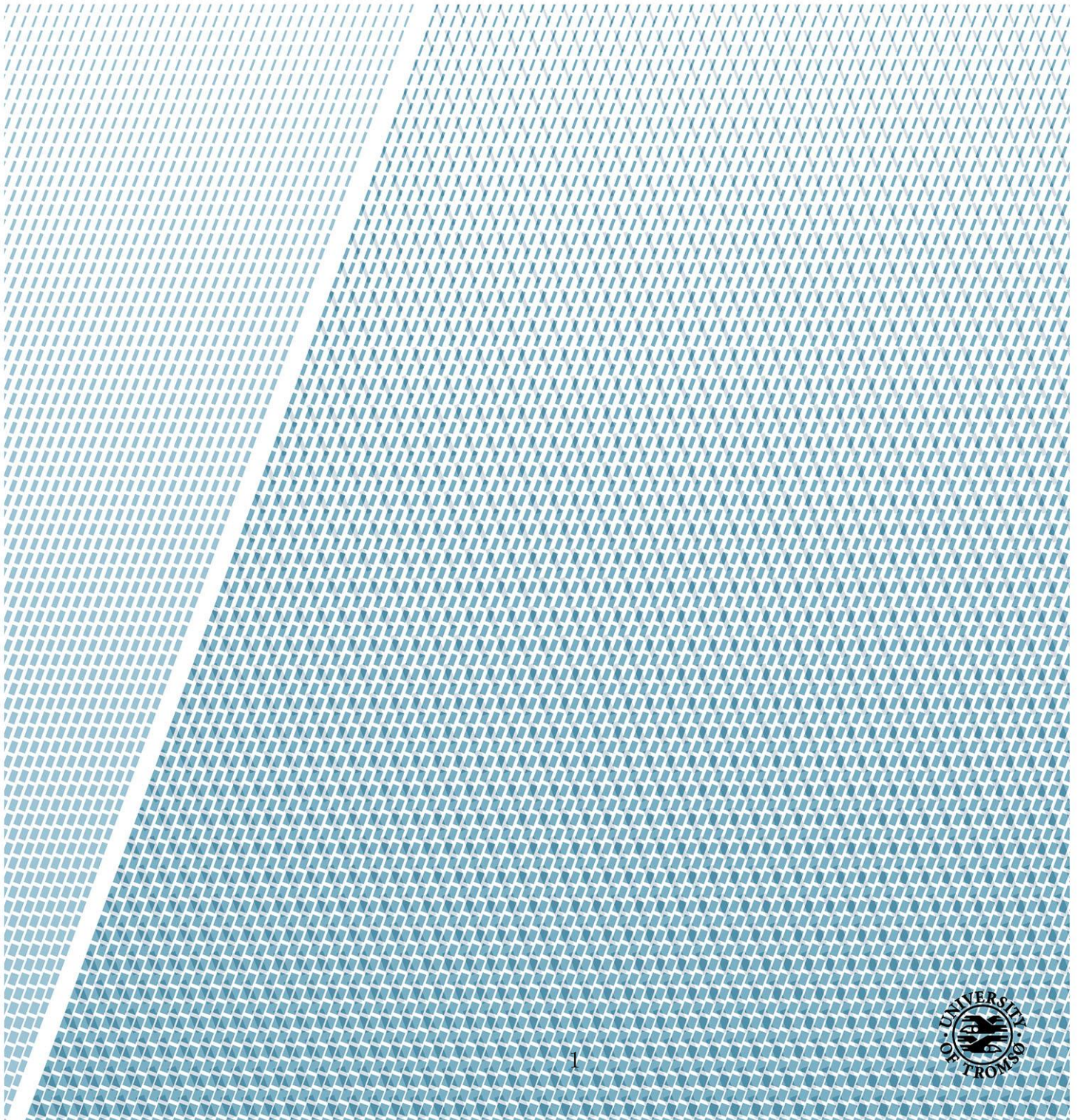


The Unidirectional Pulse Propagation Equation for Cylindrical Vector modes

—
Vegard Nilsen

MAT-3941 Master's Thesis in Applied Physics and Mathematics – Jul 2015



Abstract

A new model for the unidirectional pulse propagation equations (UPPE) was developed by Per Jacobsen[1], this model is based on the assumption of cylindrical vector (CV) modes. The model will be strong for CV type electrical field representations where only a few modes will be excited. In this thesis we will investigate the model further. The model will be implemented as a pseudo spectral method where both the Fourier and Hankel transform are necessary.

Acknowledgements

This thesis is the product of my master degree in applied mathematics at UiT The Arctic University of Norway. I would like to thank my supervisor Per Jakobsen for his excellent advice and guidance. I would also like to thank my girlfriend Karoline, and my son Jonas who has inspired me every day through this time.

I also would like to send a special thank you to the College of Optical Science in the state of Arizona, USA. For hosting my stay there for parts of my study.

Last I want to thank my friends and fellow students for all the good times we have experienced together.

Contents

Abstract	i
Acknowledgements	iii
1 Introduction	1
1.1 Numerical models	2
1.2 Structure	2
2 Maxwell equations for UPPE	5
2.1 Maxwell equations	5
2.2 Polarization	8
3 Method of Verification	11
3.1 Numerical Verification	11
3.2 The MoMS in UPPE equations	13
4 TE model	17
4.1 Derivation of TE model	17
4.2 A Simple Example	24
4.3 Rescaling the TE model	29
4.4 Implementation of TE model	32
4.4.1 The model	32
4.4.2 UPPE setup	34
4.4.3 Verification	35
4.5 Numerical Results	36
4.5.1 TE model	36
4.5.2 Verification	39
4.6 Discussion	42
5 Vectorial model	47
5.1 Vector Cylindrical Model	47
5.2 Rescaling the Vector Model	74
5.3 Numerical Vectorial	81
5.3.1 The model	81

5.3.2	Parallel programming in the model	85
5.3.3	Experimental setup	86
5.3.4	Verification	86
5.4	Numerical Results	88
5.4.1	Experimental results	88
5.4.2	Verification	92
5.5	Discussion	95
6	Summary	99
6.1	Future work	100
A	Appendix A	101
A.1	Fourier Transform	101
A.2	Hankel Transform	106
A.3	Interpolation	110
A.4	The First Order Finite Difference Method	114
B	Appendix B	119
B.1	The Sellmeier formula	119
B.2	The Cylindrical Derivative Operators	121
C	Appendix C	123
	Bibliography	125

Chapter 1

Introduction

The main part of this thesis we will discuss the cylindrical vector modes (CV). These have been of interest since the invention of the laser. A lot of research has been devoted solely to express beams using linear optical elements, a review on this matter can be found in[2]. The main interest is in the nonlinear interaction experienced in optics and solitary pulses[3][4][5].

In the 80s Durnin stated that Bessel beam[6] solutions for the scalar wave equation can be regarded as diffraction free in the ideal case. Since then a lot of research has pointed towards generation and modulation of such beams. Most of the research has been reviewed in the recent book[7].

These types of theoretical models have been studied through the scalar wave equation approximation of the Maxwell equations. This together with the nonlinear schroedinger equation, which is studied in [8], has been the two main equations to model optical beams of this type. The search for a more general model for vector modes representation has been going on since the beginning[9].

Lately there has been ongoing research by Per Jakobsen in[1]. The focus was to find a more general model to the cylindrical vector modes of arbitrary nonlinear polarization.

1.1 Numerical models

In this thesis we derive and implement a system for CV pulse propagation by using cylindrical vector modes. The materials we want to model are of arbitrary polarization. Such a formulation proves to be more effective than other models if the goal is to simulate weakly nonlinear propagation in for instance axisymmetric radially polarized pulses. Such fields can be represented through only a few modes in the CV modes, while regular plane wave modes will use a large set of modes.

The typical conditions for which this type of formulation applies is nonlinear propagation of ultrashort CV pulses in dispersive nonlinear materials, such as air. For standard time domain models as FDTD, the problem lies in representing the linear polarization in terms of differential equations because of a broad temporal band. The propagation distances are often very long compared to optical wavelengths, and coupled with a complex transverse structure renders the problem difficult in computational terms.

The type of model we will focus on is the UPPE[10]. The backbone of the model is the assumption of no scattered fields. This assumption proves to be correct even for the most extreme cases[11]. Such models can with ease handle any arbitrary linear and nonlinear polarization.

These types of models have been investigated before. Instead of CV modes the waves have been formulated as spectral amplitudes for the electrical field in terms of Fourier plane wave modes. Such formulation needs many spectral modes in order to represent a radially or azimuthally polarized CV pulse. For long propagation distances and broad temporal spectrum, the numerical solutions for UPPE equations becomes extremely difficult compared to a cylindrical formulation.

1.2 Structure

The main goal of this thesis is the cylindrical formulation of the CV modes. We will start off by first introducing the Maxwell equations in its natural form in chapter 2.

Chapter 3 is dedicated to the numerical verification method. We will first discuss the formulation of the method, and then explain how it can be applied to the Maxwell equations.

In chapter 4 we will introduce our first model. This model is based upon the assumption of the transverse electrical (TE) field. Such a model will result in a single scalar equation. We will then proceed with a simple example to better understand the true meaning of UPPE conditions. The representation of the model can be made dimensionless through a rescaling method, as is done in section 3.3. The next section we describe the numerical solution to the model, where we for the first time introduce the pseudo spectral method.

The last model is introduced in chapter 5. This is the cylindrical formulation of the CV modes. We will first go through the derivation and along the way discuss the limitations such a formulation will put on the model. We will rescale it to a non dimensional system and then propose a numerical solution.

The summary in chapter 6 we go through what we have done in the thesis, and make a few conclusive sentences.

Chapter 2

Maxwell equations for UPPE

The Maxwell equations are used to describe electromagnetic behaviour in physics, and the field of optical sciences are no different in this regard. This chapter is devoted to give a quick introduction to how the Maxwell equations are used in the framework of spatially propagating UPPE models.

2.1 Maxwell equations

In Nonlinear Optics we gaze upon the interaction between light and matter. This interaction can often be so strong that the matter itself will deform and change under the influence of light. Light is best explained as electromagnetic radiation, and its movements is governed by the Maxwell equations. In its most basic form it is called the microscopic Maxwell equations

$$\begin{aligned}\nabla \times \mathbf{e} + \partial_t \mathbf{b} &= 0 \\ \nabla \cdot \mathbf{b} &= 0 \\ \nabla \cdot \mathbf{e} &= \frac{\rho}{\epsilon_0} \\ \nabla \times \mathbf{b} - \epsilon_0 \mu_0 \partial_t \mathbf{e} &= \mu_0 \mathbf{J}\end{aligned}\tag{2.1}$$

where \mathbf{e} is the electrical field, \mathbf{b} is the magnetic field, ρ is the charge, \mathbf{J} is the current, ϵ_0 and μ_0 is the permittivity and the permeability. In free space the

product of the last two holds the relation between them as the speed of light in vacuum

$$\frac{1}{\sqrt{\mu_0\epsilon_0}} = c$$

The set of equations (2.1) gives a set of coupled Maxwell equations for every charge ρ_i . For propagating light the distances are often measured in meters, while electrons are at atomic scale. These equations are thus infeasible for numerical calculations on the natural length scales of light propagation. It is possible to do a spatial average to find the macroscopic Maxwell equations which is done in [12][8].

$$\begin{aligned}\nabla \times \mathbf{E} + \partial_t \mathbf{B} &= 0 \\ \nabla \cdot \mathbf{B} &= 0 \\ \nabla \cdot \mathbf{D} &= \rho_F \\ \nabla \times \mathbf{H} - \partial_t \mathbf{D} &= \mathbf{J}_F\end{aligned}\tag{2.2}$$

where \mathbf{E} is the total electric field, \mathbf{B} is the total magnetic field, \mathbf{D} is the displacement field and \mathbf{H} is the magnetizing field at the positions and time (x, y, z, t) . For the displacement field we have the relation

$$\mathbf{D} = \epsilon_0 \mathbf{E} + \mathbf{P}$$

where \mathbf{P} is the polarization. The two last quantities are the total amount of free charges ρ_F and the free current \mathbf{J}_F . In the set of equations (2.2) we deal with densities, such that these are feasible for calculations over greater distances than (2.1).

In most cases it is natural to assume the material light is propagating through, to consist of a linear magnetizing field.

$$\mu_0 \mathbf{H} = \mathbf{B}$$

It is also common to assume the material to possess no free charges or current such that

$$\rho_F = \mathbf{J}_F = 0$$

This reduces the Maxwell equations¹ to

$$\begin{aligned} \nabla \times \mathbf{E} + \partial_t \mathbf{B} &= 0 \\ \nabla \cdot \mathbf{B} &= 0 \\ \nabla \cdot (\epsilon_0 \mathbf{E} + \mathbf{P}) &= 0 \\ \nabla \times \mathbf{B} - \mu_0 \partial_t (\epsilon_0 \mathbf{E} + \mathbf{P}) &= 0 \end{aligned} \tag{2.3}$$

In general the polarization is a function of the magnetic and/or electrical field. The set of equations (2.3) can be written in component form, that leads to a system of eight equations for six unknown field components. This means the set of equations are redundant, and two of the equations has to either be removed or be made implicit. For time propagating models the two divergence terms appears as constraints on the field components, such models are derived in[13], and are the most common models when solving the Maxwell equations.

For spatially propagating UPPE models we work with pulses that is assumed known for all time. If the chosen propagation direction is z, the two equations without a z derivative will become the constraints instead of divergence operators have in time propagating models.

¹From this point we mean the macroscopic Maxwell equations when we refer to the Maxwell equations.

2.2 Polarization

For weak fields the polarization can be expressed through a power series as shown in [14], we have

$$\mathbf{P} = \epsilon_0 (\chi^{(1)}\mathbf{E} + \chi^{(2)}\mathbf{E}^2\chi^{(3)}\mathbf{E}^3 \dots) \quad (2.4)$$

where χ are tensors with rank corresponding to the exponent number. The first term is the linear polarization and can be expressed as

$$\mathbf{P}_L(t) = \int_0^{\infty} d\tau \chi^{(1)}(\tau) E(t - \tau)$$

It is assumed $\chi^{(1)}(\tau)$ respects the causality condition and holds the value 0 for $\tau < 0$. For time domain models the integral has to be evaluated for each time step. For spatial models we can rewrite this integral through the use of pseudo operators. Inserting the Fourier transform of both $\chi^{(1)}$ and $E(t)$ in (2.4) we can through a few modifications get

$$P_L(x, t) = \epsilon_0 \int_{-\infty}^{\infty} d\omega \hat{\chi}(\omega) \hat{E}(x, \omega) e^{-i\omega t} \quad (2.5)$$

where we have introduced hat notation for the quantities to represent Fourier transformation. We can expand the the first order tensor as a series

$$P_L(x, t) = \epsilon_0 \int_{-\infty}^{\infty} d\omega \left(\sum_{n=0}^{\infty} \frac{\hat{\chi}^n(0)}{n!} \omega^n \right) \hat{E}(x, \omega) e^{-i\omega t} \quad (2.6)$$

If we do a few manipulations of (2.6) we get

$$P_L(x, t) = \epsilon_0 \sum_{n=0}^{\infty} \frac{\widehat{\chi}^n(0)}{n!} \left(\int_{-\infty}^{\infty} d\omega \omega^n \widehat{E}(x, \omega) e^{-i\omega t} \right) \quad (2.7)$$

$$P_L(x, t) = \epsilon_0 \sum_{n=0}^{\infty} \frac{\widehat{\chi}^n(0)}{n!} \left(\int_{-\infty}^{\infty} d\omega (i\partial_t)^n \widehat{E}(x, \omega) e^{-i\omega t} \right) \quad (2.8)$$

$$P_L(x, t) = \epsilon_0 \sum_{n=0}^{\infty} \frac{\widehat{\chi}^n(0)}{n!} (i\partial_t^n) \left(\int_{-\infty}^{\infty} d\omega \widehat{E}(x, \omega) e^{-i\omega t} \right) \quad (2.9)$$

In the parenthesis we have the inverse Fourier transform of the electrical field, such that the first order polarization can be written as

$$P_L(x, t) = \epsilon_0 \widehat{\chi}(i\partial_t) E(x, t) \quad (2.10)$$

When the transform of the linear polarization is taken, we have $\widehat{\chi}(\omega)$ directly.

For the higher order parts of the polarization $P^{(2)}$ and $P^{(3)}$ there exists several effects such as second harmonic generation (SHG), sum frequency generation (SFG), difference frequency generation (DFG) and more. For the third order we have the same families of polarization, but we will focus on the Kerr effect[15]

$$\mathbf{P}_{NL}(t) = \epsilon_0 \chi^{(3)}(\mathbf{E} \cdot \mathbf{E}) \mathbf{E} \quad (2.11)$$

It is typical that the intensity of the laser will modify the medium to an optical lens, which in turn will refocus the beam from its dispersion. In this setting the tensor $\chi^{(3)}$ is a material dependant constant. To further investigate the Kerr effect we will go through an example

Example 2.1. Kerr effect *To further investigate the Kerr effect we will go through a short example, let us assume a wavepacket on the following form*

$$\phi(z, t) = e^{-(t-vz)} \left(\frac{e^{i\omega_0 t} + e^{-i\omega_0 t}}{2} \right)$$

Inserting this into (2.11) gives

$$\phi^3(z, t) = e^{-3(t-vz)} \left(\frac{3e^{i\omega_0 t} + 3e^{-i\omega_0 t} + e^{i3\omega_0 t} + e^{-i3\omega_0 t}}{8} \right)$$

Which shows that frequencies at $3\omega_0$ will be produced when the Kerr effect is present. To know what the nonlinear term will produce is of great interest before one attempts to develop a model.

This is the formulation of the Maxwell equations, including the linear polarization we will use to develop our numerical models.

Chapter 3

Method of Verification

In this chapter we will go through the general scheme to verify the numerical implementations. Then we will discuss the specifics for the Maxwell equations and the UPPE framework.

3.1 Numerical Verification

To verify the numerical implementation we have chosen to use Method of Manufactured Solutions (MoMS)[16][17]. The method has been widely used in other sciences, such as fluid mechanics. We will now introduce this method of verifying numerical implementation to the field of optics.

In general the method is straight forward, but will more often than not result in rather complicated algebraic manipulations.

For a typical system of partial differential equations an analytical solution is hard to come by. For such systems we can modify the equations to a form where an analytical solution is trivial to find. Assume the dynamical system of equations

$$\mathcal{L}_1 E_1 = 0$$

$$\mathcal{L}_2 E_2 = 0$$

$$\mathcal{L}_3 E_3 = 0$$

where the operators \mathcal{L}_1 , \mathcal{L}_2 and \mathcal{L}_3 are some complicated operator involving derivatives and the other functions E_1 , E_2 and E_3 . If an analytical solution cannot be found, we can manipulate the equations by adding artificial sources

$$\mathcal{L}_1 E_1 = \rho_1$$

$$\mathcal{L}_2 E_2 = \rho_2$$

$$\mathcal{L}_3 E_3 = \rho_3$$

where ρ_1 , ρ_2 and ρ_3 is arbitrary functions. For this system we can easily find an analytical solution by simply choosing E_1 , E_2 and E_3 which satisfies the initial conditions for the system. The source of each equation will now be chosen such that the set of equations is consistent. Let us do an example to clarify

Example 3.1. *The heat equation* *Let us assume the heat equation with the following initial conditions*

$$\partial_t f(x, t) - \alpha \partial_{xx} f(x, t) = 0, \quad f(-0.1, 0) = f(0.1, 0) = 300 \quad (3.1)$$

For this example we will choose the function

$$f(x, t) = 300 + (0.01 - x^2)t \quad (3.2)$$

The function $f(x, t)$ obviously satisfies the initial condition, which is a requirement. But the function is not a solution to the differential equation (3.1). By direct insertion we get

$$0.01 - x^2 + 2\alpha t = 0$$

The function can be made a solution to the modified system with an artificial source

$$\partial_t f(x, t) - \alpha \partial_{xx} f(x, t) = \rho(x, t)$$

where by insertion we now have

$$0.01 - x^2 + 2\alpha t = \rho(x, t)$$

By choosing $\rho(x, t)$ such that the equation is satisfied we have a consistent system to verify the numerical implementation.

For the best results the exact solution and the source should both be smooth functions, without any singularities. In general this is a mathematical formulation, and disregard any physical assumptions. If the numerical scheme simulates a physical system with assumptions out of the ordinary, these have to be properly implemented within the source and the exact solution. The general numerical scheme, without assumptions can also be tested, if possible.

In the method the source terms is arbitrary. We can choose the source to neglect certain terms of the model. By choosing the function $\rho(x, t) = \partial_t f(x, t) + \rho'(x, t)$ as the source in our example, we can neglect the first derivative from the model. This way we can systematically verify each part of the model. For the process of creating the numerical model, this can be a very powerful tool, as we get direct verification for each step along the way.

3.2 The MoMS in UPPE equations

For the UPPE scheme we want to solve a system of equations which originates from the Maxwell equations. We found the system relevant to be

$$\begin{aligned}
\nabla \cdot \mathbf{B} &= 0 \\
\nabla \cdot \mathbf{D} &= 0 \\
\nabla \times \mathbf{B} - \frac{1}{c^2} \partial_t \mathbf{E} &= \mu_0 \partial_t \mathbf{P} \\
\nabla \times \mathbf{E} - \partial_t \mathbf{B} &= 0
\end{aligned} \tag{3.3}$$

For complicated versions of the polarization, it is nontrivial to find a solution satisfying all the equations. It is possible to simplify the search by expressing the fields in terms of their potential

$$\mathbf{E} = -\nabla\phi - \partial_t \mathbf{A} \tag{3.4}$$

$$\mathbf{B} = \nabla \times \mathbf{A} \tag{3.5}$$

By a choice of the function ϕ and vector \mathbf{A} we can find any arbitrary solution satisfying the system (3.3), where it is known that both a electrical field and magnetic field exists. The Maxwell equations can be approximated to the scalar equation when the TE field is assumed[8]. For this example we will investigate the equation

$$\partial_{zz} E - \frac{1}{c^2} \partial_{tt} (\chi(i\partial_t) + 1) E = \frac{\mu_0}{c} \partial_{tt} P^{NL} \tag{3.6}$$

The polarization is usually defined as a function of the electrical and/or the magnetic field. In order to create a source, we can assume this arbitrary polarization to be the source element. The choice of polarization can thus be written as

$$P^{NL}(E, B) = P^{NL'}(E, B) + \rho(E, B)$$

Choosing the functions in (3.5) as $\phi = 0$ and $\mathbf{A} = \partial_t \mathbf{f}$ and inserting them into equation (3.6) gives

$$\partial_{tt}(-\partial_{zz}f + \frac{1}{c^2}\partial_{tt}(\chi(i\partial_t) + 1)f + \frac{\mu_0}{c^2}(P^{NL'}(-\partial_{tt}f, \nabla \times \partial_t f) + \rho)) = 0$$

Dependant on the nonlinear term $P^{NL'}$ finding a source term ρ can either be trivial or extremely complicated. The initial conditions of the equation have to follow the exact solution as

$$\mathbf{E} = -\partial_{tt}\mathbf{f}, \quad \mathbf{B} = \nabla \times \partial_t\mathbf{f}$$

The solution can now be found through one function alone \mathbf{f} , where we have ensured both a magnetic and electrical field to exist. The calculations done here assumes the general system for the equation (3.6).

Chapter 4

TE model

In this chapter we will derive our first model which is based upon the Transverse Electrical (TE) field. This is the same model as discussed in [8], where we through a multiple scales method approximated the model to the nonlinear schroedinger equation.

We will then proceed to do a simple example of a analytically comprehensive model, in order to understand what UPPE models are about. In the next parts we will take the model through a scaling process where we end up with a dimensionless system, and finally propose a suggestive method to solving the problem numerically.

4.1 Derivation of TE model

The starting point of the model is the Maxwell equations as we derived them in chapter 2.

$$\begin{aligned}\nabla \times \mathbf{E} + \partial_t \mathbf{B} &= 0 \\ \nabla \times \mathbf{B} - \frac{1}{c^2} \partial_t \mathbf{E} &= \mu_0 \partial_t \mathbf{P} \\ \nabla \cdot \mathbf{B} &= 0 \\ \nabla \cdot \epsilon_0 (\mathbf{E} + \mathbf{P}) &= 0\end{aligned}\tag{4.1}$$

where the polarization consist of a linear term, and some nonlinear or linear term.

$$\mathbf{P} = \mathbf{P}^L + \mathbf{P}^{NL}$$

For the linear polarization we are going to use the causal operator $\widehat{\chi}(i\partial_t)$. The nonlinear term we are going to leave as any arbitrary function.

The chosen direction of propagation is z . The TE field is defined as the electromagnetic field perpendicular to the propagation direction of the field. It can be written in Cartesian coordinates as

$$\mathbf{E}(\mathbf{x}, t) = E(z, x, t)\mathbf{j}$$

$$\mathbf{B}(\mathbf{x}, t) = B_1(z, x, t)\mathbf{i} + B_2(z, x, t)\mathbf{k}$$

$$\mathbf{P}(\mathbf{x}, t) = P(z, x, t)\mathbf{j}$$

By inserting our TE field into the Maxwell equations (4.1), the equations can be reduced into component form

$$\partial_z E = \partial_t B_1 \tag{4.2}$$

$$\partial_x E = -\partial_t B_1 \tag{4.3}$$

$$\partial_x B_1 = -\partial_z B_2 \tag{4.4}$$

$$\partial_z B_1 - \partial_x B_2 = \frac{1}{c^2} \partial_t (E + \chi(i\partial_t)E) + \frac{1}{\epsilon_0} P^{NL} \tag{4.5}$$

There are four equations in this set. We only need three to find a solution to all our three field components. This means that the equations are redundant. The three equations with the z derivative, equations (4.2), (4.4) and (4.5) will be our dynamical system, and the last equation (4.3) is a constraint. Observe the following

$$\begin{aligned}
\partial_x E + \partial_t B_2 &= 0 \\
\partial_z(\partial_x E + \partial_t B_2) &= 0 \\
\partial_{zx} E - \partial_{tx} B_1 &= 0 \\
\partial_{zx} E - \partial_{zx} E &= 0
\end{aligned}$$

This means the constraint is automatically fulfilled.

If we take the time derivative of equation (4.5), and replace $\partial_t B_1$ with equation (4.2), and $\partial_t B_2$ with equation (4.3), we can remove the magnetic field from equation (4.4)

$$\partial_{zz} E + \partial_{xx} E = \frac{1}{c^2} \partial_{tt} ((1 + \chi(i\partial_t)) E + \frac{1}{\epsilon_0} P^{NL}) \quad (4.6)$$

We are now going to look for a solution to this system by mode expansion to the linear part of the equation. We start by removing the nonlinearity P^{NL} from the equation.

$$\partial_{zz} E + \partial_{xx} E = \frac{1}{c^2} \partial_{tt} (1 + \chi(i\partial_t)) E$$

If the medium is homogeneous we can reduce the equation to an algebraic equation through Fourier transform in space and time.

$$-(k^2 + \xi^2) \hat{E} = \left(\frac{\omega}{c}\right)^2 (1 + \hat{\chi}(\omega)) \hat{E}$$

where we denote k as the longitudinal, ξ as the transverse wave number and ω is frequency. We have denoted \hat{E} as the Fourier transform of E . We introduce the refractive index as

$$n^2(\omega) = 1 + \widehat{\chi}(\omega)$$

By solving the equation for the longitudinal wave number k we can find the dispersion relation as

$$k = \pm\beta(\omega, \xi) = \pm\sqrt{\left(\frac{\omega}{c}\right)^2 n^2(\omega) - \xi^2}$$

By expressing the longitudinal wave number in this way we can use it to expand the electrical field in terms of a integral in the transverse direction and frequency.

$$E(z, x, t) = \frac{1}{4\pi^2} \int_0^\infty d\omega \int_{-\infty}^\infty d\xi \{ A_+(z, \xi, \omega) e^{i\beta z} + A_-(z, \xi, \omega) e^{-i\beta z} \} e^{i\xi x - \omega t} + (*) \quad (4.7)$$

where we have used the notation (*) for the complex conjugate. The complex conjugate ensures the reality of the electrical field. From the exponents we can deduce that the amplitude A_+ is travelling to the right, while the amplitude A_- is travelling to the left.

The expansion can be simplified through rewriting the complex conjugate in the following way

$$\begin{aligned} & \int_0^\infty d\omega \int_{-\infty}^\infty d\xi \{ A_+^*(z, \xi, \omega) e^{-i\beta z} + A_-^*(z, \xi, \omega) e^{i\beta z} \} e^{i(\omega t - \xi x)} \\ & \int_0^\infty d\omega \int_{-\infty}^\infty d\xi \{ A_+^*(z, -\xi, -\omega) e^{-i\beta z} + A_-^*(z, -\xi, -\omega) e^{i\beta z} \} e^{-i(\omega t - \xi x)} \\ & \int_{-\infty}^0 d\omega \int_{-\infty}^\infty d\xi \{ A_+^*(z, -\xi, -\omega) e^{-i\beta z} + A_-^*(z, -\xi, -\omega) e^{i\beta z} \} e^{i(\xi x - \omega t)} \end{aligned}$$

where we have assumed that $n(\omega)$ is an even function. By introducing new amplitudes we can simplify the transform to

$$E(z, x, t) = \frac{1}{4\pi^2} \int_{-\infty}^{\infty} d\omega \int_{-\infty}^{\infty} d\xi \{A(z, \xi, \omega)e^{i\beta z} + B(z, \xi, \omega)e^{-i\beta z}\} e^{-i\omega t + i\xi x} \quad (4.8)$$

where the new amplitudes are defined as

$$A(z, \xi, \omega) = \begin{cases} A_+(z, \xi, \omega), & \omega > 0 \\ A_-^*(z, -\xi, -\omega), & \omega < 0 \end{cases}$$

$$B(z, \xi, \omega) = \begin{cases} A_-(z, \xi, \omega), & \omega > 0 \\ A_+^*(z, -\xi, -\omega), & \omega < 0 \end{cases}$$

We want to use this expansion to solve the nonlinear equation (4.6). To do so we have to take the derivative in z on the expansion (4.7)

$$\begin{aligned} \partial_z E(z, x, t) = & \frac{1}{4\pi^2} \int_{-\infty}^{\infty} d\omega \int_{-\infty}^{\infty} d\xi \{ \partial_z A e^{i\beta z} \\ & + i\beta A e^{i\beta z} + \partial_z B e^{-i\beta z} - i\beta B e^{-i\beta z} \} e^{i(\xi x - \omega t)} \end{aligned}$$

The expression can be reduced by the following constraint[18]

$$\partial_z A e^{i\beta z} + \partial_z B e^{-i\beta z} = 0 \quad (4.9)$$

Taking the second z derivative of the expansion (4.7) will give the expression

$$\begin{aligned} \partial_{zz}E = & \frac{1}{4\pi^2} \int_{-\infty}^{\infty} d\omega \int_{-\infty}^{\infty} d\xi \{ -\beta^2 A e^{i\beta z} - \beta^2 B e^{-i\beta z} \\ & + i\beta \partial_z A e^{i\beta z} - i\beta \partial_z B e^{-i\beta z} \} e^{i(\xi x - \omega t)} \end{aligned}$$

where the two last terms can be rewritten as $2i\beta \partial_z A_+ e^{i\beta z}$ through equation (4.9).

Inserting this directly into the nonlinear equation (4.6), and proceeding with the Fourier transform of the right hand side will we get the equation

$$2i\beta \partial_z A e^{i\beta z} = \widehat{NL} \quad (4.10)$$

where

$$NL = \frac{1}{c^2 \epsilon_0} \partial_{tt} P^{NL} \quad (4.11)$$

and the relation between amplitude and electrical field is

$$E(z, x, t) = \frac{1}{4\pi^2} \int_{-\infty}^{\infty} d\omega \int_{-\infty}^{\infty} d\xi \{ A(z, \xi, \omega) e^{i\beta z} + B(z, \xi, \omega) e^{-i\beta z} \} e^{-i\omega t + i\xi x} \quad (4.12)$$

For the amplitude $B(\omega)$ we can observe the following

$$\begin{aligned} B^*(\omega) &= A_-^*(\omega) = A(-\omega), \quad \omega > 0 \\ B^*(\omega) &= A_+^*(-\omega) = A(-\omega), \quad \omega < 0 \end{aligned}$$

Thus we have found the relation

$$B(\omega) = A^*(-\omega), \quad \forall \omega$$

By focusing on the conjugate of the transform we can observe that

$$\frac{1}{4\pi^2} \int_{-\infty}^{\infty} d\omega \int_{-\infty}^{\infty} d\xi A^*(z, -\xi, -\omega) e^{-i\beta z} e^{-i\omega t + i\xi x} \quad (4.13)$$

$$= \left(\frac{1}{4\pi^2} \int_{-\infty}^{\infty} d\omega \int_{-\infty}^{\infty} d\xi A(z, -\xi, -\omega) e^{i\beta z} e^{i\omega t - i\xi x} \right)^* \quad (4.14)$$

Here we introduce the relations $\omega \rightarrow -\omega'$ and $\xi \rightarrow -\xi'$, such that the total integral can be simplified to

$$E(z, x, t) = \frac{1}{4\pi^2} \int_{-\infty}^{\infty} d\omega \int_{-\infty}^{\infty} d\xi \{ A(z, \xi, \omega) e^{i\beta z} e^{-i\omega t + i\xi x} + (*) \} \quad (4.15)$$

This means the amplitude $B(\omega)$ is redundant, and the electrical field can be found by considering the value $2\text{Re}(A(\omega))$.

No assumptions breaking the Maxwells equations has been made this far. For UPPE equations we assume there is no backwards travelling wave, or this wave is rather small in comparison to the dominant forward travelling wave. For UPPE equations we thus enforce the condition

$$A(z, \xi, \omega) = 0, \quad \omega < 0$$

This assumption ensures a model only creating a right travelling wave. To put further emphasis on the conditions creating such waves we will in the next section go through a simple example explaining this phenomena.

The numerical problem has been reduced from a wave equation to a single ODE solving for one amplitude $A(\omega, z)$, where the total electrical field can be found from this amplitude alone.

4.2 A Simple Example

To better understand the UPPE approximation we will here go through a simple example. We are going to assume a linearly polarized electromagnetic wave propagating in the presence of a spatially varying refractive index

The relevant equation for this specific example is

$$\partial_{zz}E - \frac{1}{c^2}\partial_{tt}E = \frac{1}{c^2}\chi(z)\partial_{tt}E \quad (4.16)$$

We start by solving the homogeneous part

$$\partial_{zz}E - \frac{1}{c^2}\partial_{tt}E = 0$$

The two modes solving this system is

$$e^{i\beta z - i\omega t}, e^{-i\beta z - i\omega t}, \quad \omega > 0$$

where $\beta(\omega) = \frac{1}{c^2}|\omega|$. By the inverse transform we can recreate any real function $E = E(z, t)$.

$$E(z, t) = \int_0^{\infty} d\omega \{A_+(z, \omega)e^{i\beta z} + A_-(z, \omega)e^{-i\beta z}\}e^{-i\omega t} + (*)$$

Similarly to the TE model we can rewrite the integral transform to the following form

$$E(z, t) = \int_{-\infty}^{\infty} d\omega \{A(z, \omega)e^{i\beta z} + B(z, \omega)e^{-i\beta z}\}e^{-i\omega t} \quad (4.17)$$

where

$$A(z, \omega) = \begin{cases} A_+(z, \omega), & \omega > 0 \\ A_-^*(z, \omega), & \omega < 0 \end{cases}$$

$$B(z, \omega) = \begin{cases} A_-(z, \omega), & \omega > 0 \\ A_+^*(z, \omega), & \omega < 0 \end{cases}$$

It is easy to show that

$$B(z, \omega) = A^*(z, -\omega) \quad (4.18)$$

Thus the amplitude B is redundant. The amplitude A is at this point arbitrary for all ω . The amplitude B will ensure that E is real.

To solve the starting point equation (4.16) we must take derivatives of our expansion (4.17).

$$\partial_z E(z, t) = \int_{-\infty}^{\infty} d\omega \{i\beta A e^{i\beta z} - i\beta B e^{-i\beta z} + \partial_z A e^{i\beta z} + \partial_z B e^{-i\beta z}\} e^{-i\omega t}$$

The expansion (4.17) is redundant. We have four half range frequencies where we only need two. This is because the reality of the electrical field satisfies

$$\widehat{E}(z, \omega) = \widehat{E}^*(z, -\omega)$$

We reduce this redundancy by introducing the constraint[18]

$$\partial_z A e^{i\beta z} + \partial_z B e^{-i\beta z} = 0 \quad (4.19)$$

Taking the second derivative of (4.17) will give

$$\partial_{zz}E(z, t) = \int_{-\infty}^{\infty} d\omega \{i\beta\partial_z A e^{i\beta z} - i\beta\partial_z B e^{-i\beta z} - \beta^2 A e^{i\beta z} - \beta^2 B e^{-i\beta z}\} e^{-i\omega t} \quad (4.20)$$

Inserting (4.20) and (4.17) into equation (4.16) we get

$$\begin{aligned} & \int_{-\infty}^{\infty} d\omega \left(\frac{\omega^2}{c^2} - \beta^2 \right) \{A e^{i\beta z} + e^{-i\beta z}\} e^{-i\omega t} \\ & \int_{-\infty}^{\infty} d\omega \{i\beta\partial_z A e^{i\beta z} - i\beta\partial_z B e^{-i\beta z}\} e^{-i\omega t} \\ & = - \int_{-\infty}^{\infty} d\omega \frac{\omega^2}{c^2} \hat{\chi}(z) \{A e^{i\beta z} + B e^{-i\beta z}\} e^{-i\omega t} \end{aligned}$$

The first integral cancels, and in spectral domain we are left with

$$\begin{aligned} & i\beta\partial_z A e^{i\beta z} - i\beta\partial_z B e^{-i\beta z} \\ & = -\frac{\omega^2}{c^2} \hat{\chi}(z) \{A e^{i\beta z} + B e^{-i\beta z}\} \end{aligned}$$

Using (4.19) again will give

$$2i\beta\partial_z A e^{i\beta z} = -\frac{\omega^2}{c^2} \hat{\chi}(z) \{A e^{i\beta z} + B e^{-i\beta z}\} \quad (4.21)$$

Introducing (4.18) to (4.21) and a few manipulations give

$$\partial_z A(z, \omega) = i\alpha f(z) \{A(z, \omega) + A^*(z, -\omega) e^{-2i\beta z}\} \quad (4.22)$$

where

$$\alpha = \frac{\omega^2 \widehat{\chi}_0}{2\beta c^2} = \frac{1}{2}\beta \widehat{\chi}_0$$

and

$$\widehat{\chi}(z) = \widehat{\chi}_0 f(z)$$

where $\widehat{\chi}_0$ is the strength of the function $f(z) = O(1)$.

Underlying the UPPE assumption is a unidirectional wave. In order to achieve this we will assume that $A(z, \omega) = 0$ for $\omega < 0$. For equation (4.22) this will for $\omega > 0$ mean that

$$\partial_z A(z, \omega) = i\alpha f(z) A(z, \omega) \quad (4.23)$$

We now check for consistency in according to the full system (4.22). For $\omega < 0$ we get

$$\partial_z A(z, \omega) = i\alpha f(z) \{A(z, -|\omega|) + A^*(z, |\omega|) e^{-2i\beta z}\} \quad (4.24)$$

Even for the simple case where we assume that $A(0, -|\omega|) = 0$, the equation (4.24) gives

$$\partial_z A(0, -\omega) = i\alpha f(0) \{A^*(0, |\omega|)\} \neq 0$$

Thus a solution to (4.22) does not even exist.

In order for (4.23) to be an approximation to (4.22) we need $A(z, \omega) \approx 0$ for all $\omega < 0$. For the assumption $A(z, -|\omega|) \approx 0$ we have for equation (4.22)

$$\partial_z A(z, |\omega|) = i\alpha f(z)A(z, |\omega|) \quad (4.25)$$

$$\partial_z A(z, -|\omega|) = i\alpha f(z)A^*(z, |\omega|)e^{-2i\beta z} \quad (4.26)$$

In (4.26) we observe that

$$A(z, -|\omega|) = i\alpha \int_{z_0}^z dz' f(z')A^*(z', |\omega|)e^{2i\beta z'}$$

We observe from (4.25) that the characteristic length scale of variation of $A(z, |\omega|)$ is

$$L_+ \sim \frac{1}{\alpha}$$

In (4.26) the oscillatory exponent will vary on a length scale of

$$L_- \sim \frac{1}{\beta}$$

If it was the case that

$$L_+ \gg L_- \quad (4.27)$$

it would mean that the integral in (4.26) would be very small due to cancellations.

This is an example of the Riemann-Lebesgue lemma from theory of integration. The unidirectional wave assumption is thus only valid whenever (4.27) holds. For such cases when we have $A(z_0, -|\omega|) \approx 0$ then $A(z, -|\omega|) \approx 0$ for $z > z_0$ due to integral cancellations. This is the assumption leading to existence of UPPE models.

4.3 Rescaling the TE model

From the derivation of the TE model we remember that we had the following equations as our proposed numerical system

$$2i\beta\partial_z A_+ e^{i\beta z} = \widehat{NL} \quad (4.28)$$

where the electrical field can be found through the transform

$$E(z, x, t) = \frac{1}{4\pi^2} \int_{-\infty}^{\infty} d\omega \int_{-\infty}^{\infty} d\xi A_+(z, \xi, \omega) e^{i\beta z} e^{-i\omega t + i\xi x} \quad (4.29)$$

and the origin of the differential equation were

$$\partial_{zz}E + \partial_{xx}E = \frac{1}{c^2} \partial_{tt}((1 + \chi(i\partial_t))E) + \frac{1}{\epsilon_0} P^{NL} \quad (4.30)$$

We will here start by introducing new variables. The variables will be dimensionless, while the corresponding constant will typically be set by the initial condition.

$$z = z_0 z', \quad x = x_0 x', \quad E = E_0 E', \quad t = t_0 t' \quad (4.31)$$

By inserting the new variables (4.31) into (4.30) and a few manipulations we get

$$\alpha \partial_{x'x'} E' + \partial_{z'z'} E' - \partial_{t't'} E' = \partial_{t't'} \chi \left(\frac{i}{t_0} \partial_{t'} \right) E' + \partial_{t't'} P^{NL'} \quad (4.32)$$

where we have introduced the relation $z_0 = ct_0$. The new constant α is

$$\alpha = \frac{c^2 t_0^2}{x_0^2} = \left(\frac{z_0}{x_0} \right)^2$$

which is a constant of proportionality. The constant is length divided by length and thus dimensionless.

The transversal part can be removed from equation (4.32) by

$$\lim_{x_0 \rightarrow \infty} \alpha = \lim_{x_0 \rightarrow \infty} \left(\frac{z_0}{x_0} \right)^2 \approx 0$$

The numerical approach we want for this model is based upon this assumption. The relation between the amplitude and the electrical field can be found through the transform (4.29). We will first look at the dispersion

$$\beta = \sqrt{\left(\frac{\omega}{c} \right)^2 n^2(\omega)}$$

We will use $\omega_0 t_0 = 1$ as the relationship between time and frequency. Together with the aforementioned relationship for the speed of light $z_0 = ct_0$ we have

$$\beta = \frac{1}{z_0} \sqrt{(\omega')^2 n^2(\omega' \omega_0)}$$

where the function $n(\omega \omega_0)$ is a dimensionless quantity. For the transform this will ensure the exponent to be in dimensionless form. For the rest of the transform (4.29) we have

$$E_0 E'(z', x', t') = \frac{A_0}{t_0} \frac{1}{2\pi} \int_{-\infty}^{\infty} d\omega' A(z', \omega') e^{i\beta' z'} e^{-i\omega' t'}$$

where we observe that in terms of A_0 we have E_0 as

$$E_0 \sim \frac{A_0}{t_0} \tag{4.33}$$

direct insertion of 4.33) into (4.28) the equation gives

$$\frac{A_0}{z_0^2} 2i\beta' \partial_z A' e^{i\beta' z'} = \widehat{NL}$$

where the nonlinearity has the dimension

$$NL' = \frac{E_0}{c^2 t_0^2} P^{NL'} = \frac{E_0}{z_0^2} P^{NL'}$$

From the Fourier transform we will get an extra factor t_0 . We have

$$A_0 2i\beta' \partial_z A'_+ e^{i\beta' z'} = t_0 E_0 \widehat{NL}'$$

through the relation of the initial electrical field E_0 and the amplitude A_0 , we observe that the differential equation is a dimensionless equation. We know the Maxwell equations is a physical law and is dimensionless, this will thus be a weak verification of the derivations done in the previous section. The dimensionless equations are the ones we will use in our numerical implementation. The problem has now through the assumption of $\alpha = 0$ been reduced to solving

$$2i\beta' \partial_z A'_+ e^{i\beta' z'} = \widehat{NL}'$$

where the electrical field can be found through

$$E'(z', x', t') = \frac{1}{2\pi} \int_{-\infty}^{\infty} d\omega' A(z', \omega') e^{i\beta' z'} e^{-i\omega' t'} \quad (4.34)$$

and the arbitrary nonlinearity is expressed as

$$NL' = P^{NL'}$$

In this section we introduced new dimensionless variables. We made reasonable

relations between the different quantities in terms of the physical phenomena we want to model.

Next we went on to assume that the transverse part is gone by setting the constant $\alpha = 0$. This simplified our system to a propagating direction and a time dependency.

4.4 Implementation of TE model

In this section we will explain the implementation of the TE model. We will treat the model as the general Maxwell equation without the UPPE assumptions. We will then go two different directions, one where we discuss the implementation of the UPPE assumptions, and one where we discuss the verification of the numerical system.

4.4.1 The model

To evolve the amplitude involves evaluating the polarization each time. The polarization is some function of the fields E or B . If we assume that the polarization is of the type Kerr effect we have in the temporal domain

$$NL = E^3$$

which in the spectral domain represents a double convolution. The convolution can be avoided by reconstructing the electrical field, do the multiplication, and then bring the polarization back to spectral domain. This type of method is called a pseudo spectral method. To do so we have to implement the relation between the electrical field and the amplitude

$$E(z, t) = \frac{1}{2\pi} \int_{-\infty}^{\infty} d\omega A(\omega, z) e^{i\beta z - i\omega t} + (*) \quad (4.35)$$

Since the algorithm is based on repetitive use of the Fourier transform we have chosen to implement a version of the Fast Fourier Transform (FFT) algorithm. The FFT algorithm has a $N \log(N)$ complexity, compared to its counterpart the Discrete Fourier Transform (DFT), which has a N^2 complexity.

The algorithm itself does not have to be implemented, but in order to utilize the FFT we have to go through a scale and shift process for our transform (4.35). The full derivation is described in Appendix A.

We have chosen to implement the transform (4.35) with periodic boundaries. Such an implementation has the advantage of recycling the domain, and thus requires a smaller time domain for long distance propagation. For the general wave it is enough to have the wave fully encapsulated by the time domain, and the frequencies within the spectral domain.

To utilize the FFT algorithm, the domain of interest has to be discretized into 2^m points. If the amount of points for the current discretization is not enough, one will have to double the amount of points to achieve a finer discretization. The general idea of the model is to simulate nonlinear interactions for few cycle pulses. Nonlinear interactions like the Kerr effect produces new frequencies at three times the mother frequency, as we discovered in Chapter 2. This means that the discretization itself has to be fine enough to represent the pulse, and at the same time leave room for these frequencies to appear in the spectral domain.

The evolution equation to find the amplitude at a given point z is expressed as the differential equation

$$2i\beta\partial_z A(\omega, z)e^{i\beta z} = \widehat{NL}(\omega, z) \quad (4.36)$$

To solve such a system we have used a standard ODE solver. The number of differential equations equates the number of points in frequency. For nonlinear ODEs it is advisable to use implicit methods. Because of the high number of points in the system one should choose a solver which does not require the Jacobian to be calculated beforehand. The chosen solver for this problem was the Adam Basforth algorithm.

The major part of time spent in the algorithm is on the right hand side. In general this is where the numerical implementation should be made in as few steps as possible where speed really matters. The outlay of our implementation can be shown in a four step algorithm:

1. Reconstruct the electrical field from the transform (4.35)
2. Evaluate the polarization at this point z .
3. Bring the polarization into spectral domain and set it as the right hand side of (4.36).
4. repeat to evolve further.

This implementation is the same for both the UPPE conditions and the verification of the model.

4.4.2 UPPE setup

To simulate real UPPE conditions we can modify the general propagation model. As indicated in the first section of this chapter, we can set all negative frequencies to zero, to simulate a right travelling wave. To initialize such a wave we can start with a wave packet of the form

$$f_0(t) = e^{-\gamma t} \cos(\omega_0 t)$$

Choosing the constants γ and ω_0 properly will ensure this simulates a few cycle pulse. Taking the Fourier transform of the function will give a wave propagating in both negative and positive direction. We will keep only the positive frequencies and use this to initiate the amplitude $A(\omega, z)$.

The electrical field can then be found through reconstruction as explained previously. From the constant ω_0 we will get the initial frequency spike, if the non-linearity is of the type Kerr effect, we will get new child frequencies at the points $3\omega_0$ in the spectrum. The choice of ω_0 should be chosen such that the point $\omega = 0$

is unpopulated, yet the domain does not get saturated from production of child frequencies too fast.

Whenever we reconstruct the electrical field and conduct an evaluation of the nonlinearity we will produce negative frequencies, these have to be set to zero each time we want to propagate the amplitude $A(\omega, z)$. Since we know that negative frequencies does not exist for $A(\omega, z)$ we can also choose to not propagate the negative frequencies, and thus get a general speed up for the propagation model.

4.4.3 Verification

To verify the numerical implementation we will use the method described in chapter 3. To produce an environment where the UPPE conditions are fulfilled requires tinkering with the chosen analytical solution. In terms of testing the numerical implementations as a system working together, it is sufficient to test the more general model. We will thus assume both positive and negative frequencies exists for this test.

The evolution of the electrical field will follow the differential equation which was the origin of the amplitude equation

$$\partial_{zz}E - \partial_{tt}E - \partial_{tt}\chi(i\partial_t)E = \partial_{tt}P^{NL} \quad (4.37)$$

The polarization has been treated as a general function of unknown type. For verification purpose we can assume this to be any function of our choosing, and thus represent our source term. In the TE model, the chosen representation of the polarization is

$$\partial_{tt}P^{NL}(z, t) = \partial_{tt}P^{NL'}(z, t) + \partial_{tt}\rho(z, t)$$

where $P^{NL'}$ will be represented as the Kerr effect. The polarization can also be represented as any kind of magnetic function, as we can ensure this through the representation

$$-\partial_{tt}f(z, t) = E(z, t)$$

The original equation is the driven wave equation. To analytically solve it we need atleast two initial conditions. We choose the equations

$$E(z, t) = \frac{1}{2\pi} \int_{-\infty}^{\infty} d\omega \{A(z, \omega)e^{i\beta z} + B(z, \omega)e^{-i\beta z}\}e^{-i\omega t}$$

$$\partial_z E(z, t) = \frac{1}{2\pi} \int_{-\infty}^{\infty} d\omega \{i\beta A e^{i\beta z} - i\beta B e^{-i\beta z}\}e^{-i\omega t}$$

This is a system of two equations and two unknowns. We only have to solve it for the amplitude $A(\omega, z)$ since the amplitude $B(\omega, z)$ is redundant. This will initialize the general model.

4.5 Numerical Results

We will present the numerical results in the same order as we presented the suggested numerical solutions of the systems.

4.5.1 TE model

For the polarization we have chosen to simulate the Kerr effect, and the material Air

$$P'_{kerr} = \zeta E'^3$$

where the constant $\zeta = \eta E_0^2$, and is regarded as the strength of the nonlinearity. The Kerr constant η is material dependant, and for air it holds the value $\eta = 1.7 * 10^{-25}$. The initial electrical field E_0 is given by the intensity of the incident laser beam, and can be found through the relation

$$E_0 = \left(\frac{2I}{\epsilon_0 c} \right) \times 10^2$$

The intensity of the laser we have chosen to model is of the strength $I = 10^{15} \text{W/cm}^2$. The strength of the nonlinearity in this case will thus have the value

$$\zeta = \eta E_0^2 = 0.001281$$

The refractive index is material dependant. In order to find analytical function of the refractive index it is common to use the Sellmeier formulas. A short introduction is given in the Appendix B. For Air the formula is given as

$$n(\omega) = 1 + \frac{5.85096 \times 10^{-16}}{1.99884 \times 10^{-11} - \omega^2} + \frac{2.01822 \times 10^{-14}}{8.29399 \times 10^{-10} - \omega^2}$$

This function can be verified through the STP conditions of the medium. Inserting the frequency $\omega = 0$ into the formula for the refractive index gives the value 1.00027 which is the exact value for STP conditions in air.

To find the initial mode of the system we have chosen the function

$$f_0(t) = e^{-t/2} \cos(5t)$$

The test run was ran with a time domain from -15 to 15 , the discretization in time direction was chosen to be $T = 1024$. For the only spatial direction we have chosen to print the results with steplength $dz = 0.1$.

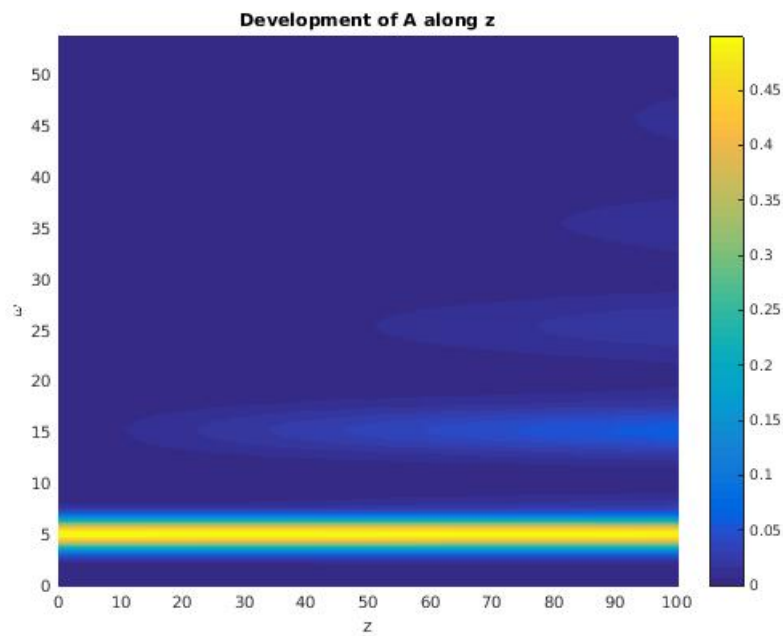


FIGURE 4.1: The figure shows the development of A with ω on the y axis and propagation direction z on the x axis. The discretization for ω is 1024 while in z direction we have 1000 points.

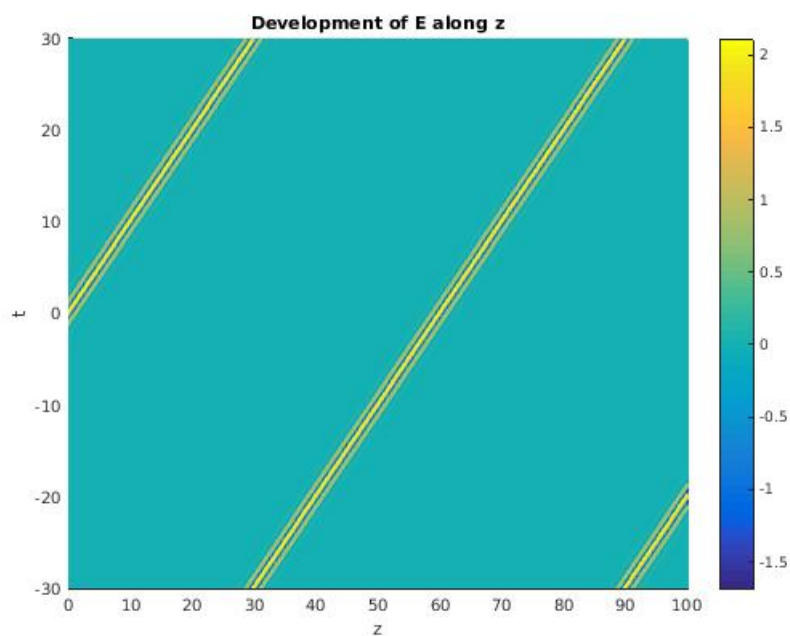


FIGURE 4.2: This is the same function in the time domain. The y axis is now time instead, discretized with 1024 points. The z discretization is the same as the previous picture 1000 points. We can see the short pulse travelling through the medium with periodic boundaries doing its work.

The first figure (4.1) is the development of the spectrum, where the y axis is frequency and the x axis is z. The chosen representation is a density plot where we can see the mother frequency at the point $\omega = 5$, and child frequencies emerge along the frequency axis.

In the next figure (4.2) we have the same system in time and space. The pulse is here travelling through the domain and reappearing on the negative side of the time axis.

4.5.2 Verification

Both the Kerr coefficient, incident laser intensity and refractive index will be present in this simulation as well. For this case however, we will simulate an exact solution, and these functions and constants will not play the same role as in the real experimental test.

For verification purpose the numerical constant was set to $\zeta = 0.002$. And the refractive index was set to be a constant $n(\omega) = 1$. To find an exact solution we chose the function

$$f(z, t) = e^{-(t-2z)^2} \cos(10t)$$

The time domain spans from -30 to 30 , where the discretization is of 1024 points.

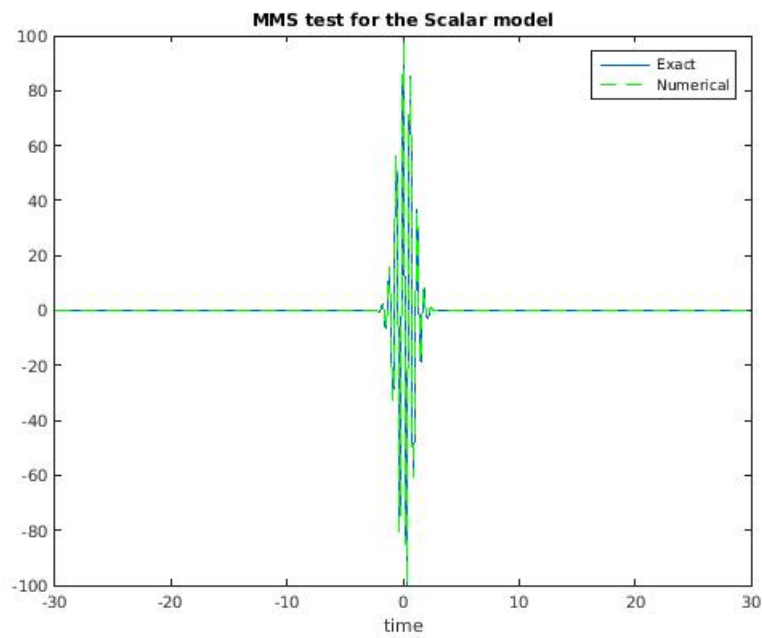


FIGURE 4.3: The figure shows the exact solution in blue, and numerical solution in green in the same plot. The discretization in time is 1024 points, and this is at the point $z = 0.1$. We can see that the solutions perfectly overlap each other.

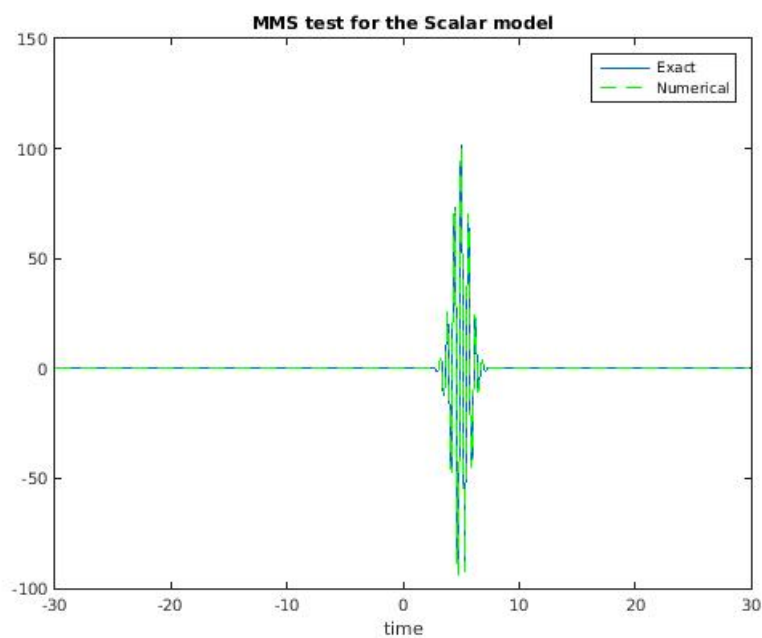


FIGURE 4.4: The figure shows the exact solution in blue, and numerical solution in green in the same plot. The discretization in time is 1024 points, and this is at the point $z = 2.5$. We can see that the solutions perfectly overlap each other.

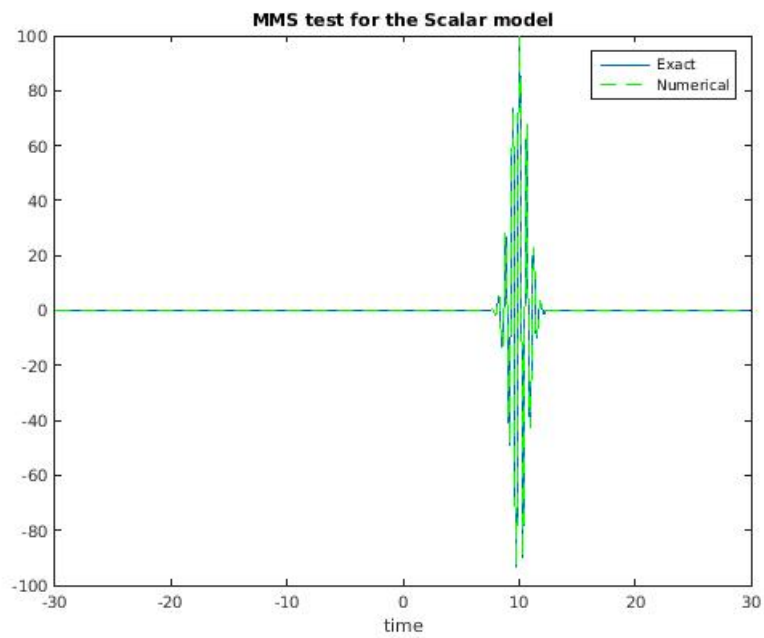


FIGURE 4.5: The figure shows the exact solution in blue, and numerical solution in green in the same plot. The discretization in time is 1024 points, and this is at the point $z = 5.0$. We can see that the solutions perfectly overlap each other.

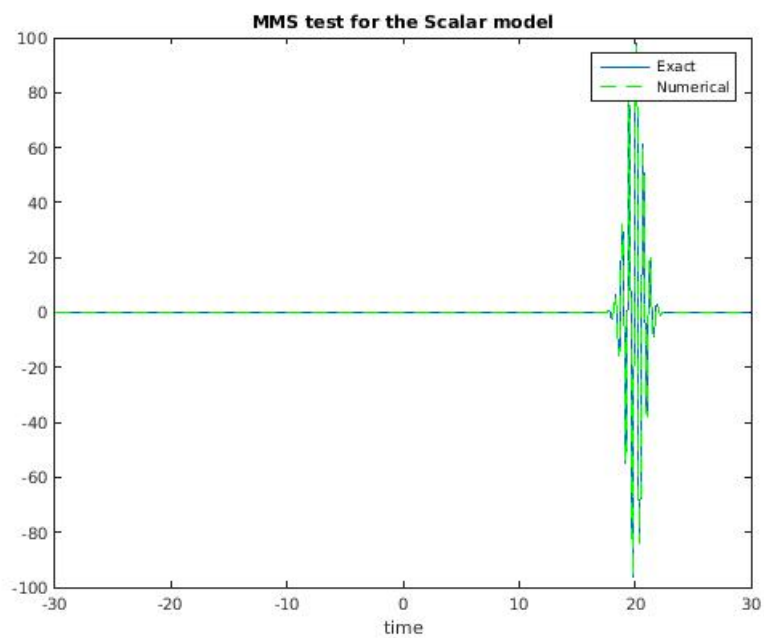


FIGURE 4.6: The figure shows the exact solution in blue, and numerical solution in green in the same plot. The discretization in time is 1024 points, and this is at the point $z = 10$. We can see that the solutions perfectly overlap each other.

The figures 4.3, 4.4, 4.5 and 4.6 shows the exact solution in blue against the numerical solution in green. The figures shows the wave at the points $z = 0.1$,

$z = 2.5$, $z = 5.0$ and $z = 10.0$. As we observe from the figures the numerical solution and the exact solution are on top of each other. This is an indication that the numerical solution does indeed simulate the exact solution.

4.6 Discussion

The final product of this derivation is a highly reduced model for a very specific electrical field composition. The model is small enough to comprehend what to expect from the different parts of the numerical scheme, and at the same time produce a full solution. We have used this to get an introduction to the pseudo spectral method, where the nonlinearity will be calculated in the time domain, and the amplitude $A(\omega, z)$ will be propagated in the spectral domain.

From the test of the UPPE conditions we can observe the periodic boundaries in work. These figures really shows the upper hand such an implementation has over regular FDTD implementations, or non periodic boundary implementations. The total discretization needed is reduced dramatically when the goal is to propagate the pulse over greater distances.

Finding an analytical solution to the UPPE conditions proves difficult. In the contrary, an through an artificial source it is rather trivial to find any solution to the general system. Since the artificial source is an analytical expression it cannot simulate the wave through the time domain several times. This means we cannot measure the total inaccuracy from recycling the time domain.

For the first run through the time domain we are able to measure the total error of the implementation.

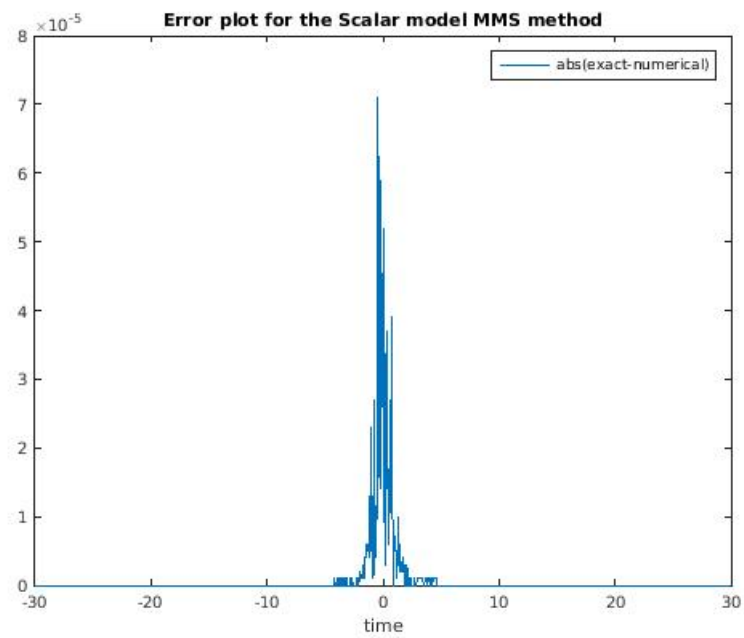


FIGURE 4.7: The absolute value of the difference between the exact solution and the numerical solution at the point $z = 0.1$.

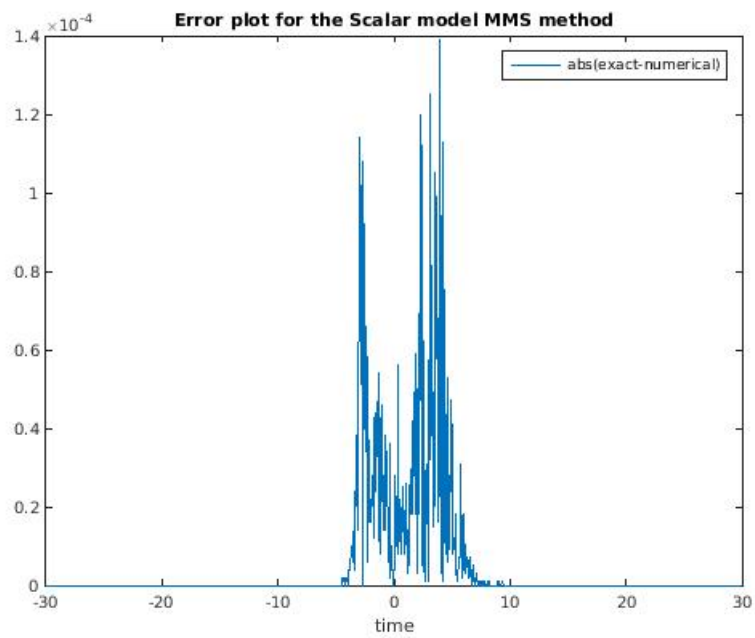


FIGURE 4.8: The absolute value of the difference between the exact solution and the numerical solution at the point $z = 2.5$.

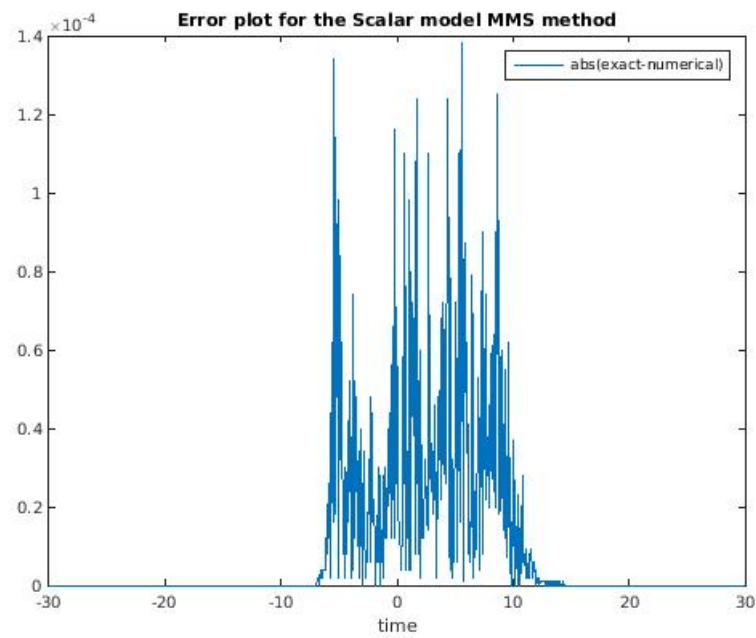


FIGURE 4.9: The absolute value of the difference between the exact solution and the numerical solution at the point $z = 5.0$.

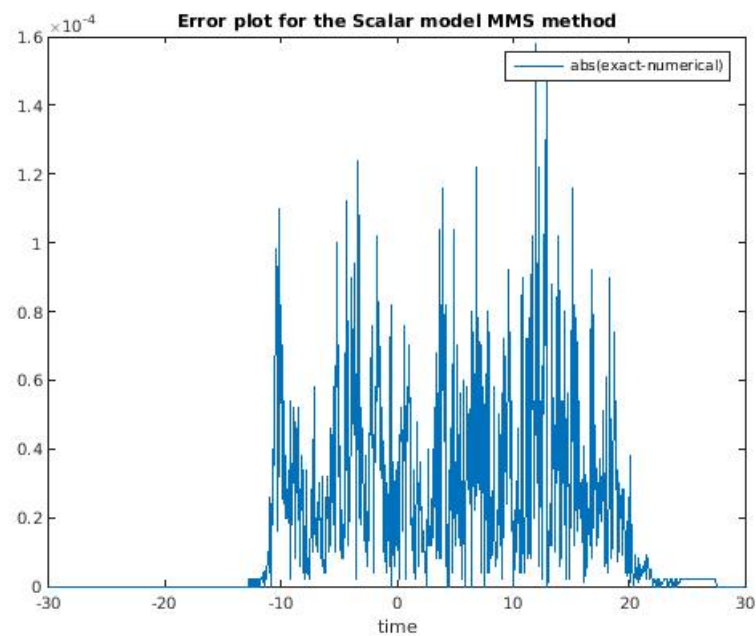


FIGURE 4.10: The absolute value of the difference between the exact solution and the numerical solution at the point $z = 10$.

The following figures (4.7) to (4.10) shows the total error within the system as $err = |exact - numerical|$. The chosen points is $z = 0.1$, $z = 2.5$, $z = 5.0$ and $z = 10.0$. As we can see from the figures, the error grows from 10^{-5} in figure (4.7)

to 10^{-4} in figure (4.10). The total error of the system also spreads along the axis as the pulse propagates.

The main source of error comes from the midpoint rule which has a weak error estimation of $\mathcal{O}(h^2)$. The transform is repetitively used at each point, and the error should thus stack up for each reconstruction of the electrical field. As we observe from the error plots the total error spreads as the wave propagate. The linear speed of the initial condition should be located at $t = 10$ in the last picture, the exact solution at $t = 20$, as can be seen from the exact solution chosen. The total error is however small in comparison to the exact solution, and we have atleast 6 significant digits of accuracy.

It is clear that the numerical verification is not the same as testing the true UPPE conditions model. To run a UPPE conditions model we can highly reduce the run time of the implementation by reducing the amount of frequency we have to work with, this however requires modification of the numerical implementation. The second and maybe most important aspect is the right hand side, in contrary to the UPPE conditions, the verification method runs with a very significant right hand side, and thus gives stronger change in the amplitude $A(\omega, z)$. It is to expect for the verification to give a higher amount of total error than the true UPPE conditions example.

Chapter 5

Vectorial model

5.1 Vector Cylindrical Model

We will now derive a formulation for the Maxwell equations based upon cylindrical coordinates, this derivation is based upon the work done by Per Jakobsen[1]. The base is the macroscopic Maxwell equations

$$\nabla \times \mathbf{E} + \partial_t \mathbf{B} = 0 \quad (5.1)$$

$$\nabla \times \mathbf{B} - \frac{1}{c^2} \partial_t \mathbf{E} = \mu_0 \partial_t \mathbf{P} \quad (5.2)$$

$$\nabla \cdot \mathbf{B} = 0 \quad (5.3)$$

$$\nabla \cdot (\epsilon_0 \mathbf{E} + \mathbf{P}) = 0 \quad (5.4)$$

polarization \mathbf{P} will be expressed as

$$\mathbf{P}(\mathbf{x}, t) = \epsilon_0 \chi(i\partial_t) \mathbf{E}(\mathbf{x}, t) + \mathbf{P}^{NL}(\mathbf{x}, t) \quad (5.5)$$

where the nonlinear polarization is assumed to be some arbitrary function.

The fields will be expressed in terms of cylindrical coordinates

$$\mathbf{E}(x, y, z, t) = E_r(r, \theta, z, t)\mathbf{r} + E_\theta(r, \theta, z, t)\theta + E_z(r, \theta, z, t)\mathbf{z} \quad (5.6)$$

$$\mathbf{B}(x, y, z, t) = B_r(r, \theta, z, t)\mathbf{r} + B_\theta(r, \theta, z, t)\theta + B_z(r, \theta, z, t)\mathbf{z} \quad (5.7)$$

$$\mathbf{P}(x, y, z, t) = P_r(r, \theta, z, t)\mathbf{r} + P_\theta(r, \theta, z, t)\theta + P_z(r, \theta, z, t)\mathbf{z} \quad (5.8)$$

Where we have allowed the components of the fields to vary in space and time. By representing the fields in cylindrical coordinates instead of cartesian coordinates a constraint is set on the model. It is evident that the cylindrical system has a singularity at the point $r = 0$, and any field can not be represented at this point.

We proceed by inserting the fields into the first equation of Maxwell (5.1), and get

$$\frac{1}{r}\partial_\theta E_z - \partial_z E_\theta + \partial_t B_r = 0 \quad (5.9)$$

$$\partial_z E_r - \partial_r E_z + \partial_t B_\theta = 0 \quad (5.10)$$

$$\frac{1}{r}(\partial_r(rE_\theta) - \partial_\theta E_r) + \partial_t B_z = 0 \quad (5.11)$$

For the second Maxwell equation (5.2) we have

$$\frac{1}{r}\partial_\theta B_z - \partial_z B_\theta - \frac{1}{c^2}((1 + \chi(i\partial_t))E_r) = \mu_0\partial_t P_r^{NL} \quad (5.12)$$

$$\partial_z B_r - \partial_r B_z - \frac{1}{c^2}((1 + \chi(i\partial_t))E_r) = \mu_0\partial_t P_\theta^{NL} \quad (5.13)$$

$$\frac{1}{r}(\partial_r(rB_\theta) - \partial_\theta B_r) - \frac{1}{c^2}((1 + \chi(i\partial_t))E_r) = \mu_0\partial_t P_z^{NL} \quad (5.14)$$

The two divergence equations of Maxwell (5.3) and (5.4) gives

$$\frac{1}{r}\partial_r(rB_r) + \frac{1}{r}\partial_\theta B_\theta + \partial_z B_z = 0 \quad (5.15)$$

$$\begin{aligned} \epsilon_0(1 + \chi(i\partial_t))\left(\frac{1}{r}\partial_r(rE_r) + \frac{1}{r}\partial_\theta E_\theta + \partial_z E_z\right) = \\ \frac{1}{r}\partial_r(rP_r^{NL}) + \frac{1}{r}\partial_\theta P_\theta^{NL} + \partial_z P_z^{NL} \end{aligned} \quad (5.16)$$

This is a system of eight equations for six unknowns, and therefore overdetermined. We need six equations to form our dynamical system for the six field components, the chosen equations are

$$\frac{1}{r}\partial_\theta E_z - \partial_z E_\theta + \partial_t B_r = 0 \quad (5.17)$$

$$\partial_z E_r - \partial_r E_z + \partial_t B_\theta = 0 \quad (5.18)$$

$$\frac{1}{r}\partial_\theta B_z - \partial_z B_\theta - \frac{1}{c^2}((1 + \chi(i\partial_t))E_r) = \mu_0\partial_t P_r^{NL} \quad (5.19)$$

$$\partial_z B_r - \partial_r B_z - \frac{1}{c^2}((1 + \chi(i\partial_t))E_r) = \mu_0\partial_t P_\theta^{NL} \quad (5.20)$$

$$\frac{1}{r}\partial_r(rB_r) + \frac{1}{r}\partial_\theta B_\theta + \partial_z B_z = 0 \quad (5.21)$$

$$\begin{aligned} \epsilon_0(1 + \chi(i\partial_t))\left(\frac{1}{r}\partial_r(rE_r) + \frac{1}{r}\partial_\theta E_\theta + \partial_z E_z\right) = \\ \frac{1}{r}\partial_r(rP_r^{NL}) + \frac{1}{r}\partial_\theta P_\theta^{NL} + \partial_z P_z^{NL} \end{aligned} \quad (5.22)$$

The two remaining equations forms a constraint to the solution of the system. We can express them as

$$K_1 \equiv \frac{1}{r}(\partial_r(rE_\theta) - \partial_\theta E_r) + \partial_t B_z = 0 \quad (5.23)$$

$$\begin{aligned} K_2 \equiv \frac{1}{r}(\partial_r(rB_\theta) - \partial_\theta B_r) \\ - \frac{1}{c^2}((1 + \chi(i\partial_t))E_r) - \mu_0\partial_t P_z^{NL} = 0 \end{aligned} \quad (5.24)$$

The constraints (5.23) and (5.24) are preserved when the wave propagates. This can be verified through the z derivative of the constraints them self. Observe that

$$\begin{aligned}
\partial_z K_1 &= \frac{1}{r} (\partial_r (r \partial_z E_\theta) - \partial_{\theta z} E_r) + \partial_{tz} B_z \\
&= \frac{1}{r} (\partial_{r\theta} E_z + \partial_r (r \partial_t B_r) - \partial_{\theta z} E_z \\
&\quad + \partial_{\theta t} B_\theta - \partial_r (r \partial_t B_r) - \partial_{\theta t} B_\theta) = 0
\end{aligned} \tag{5.25}$$

where we use (5.17), (5.18) and (5.21) to manipulate equation (5.23). For the next equation (5.24) we have

$$\begin{aligned}
\partial_z K_2 &= \frac{1}{r} (\partial_r (r \partial_z B_\theta) - \partial_{\theta z} B_r) - \\
&\quad \frac{1}{c^2} ((1 + \chi(i\partial_t)) \partial_z E_r) - \mu_0 \partial_{tz} P_z^{NL} \\
&= -\frac{1}{c^2} \partial_t (1 + \chi(i\partial_t)) (\partial_z E_z + \frac{1}{r} \partial_\theta E_\theta \\
&\quad + \mu_0 (1 + \chi(i\partial_t))^{-1} \left(\frac{1}{r} \partial_r (r P_r^{NL}) + \frac{1}{r} \partial_\theta P_\theta^{NL} + \partial_z P_z^{NL} \right) = 0
\end{aligned} \tag{5.26}$$

where we use the relations (5.19) and (5.20). These two constraints serve the same purpose as the divergence constraints for Maxwells equations as a dynamical system in time. The constraints has to be imposed at one point, and this is usually done at the entrance to the medium.

We will now remove the magnetic field components from the equations. Thus we get a system consisting of electrical field components only. We begin by taking the z derivative of equation (5.17)

$$\partial_{zz} E_\theta = \frac{1}{r} \partial_{z\theta} E_z + \partial_{tz} B_r \tag{5.27}$$

$$\begin{aligned}
&= \frac{1}{r} \partial_{\theta z} E_z - \partial_r \left(\frac{1}{r} \partial_r (r E_\theta) \right) + \partial_r \left(\frac{1}{r} \partial_\theta E_r \right) \\
&\quad + \frac{1}{c^2} \partial_{tt} ((1 + \chi(i\partial_t)) E_\theta) + \mu \partial_{tt} P_\theta^{NL}
\end{aligned} \tag{5.28}$$

where we have used equation (5.20) and (5.23). For the next component we get

$$\partial_{zz}E_r = \partial_{zr}E_z - \partial_{zt}B_\theta \quad (5.29)$$

$$\begin{aligned} &= \partial_{zr}E_z + \frac{1}{r}\partial_\theta \left(\frac{1}{r}(\partial_r(rE_\theta)) \right) - \frac{1}{r}\partial_\theta \left(\frac{1}{r}\partial_\theta E_r \right) \\ &\quad + \frac{1}{c^2}\partial_{tt}((1 + \chi(i\partial_t))E_r) + \mu_0\partial_{tt}P_r^{NL} \end{aligned} \quad (5.30)$$

where we use equation (5.19) and (5.24). Then equations (5.28), (5.30) and (5.22) creates the three equations for the three electrical field components

$$\begin{aligned} \partial_{zz}E_\theta &= \frac{1}{r}\partial_{\theta z}E_z - \partial_r \left(\frac{1}{r}\partial_r(rE_\theta) \right) + \partial_r \left(\frac{1}{r}\partial_\theta E_r \right) \\ &\quad + \frac{1}{c^2}\partial_{tt}((1 + \chi(i\partial_t))E_\theta) + \mu\partial_{tt}P_\theta^{NL} \end{aligned} \quad (5.31)$$

$$\begin{aligned} \partial_{zz}E_r &= \partial_{zr}E_z + \frac{1}{r}\partial_\theta \left(\frac{1}{r}(\partial_r(rE_\theta)) \right) - \frac{1}{r}\partial_\theta \left(\frac{1}{r}\partial_\theta E_r \right) \\ &\quad + \frac{1}{c^2}\partial_{tt}((1 + \chi(i\partial_t))E_r) + \mu_0\partial_{tt}P_r^{NL} \end{aligned} \quad (5.32)$$

$$\begin{aligned} \partial_z E_z &= -\frac{1}{r}\partial_r(rE_r) - \frac{1}{r}\partial_\theta E_\theta \\ &\quad - (\epsilon_0(1 + \chi(i\partial_t)))^{-1} \left(\frac{1}{r}\partial_r(rP_r^{NL}) + \frac{1}{r}\partial_\theta P_\theta^{NL} + \partial_z P_z^{NL} \right) \end{aligned} \quad (5.33)$$

Since the term $\partial_z P_z^{NL}$ contains the z derivative of all the electric field components including E_z , equation(5.33) has to be solved implicitly. The nonlinear polarization can be assumed a small perturbation, and equation (5.33) can be solved by iteration.

From this set of equations (5.31) to (5.33) we will derive the spectral evolution equations. Take note that to solve (5.33) we need the five quantities E_r , E_θ , E_z , $\partial_z E_r$ and $\partial_z E_\theta$. We can find a hidden constraint for these by the collection of equations

$$\partial_r E_z - \partial_t B_\theta - \partial_z E_r = 0 \quad (5.34)$$

$$\frac{1}{r} \partial_\theta E_z + \partial_t B_r - \partial_z E_\theta = 0 \quad (5.35)$$

$$\frac{1}{r} (\partial_r (r E_\theta) - \partial_\theta E_r) + \partial_t B_z = 0 \quad (5.36)$$

$$\begin{aligned} & \frac{1}{r} (\partial_r (r B_\theta) - \partial_\theta B_r) \\ & - \frac{1}{c^2} \partial_t ((1 + \chi(i\partial_t)) E_z) = \mu_0 \partial_t P_z^{NL} \end{aligned} \quad (5.37)$$

The first two equations comes directly from Maxwells equations (5.17) and (5.18). The next two equations are the same constraints we found earlier as K_1 (5.23) and K_2 (5.24). The system now has four constraints for three components, and is overdetermined. These equations can only be true if we either can remove one of them or combine some of them in order to lift the redundancy.

We can remove the magnetic field from the equations, by starting with the time derivative of the equation (5.37) we get

$$\begin{aligned} & \frac{1}{r} (\partial_{rt} (r B_\theta) - \partial_{\theta t} B_r) - \frac{1}{c^2} \partial_t ((1 + \chi(i\partial_t)) E_z) = \mu_0 \partial_{tt} P_z^{NL} \\ & \frac{1}{r} (\partial_r (r (\partial_r E_z - \partial_z E_r))) - \partial_\theta (-\frac{1}{r} \partial_\theta E_z + \partial_z E_\theta) \\ & \quad - \frac{1}{c^2} \partial_t ((1 + \chi(i\partial_t)) E_z) = \mu_0 \partial_{tt} P_z^{NL} \\ & \quad - \frac{1}{c^2} \partial_t ((1 + \chi(i\partial_t)) E_z + \nabla_\perp^2 E_z \\ & \quad - \frac{1}{r} \partial_r (r \partial_z E_r) - \frac{1}{r} \partial_{\theta z} E_\theta = \mu_0 \partial_{tt} P_z^{NL} \end{aligned} \quad (5.38)$$

where we used the equations (5.34) and (5.35) to get to this point. This constraint is preserved when the beam propagates, and only have to be imposed at the entrance of the medium.

We will now look to expand the linear part of the equations (5.31), (5.33) and (5.33) into modes, and use this expansion to get a full solution to the nonlinear problem. The equations without the nonlinearities P_i^{NL} reads

$$\begin{aligned}\partial_{zz}E_\theta &= \frac{1}{r}\partial_{\theta z}E_z - \partial_r\left(\frac{1}{r}\partial_r(rE_\theta)\right) + \partial_r\left(\frac{1}{r}\partial_\theta E_r\right) \\ &\quad + \frac{1}{c^2}\partial_{tt}((1 + \chi(i\partial_t))E_\theta)\end{aligned}\tag{5.39}$$

$$\begin{aligned}\partial_{zz}E_r &= \partial_{zr}E_z + \frac{1}{r}\partial_\theta\left(\frac{1}{r}(\partial_r(rE_\theta))\right) - \frac{1}{r}\partial_\theta\left(\frac{1}{r}\partial_\theta E_r\right) \\ &\quad + \frac{1}{c^2}\partial_{tt}((1 + \chi(i\partial_t))E_r)\end{aligned}\tag{5.40}$$

$$\partial_zE_z = -\frac{1}{r}\partial_r(rE_r) - \frac{1}{r}\partial_\theta E_\theta\tag{5.41}$$

This can be solved by assuming no angular or radial electric field. Thus giving the solution

$$E_r = E_\theta = 0, \quad E_z = \phi(r, \theta, t)$$

that is the trivial solution. Instead we will seek nonzero solutions involving the angular and radial terms. We start by removing the dependency of E_z from the angular and radial parts

$$\begin{aligned}\partial_{zz}E_r &= -\partial_r\left(\frac{1}{r}\partial_r(rE_r)\right) - \frac{1}{r}\partial_\theta\left(\frac{1}{r}\partial_\theta E_r\right) + \frac{1}{c^2}\partial_{tt}((1 + \chi(i\partial_t))E_r) \\ &\quad - \partial_r\left(\frac{1}{r}\partial_\theta E_\theta\right) + \frac{1}{r}\partial_\theta\left(\frac{1}{r}(\partial_r(rE_\theta))\right) \\ \partial_{zz}E_\theta &= -\partial_r\left(\frac{1}{r}\partial_r(rE_\theta)\right) - \frac{1}{r^2}\partial_{\theta\theta}E_\theta + \frac{1}{c^2}\partial_{tt}((1 + \chi(i\partial_t))E_\theta) \\ &\quad - \frac{1}{r^2}\partial_{\theta r}(rE_r) + \partial_r\left(\frac{1}{r}\partial_\theta E_r\right)\end{aligned}$$

These two equations can be further reduced by manipulating the derivatives. We get

$$\begin{aligned}-\partial_r\left(\frac{1}{r}\partial_\theta E_\theta\right) + \frac{1}{r}\partial_\theta\left(\frac{1}{r}(\partial_r(rE_\theta))\right) = \\ \frac{1}{r^2}\partial_\theta E_\theta - \frac{1}{r}\partial_{r\theta}E_\theta + \frac{1}{r^2}\partial_\theta E_\theta + \frac{1}{r}\partial_{\theta r}E_\theta = \frac{2}{r^2}\partial_\theta E_\theta\end{aligned}$$

and similarly

$$-\frac{1}{r^2}\partial_{\theta r}(rE_r) + \partial_r\left(\frac{1}{r}\partial_{\theta}E_r\right) =$$

$$-\frac{1}{r^2}\partial_{\theta}E_r - \frac{1}{r}\partial_{\theta r}E_r - \frac{1}{r^2}\partial_{\theta}E_r + \frac{1}{r}\partial_{\theta r}E_r = -\frac{2}{r^2}\partial_{\theta}E_r$$

The two equations now reads

$$\begin{aligned}\partial_{zz}E_r &= -\partial_r\left(\frac{1}{r}\partial_r(rE_r)\right) - \frac{1}{r}\partial_{\theta}\left(\frac{1}{r}\partial_{\theta}E_r\right) \\ &\quad + \frac{1}{c^2}\partial_{tt}\left((1 + \chi(i\partial_t)E_r)\right) + \frac{2}{r^2}\partial_{\theta}E_{\theta} \\ \partial_{zz}E_{\theta} &= -\partial_r\left(\frac{1}{r}\partial_r(rE_{\theta})\right) - \frac{1}{r^2}\partial_{\theta\theta}E_{\theta} \\ &\quad + \frac{1}{c^2}\partial_{tt}\left((1 + \chi(i\partial_t)E_{\theta})\right) - \frac{2}{r^2}\partial_{\theta}E_r\end{aligned}$$

observe that these equations are similar in terms of derivatives. We introduce the operators according to

$$\begin{aligned}\mathbf{L}f &= -\partial_r\left(\frac{1}{r}(rf)\right) - \frac{1}{r^2}\partial_{\theta\theta}f + \frac{1}{c^2}\partial_{tt}\left((1 + \chi(i\partial_t)f)\right) \\ \mathbf{Q}f &= \frac{2}{r^2}\partial_{\theta}f\end{aligned}$$

This is the point we where want to expand the equation in modes. To do so we have to find the spectral resolution to the operator

$$\mathcal{G} = \begin{pmatrix} L & Q \\ -Q & L \end{pmatrix} \tag{5.42}$$

By introducing the inner product

$$(\phi, \psi) = \int_0^{2\pi} d\theta \int_0^{\theta} dr r \phi(r, \theta) \psi(r, \theta) \quad (5.43)$$

We can observe that the $\mathbf{L}^\dagger = \mathbf{L}$ and $Q^\dagger = -Q$.

If we assume that the space contains two component functions we can introduce the new inner product as

$$[\phi, \psi] = (\phi_1, \psi_1) + (\phi_2, \psi_2) \quad (5.44)$$

Then we observe that

$$\begin{aligned} [\mathcal{G}\phi, \psi] &= \left[\begin{pmatrix} L & Q \\ -Q & L \end{pmatrix} \begin{pmatrix} \phi_1 \\ \phi_2 \end{pmatrix}, \begin{pmatrix} \psi_1 \\ \psi_2 \end{pmatrix} \right] \\ &= \left[\begin{pmatrix} L\phi_1 + Q\phi_2 \\ -Q\phi_1 + L\phi_2 \end{pmatrix}, \begin{pmatrix} \psi_1 \\ \psi_2 \end{pmatrix} \right] \\ &= (L\phi_1 + Q\phi_2, \psi_1) + (L\phi_2 - Q\phi_1, \psi_2) \\ &= (L\phi_1, \psi_1) + (Q\phi_2, \psi_1) + (L\phi_2, \psi_2) - (Q\phi_1, \psi_2) \\ &= (\phi_1, L\psi_1) - (\phi_2, Q\psi_1) + (\psi_2, L\phi_2) + (\phi_1, Q\psi_2) \\ &= (\phi_1, L\psi_1 + Q\psi_2) + (\phi_2, L\psi_2 - Q\psi_1) \\ &= \left[\begin{pmatrix} \phi_1 \\ \phi_2 \end{pmatrix}, \begin{pmatrix} L\psi_1 + Q\psi_2 \\ -Q\psi_1 + L\psi_2 \end{pmatrix} \right] \\ &= \left[\begin{pmatrix} \phi_1 \\ \phi_2 \end{pmatrix}, \begin{pmatrix} L & Q \\ -Q & L \end{pmatrix} \begin{pmatrix} \psi_1 \\ \psi_2 \end{pmatrix} \right] \end{aligned}$$

This proves that the operator \mathcal{G} is in fact self adjoint, which implies that the spectrum is real. The spectral resolution with respect to \mathcal{G} is

$$\begin{aligned} L\phi_1 + Q\phi_2 &= \lambda\phi_1 \\ L\phi_2 - Q\phi_1 &= \lambda\phi_2 \end{aligned} \quad (5.45)$$

We introduce the Fourier transform for time, and Fourier series for the angular part

$$\phi_j(r, \theta, t) = \frac{1}{r\pi^2} \sum_{m=-\infty}^{\infty} \int_{-\infty}^{\infty} d\omega \hat{\phi}_j(r, \omega, m) e^{i(m\theta - \omega t)} \quad j = 1, 2 \quad (5.46)$$

the operator L in the spectral domain is

$$L\phi_j(r, \theta, t) = \frac{1}{r\pi^2} \sum_{m=-\infty}^{\infty} \int_{-\infty}^{\infty} d\omega L_{\omega, m} \hat{\phi}_j(r, \omega, m) e^{i(m\theta - \omega t)} \quad j = 1, 2 \quad (5.47)$$

which gives the spectral form as

$$L_{\omega, m} f = -\partial_r \left(\frac{1}{r} (r f) \right) + \frac{m^2}{r^2} f - \left(\frac{\omega}{c} \right)^2 n^2(\omega) f \quad (5.48)$$

where we have introduced the refractive index as

$$n^2(\omega) = 1 + \chi(\omega)$$

In the spectral domain the system (5.45) is

$$L_{\omega, m} \hat{\phi}_1 + \frac{2im}{r^2} \hat{\phi}_2 = \lambda \hat{\phi}_1 \quad (5.49)$$

$$L_{\omega, m} \hat{\phi}_2 - \frac{2im}{r^2} \hat{\phi}_1 = \lambda \hat{\phi}_2 \quad (5.50)$$

for equation (5.49) we get

$$\begin{aligned}\partial_r\left(\frac{1}{r}\partial_r(r\widehat{\phi}_1)\right) + \frac{m^2}{r^2}\widehat{\phi}_1 - \left(\frac{\omega}{c}\right)^2 n^2(\omega)\widehat{\phi}_1 + \frac{2im}{r^2}\widehat{\phi}_2 &= \lambda\widehat{\phi}_1 \\ \partial_{rr}\widehat{\phi}_1 + \frac{1}{r}\partial_r\widehat{\phi}_1 + \xi^2\widehat{\phi}_1 - \frac{m^2+1}{r^2}\widehat{\phi}_1 - 2im\widehat{\phi}_2 &= 0 \\ r^2\partial_{rr}\widehat{\phi}_1 + r\partial_r\widehat{\phi}_1 + (r^2\xi^2 - (1+m^2))\widehat{\phi}_1 - 2im\widehat{\phi}_2 &= 0\end{aligned}$$

We can do a similar thing with (5.50)

$$\begin{aligned}-\partial_r\left(\frac{1}{r}\partial_r(r\widehat{\phi}_2)\right) + \frac{m^2}{r^2}\widehat{\phi}_2 - \left(\frac{\omega}{c}\right)^2 n^2(\omega)\widehat{\phi}_2 - \frac{2im}{r^2}\widehat{\phi}_1 &= \widehat{\phi}_1 \\ \partial_{rr}\widehat{\phi}_2 + \frac{1}{r}\partial_r\widehat{\phi}_2 + \xi^2\widehat{\phi}_2 - \frac{m^2+1}{r^2}\widehat{\phi}_2 + \frac{2im}{r^2}\widehat{\phi}_1 &= 0 \\ r^2\partial_{rr}\widehat{\phi}_2 + r\partial_r\widehat{\phi}_2 + (r^2\xi^2 - (1+m^2))\widehat{\phi}_2 + 2im\widehat{\phi}_1 &= 0\end{aligned}$$

where we have introduced the new quantity $\xi = \sqrt{\left(\frac{\omega}{c}\right)^2 n^2(\omega) + \lambda}$. This parameter can be either real positive or imaginary depending on λ , depending on whether λ is bigger or smaller than $-\left(\frac{\omega}{c}\right)^2 n^2(\omega)$. This leaves us with the following equations for the eigenvalues

$$\begin{aligned}r^2\partial_{rr}\widehat{\phi}_1 + r\partial_r\widehat{\phi}_1 + (r^2\xi^2 - (1+m^2))\widehat{\phi}_1 - 2im\widehat{\phi}_2 &= 0 \\ r^2\partial_{rr}\widehat{\phi}_2 + r\partial_r\widehat{\phi}_2 + (r^2\xi^2 - (1+m^2))\widehat{\phi}_2 + 2im\widehat{\phi}_1 &= 0\end{aligned}\tag{5.51}$$

If we add the term $2m\widehat{\phi}_j$ to the equations (5.51) we get

$$\begin{aligned}r^2\partial_{rr}\widehat{\phi}_1 + r\partial_r\widehat{\phi}_1 + (r^2\xi^2 - (1+m^2))\widehat{\phi}_1 + 2m\widehat{\phi}_1 - 2im\widehat{\phi}_2 &= 0 \\ r^2\partial_{rr}\widehat{\phi}_2 + r\partial_r\widehat{\phi}_2 + (r^2\xi^2 - (1+m^2))\widehat{\phi}_2 + 2m\widehat{\phi}_2 + 2im\widehat{\phi}_1 &= 0\end{aligned}$$

This system has the solution on the form of Bessel functions

$$\begin{aligned}\widehat{\phi}_1 &= iJ_{m+1}(\xi r) \\ \widehat{\phi}_2 &= J_{m+1}(\xi r)\end{aligned}$$

This can only be done for ξ real. For a pure imaginary ξ we will get the modified Bessel functions, these have exponential growth and cannot be used to model real physical fields. We get the following constraint on the spectrum

$$\lambda > - \left(\frac{\omega}{c}\right)^2 n^2(\omega)$$

We now have a positive ξ , and the eigenvalues of the equations have the range $(-\left(\frac{\omega}{c}\right)^2 n^2(\omega), \infty)$.

by subtracting the same term $2m\widehat{\phi}_j$ from the equations (5.51)

$$\begin{aligned}r^2\partial_{rr}\widehat{\phi}_1 + r\partial_r\widehat{\phi}_1 + (r^2\xi^2 - (1 + m^2))\widehat{\phi}_1 - 2m\widehat{\phi}_1 - 2im\widehat{\phi}_2 &= 0 \\ r^2\partial_{rr}\widehat{\phi}_2 + r\partial_r\widehat{\phi}_2 + (r^2\xi^2 - (1 + m^2))\widehat{\phi}_2 - 2m\widehat{\phi}_2 + 2im\widehat{\phi}_1 &= 0\end{aligned}$$

We will in a similar fashion we find the two new solutions to the system

$$\begin{aligned}\widehat{\phi}_1 &= J_{m-1}(\xi r) \\ \widehat{\phi}_2 &= iJ_{m-1}(\xi r)\end{aligned}$$

Together these will form the solutions to the system

$$\begin{pmatrix} iJ_{m+1}(\xi r) \\ J_{m+1}(\xi r) \end{pmatrix}, \begin{pmatrix} J_{m-1}(\xi r) \\ J_{m-1}(\xi r) \end{pmatrix}$$

that spans the eigenspace for λ . These will be used to expand the angular and radial part of the field in terms of modes for the linearised system.

$$\partial_{zz} \begin{pmatrix} E_r \\ E_\theta \end{pmatrix} = \mathcal{G} \begin{pmatrix} E_r \\ E_\theta \end{pmatrix} \quad (5.52)$$

Thus the modes of the expansion will take the form

$$A(z, \xi, \omega, m) \begin{pmatrix} iJ_{m+1}(\xi r) \\ J_{m+1} \end{pmatrix} e^{im\theta - i\omega t} \quad (5.53)$$

$$B(z, \xi, \omega, m) \begin{pmatrix} J_{m-1}(\xi r) \\ J_{m-1} \end{pmatrix} e^{im\theta - i\omega t} \quad (5.54)$$

By inserting the modes A and B into the linearised system we observe that they must satisfy

$$\partial_{zz} A = \lambda A$$

$$\partial_{zz} B = \lambda B$$

We found the quantity ξ to be a real positive variable. From the relation

$$\xi^2 = \left(\frac{\omega}{c}\right)^2 n^2(\omega) + \lambda$$

the eigenspace can be labelled $\xi \in (0, \infty)$. By defining

$$\lambda = -\beta^2$$

we get the set of equations as

$$\begin{aligned}\partial_{zz}A &= -\beta^2A \\ \partial_{zzz}B &= -\beta^2B\end{aligned}$$

where β is defined as the propagation constant

$$\beta = \sqrt{\left(\frac{\omega}{c}\right)^2 n^2(\omega) - \xi^2}$$

From these equations we will find the four modes

$$\begin{pmatrix} iJ_{m+1}(\xi r) \\ J_{m+1}(\xi r) \end{pmatrix} e^{i(\pm\beta z + m\theta - \omega t)} \quad (5.55)$$

$$\begin{pmatrix} J_{m-1}(\xi r) \\ iJ_{m-1}(\xi r) \end{pmatrix} e^{i(\pm\beta z + m\theta - \omega t)} \quad (5.56)$$

For positive frequencies we observe that the plus sign is modes travelling to the right, while negative sign is modes travelling to the left. From equation (5.41)

$$\partial_z E_z = -\frac{1}{r} \partial_r (r E_r) - \frac{1}{r} \partial_\theta E_\theta \quad (5.57)$$

To solve this equation we insert the modes found for the two other components. The derivatives of the Bessel functions can be expressed as

$$J'_{m+1}(x) = J_m(x) - \frac{m+1}{x} J_{m+1}(x)$$

and by using this to find the derivatives in (5.57) we get

$$\begin{aligned}
& -\frac{1}{r}\partial_r(riJ_{m+1}(\xi r)) - \frac{im}{r}J_{m+1}(\xi r) = \\
& -\frac{i}{r}J_{m+1}(\xi r) - i\xi(J_m(\xi r) - \frac{m+1}{\xi r}J_{m+1}(\xi r)) = \\
& -i\xi J_m(\xi r)
\end{aligned}$$

By inserting the first two modes from (5.55) into equation (5.57) we can reduce it to

$$\begin{aligned}
\partial_z E_z &= -\left(\frac{1}{r}\partial_r(riJ_{m+1}(\xi r)) - \frac{im}{r}J_{m+1}(\xi r)\right)e^{i(\pm\beta z+m\theta-\omega t)} \\
&= -i\xi J_m(\xi r)e^{i(\pm\beta z+m\theta-\omega t)} \\
E_z &= \mp\frac{\xi}{\beta}J_m(\xi r)e^{i(\pm\beta z+m\theta-\omega t)}
\end{aligned}$$

The modes for the expanding the linearised system is then

$$\begin{pmatrix} i\beta J_{m+1}(\xi r) \\ \beta J_{m+1}(\xi r) \\ \mp\xi\beta J_m(\xi r) \end{pmatrix} e^{i(\pm\beta z+m\theta-\omega t)} \quad (5.58)$$

A similar thing can be done for the J_{m-1} Bessel functions

$$J'_{m-1}(x) = \frac{m-1}{x}J_m(x) - J_m(x)$$

where we get

$$\begin{aligned}
& -\frac{1}{r}\partial_r(riJ_{m-1}(\xi r)) - \frac{im}{r}J_{m-1}(\xi r) = \\
& \frac{m-1}{r}J_{m-1}(\xi r) + \xi(J_m(\xi r) + \frac{m-1}{\xi r}J_{m+1}(\xi r)) = \\
& \xi J_m(\xi r)
\end{aligned}$$

Inserting the mode (5.56) into equation (5.57) we get

$$\begin{aligned}
\partial_z E_z &= -\left(\frac{1}{r}\partial_r(riJ_{m-1}(\xi r)) - \frac{im}{r}J_{m-1}(\xi r)\right)e^{i(\pm\beta z+m\theta-\omega t)} \\
&= \xi J_m(\xi r)e^{i(\pm\beta z+m\theta-\omega t)} \\
E_z &= \mp \frac{i\xi}{\beta}J_m(\xi r)e^{i(\pm\beta z+m\theta-\omega t)}
\end{aligned}$$

From this we get the two new modes as

$$\begin{pmatrix} \beta J_{m-1}(\xi r) \\ i\beta J_{m-1}(\xi r) \\ \mp \xi \beta J_m(\xi r) \end{pmatrix} e^{i(\pm\beta z+m\theta-\omega t)} \quad (5.59)$$

The full solution of the linearised system (5.39) can be expressed as a superposition of the modes

$$\begin{aligned}
\begin{pmatrix} E_r \\ E_\theta \\ E_z \end{pmatrix} (z, r, \theta, t) &= \frac{1}{2\pi} \sum_s \sum_m \int_{-\infty}^{\infty} d\omega \int_{-\infty}^{\infty} d\lambda \{ A_s \begin{pmatrix} i\beta J_{m+1}(\xi r) \\ \beta J_{m+1}(\xi r) \\ -s\xi J_m(\xi r) \end{pmatrix} e^{si\beta z} \\
&+ B_s \begin{pmatrix} \beta J_{m-1}(\xi r) \\ i\beta J_{m-1}(\xi r) \\ -si\xi J_m(\xi r) \end{pmatrix} e^{si\beta z} \} e^{-im\theta-i\omega t} + \begin{pmatrix} 0 \\ 0 \\ 1 \end{pmatrix} q(r, \theta, t) \quad (5.60)
\end{aligned}$$

where s can be either positive or negative. Setting $\xi = -\left(\frac{\omega}{c}\right)^2 n^2(\omega)$ we get

$$2\xi^2 = \lambda \Rightarrow 2\xi d\xi = d\lambda \quad (5.61)$$

We can absorb the factor two into the spectral amplitudes. If we apply the Hankel transform on the last term we get the expansion (5.60) on the form

$$\begin{aligned} \begin{pmatrix} E_r \\ E_\theta \\ E_z \end{pmatrix} (z, r, \theta, t) &= \frac{1}{2\pi} \sum_s \sum_m \int_{-\infty}^{\infty} d\omega \int_0^{\infty} d\xi \xi \{ A_s \begin{pmatrix} i\beta J_{m+1}(\xi r) \\ \beta J_{m+1}(\xi r) \\ -s\xi J_m(\xi r) \end{pmatrix} e^{si\beta z} \\ &+ B_s \begin{pmatrix} \beta J_{m-1}(\xi r) \\ i\beta J_{m-1}(\xi r) \\ -si\xi J_m(\xi r) \end{pmatrix} e^{si\beta z} + \frac{1}{2} Q \begin{pmatrix} 0 \\ 0 \\ J_m(\xi r) \end{pmatrix} \} e^{-im\theta - i\omega t} \quad (5.62) \end{aligned}$$

The reality of the fields is ensured by imposing the following conditions on the spectral amplitudes

$$A_+(\xi, \omega, m) = (-1)^{m+1} i B_-^*(\xi, -\omega, -m) \quad (5.63)$$

$$B_+(\xi, \omega, m) = (-1)^{m-1} i A_-^*(\xi, -\omega, -m) \quad (5.64)$$

$$Q(\xi, -\omega, -m) = (-1)^m Q^*(\xi, \omega, m) \quad (5.65)$$

where denotes (*) the complex conjugate. These amplitudes will now pose a solution to the full set of equations, where the amplitudes have a z dependence.

Let us take a closer look at the point where s is negative

$$\begin{aligned}
& \frac{1}{2\pi} \sum_m \int_{-\infty}^{\infty} d\omega \int_0^{\infty} d\xi \xi \left\{ A_- \begin{pmatrix} i\beta J_{m+1}(\xi r) \\ \beta J_{m+1}(\xi r) \\ \xi J_m(\xi r) \end{pmatrix} e^{-i\beta z} \right. \\
& \quad \left. + B_- \begin{pmatrix} \beta J_{m-1}(\xi r) \\ i\beta J_{m-1}(\xi r) \\ i\xi J_m(\xi r) \end{pmatrix} e^{-i\beta z} + \frac{1}{2} Q \begin{pmatrix} 0 \\ 0 \\ J_m(\xi r) \end{pmatrix} \right\} e^{-im\theta - i\omega t} \\
& \left(\frac{1}{2\pi} \sum_m \int_{-\infty}^{\infty} d\omega \int_0^{\infty} d\xi \xi \left\{ A_-^* \begin{pmatrix} -i\beta J_{m+1}(\xi r) \\ \beta J_{m+1}(\xi r) \\ \xi J_m(\xi r) \end{pmatrix} e^{i\beta z} \right. \right. \\
& \quad \left. \left. + B_-^* \begin{pmatrix} \beta J_{m-1}(\xi r) \\ -i\beta J_{m-1}(\xi r) \\ -i\xi J_m(\xi r) \end{pmatrix} e^{i\beta z} + \frac{1}{2} Q^* \begin{pmatrix} 0 \\ 0 \\ J_m(\xi r) \end{pmatrix} \right\} e^{im\theta + i\omega t} \right)^*
\end{aligned}$$

Introducing the new variables $m = -m'$ and $\omega = -\omega'$ we will have the conjugated modes in reversed m and ω as suggested in (5.65). The expression itself will be

$$\begin{aligned}
& \left(\frac{1}{2\pi} \sum_{-m'} \int_{-\infty}^{\infty} d\omega' \int_0^{\infty} d\xi \xi \left\{ A_-^* \begin{pmatrix} -i\beta J_{-m'+1}(\xi r) \\ \beta J_{-m'+1}(\xi r) \\ \xi J_{-m'}(\xi r) \end{pmatrix} e^{i\beta z} \right. \right. \\
& \quad \left. \left. + B_-^* \begin{pmatrix} \beta J_{-m'-1}(\xi r) \\ -i\beta J_{-m'-1}(\xi r) \\ -i\xi J_{-m'}(\xi r) \end{pmatrix} e^{i\beta z} + \frac{1}{2} Q^* \begin{pmatrix} 0 \\ 0 \\ J_{-m'}(\xi r) \end{pmatrix} \right\} e^{-im'\theta - i\omega' t} \right)^*
\end{aligned}$$

where the Bessel functions has the following identity for negative n.

$$J_{-n}(x) = (-1)^n J_n(x)$$

Using this relation in the integral gives

$$\begin{aligned}
& \left(\frac{1}{2\pi} \sum_{-m'=-\infty}^{\infty} \int d\omega' \int_0^{\infty} d\xi \xi \{ A_-^* \right. \\
& \quad \begin{pmatrix} -(-1)^{m'-1} i \beta J_{m'-1}(\xi r) \\ (-1)^{m'-1} \beta J_{m'-1}(\xi r) \\ (-1)^{m'} \xi J_{m'}(\xi r) \end{pmatrix} e^{i\beta z} \\
& \quad + B_-^* \begin{pmatrix} (-1)^{m'+1} \beta J_{m'+1}(\xi r) \\ -(-1)^{m'+1} i \beta J_{m'+1}(\xi r) \\ -(-1)^{m'} i \xi J_{m'}(\xi r) \end{pmatrix} e^{i\beta z} \\
& \quad \left. + \frac{1}{2} Q^* \begin{pmatrix} 0 \\ 0 \\ (-1)^{m'} J_{m'}(\xi r) \end{pmatrix} \right\} e^{-im'\theta - i\omega t} \Big)^*
\end{aligned}$$

Since m is just a dummy index we can reverse the sum back again, this gives us

$$\begin{aligned}
& \left(\frac{1}{2\pi} \sum_m \int_{-\infty}^{\infty} d\omega \int_0^{\infty} d\xi \xi \{ A_-^* \right. \\
& \quad \begin{pmatrix} -(-1)^{m-1} i \beta J_{m-1}(\xi r) \\ (-1)^{m-1} \beta J_{m-1}(\xi r) \\ (-1)^m \xi J_m(\xi r) \end{pmatrix} e^{i\beta z} \\
& \quad + B_-^* \begin{pmatrix} (-1)^{m+1} \beta J_{m+1}(\xi r) \\ -(-1)^{m+1} i \beta J_{m+1}(\xi r) \\ -(-1)^m i \xi J_m(\xi r) \end{pmatrix} e^{i\beta z} \\
& \quad \left. + \frac{1}{2} Q^* \begin{pmatrix} 0 \\ 0 \\ (-1)^m J_m(\xi r) \end{pmatrix} \right\} e^{-im\theta - i\omega t} \Big)^* \tag{5.66}
\end{aligned}$$

Comparing (5.66) with the original transform (5.62) we can see that through the reality conditions suggested in (5.65), we only have to consider the positive modes in order to recreate the electrical field components.

We see that we have four half range spectral amplitudes in A_+ , B_+ , A_- , B_- , and one half range frequency in Q . Thus we have five half range frequencies determining the three field components. The system is therefore redundant. To lift the redundancy we introduce the following constraints[15]

$$\begin{aligned}\partial_z A_+ e^{i\beta z} + \partial_z A_- e^{-i\beta z} &= 0 \\ \partial_z B_+ e^{i\beta z} + \partial_z B_- e^{-i\beta z} &= 0\end{aligned}\quad (5.67)$$

This constraint will in no way restrict the space of solutions to (5.31), (5.32) and (5.33). The modal expansion can be written as

$$\begin{aligned}\begin{pmatrix} E_r \\ E_\theta \end{pmatrix} &= \frac{1}{2\pi} \sum_s \sum_m \int_{-\infty}^{\infty} d\omega \int_0^{\infty} d\xi \xi \left\{ A_s \begin{pmatrix} i\beta J_{m+1}(\xi r) \\ \beta J_{m+1}(\xi r) \end{pmatrix} e^{si\beta z} \right. \\ &\quad \left. + B_s \begin{pmatrix} \beta J_{m-1}(\xi r) \\ i\beta J_{m-1}(\xi r) \end{pmatrix} e^{si\beta z} \right\} e^{i(-m\theta\omega t)}\end{aligned}\quad (5.68)$$

$$\begin{aligned}E_z &= \frac{1}{2\pi} \sum_s \sum_m \int_{-\infty}^{\infty} d\omega \int_0^{\infty} d\xi \xi \left\{ \right. \\ &\quad \left. - s A_s \xi J_m(\xi r) e^{si\beta z} - s \beta i \xi J_m(\xi r) e^{si\beta z} \right. \\ &\quad \left. + \frac{1}{2} Q J_m(\xi r) \right\} e^{-i(m\theta + \omega t)}\end{aligned}\quad (5.69)$$

This will now be used to find a solution to the system (5.31) as the following

$$\partial_{zz} \begin{pmatrix} E_r \\ E_\theta \end{pmatrix} = \mathcal{G} \begin{pmatrix} E_r \\ E_\theta \end{pmatrix} + \begin{pmatrix} N_1 \\ N_2 \end{pmatrix}\quad (5.70)$$

$$\partial_z E_z = \mathcal{R} \begin{pmatrix} E_r \\ E_\theta \end{pmatrix} + N_3\quad (5.71)$$

where the new operator

$$\mathcal{R}f = \left(-\frac{1}{r} \partial_r (rf), -\frac{1}{r} \partial_\theta f \right)\quad (5.72)$$

and the nonlinearities are

$$\begin{aligned}
N_1 &= \mu_0 \partial_{tt} P_r^{NL} \\
N_2 &= \mu_0 \partial_{tt} P_\theta^{NL} \\
N_3 &= -\frac{(1+L)^{-1}}{\epsilon_0} \left(\frac{1}{r} \partial_r (r P_r^{NL}) + \frac{1}{r} \partial_\theta P_\theta^{NL} + \partial_z P_z^{NL} \right)
\end{aligned}$$

To solve these equations we take the z derivative of the angular and radial part of (5.68) to get

$$\begin{aligned}
\partial_z \begin{pmatrix} E_r \\ E_\theta \end{pmatrix} &= \frac{1}{2\pi} \sum_s \sum_m \int_{-\infty}^{\infty} d\omega \int_0^{\infty} d\xi \xi \left\{ A_s \begin{pmatrix} i\beta J_{m+1}(\xi r) \\ \beta J_{m+1}(\xi r) \end{pmatrix} e^{si\beta z} \right. \\
&\quad \left. + B_s \begin{pmatrix} \beta J_{m-1}(\xi r) \\ i\beta J_{m-1}(\xi r) \end{pmatrix} e^{si\beta z} \right\} e^{i(-m\theta - \omega t)}
\end{aligned}$$

where we have used the constraint (5.67). We can then take the double z derivative of (5.68) and get

$$\begin{aligned}
\partial_{zz} \begin{pmatrix} E_r \\ E_\theta \end{pmatrix} &= \frac{1}{2\pi} \sum_s \sum_m \int_{-\infty}^{\infty} d\omega \int_0^{\infty} d\xi \xi \left\{ -\beta^2 A_s \begin{pmatrix} i\beta J_{m+1}(\xi r) \\ \beta J_{m+1}(\xi r) \end{pmatrix} e^{si\beta z} \right. \\
&\quad \left. + -\beta^2 B_s \begin{pmatrix} \beta J_{m-1}(\xi r) \\ i\beta J_{m-1}(\xi r) \end{pmatrix} e^{si\beta z} + si\beta \partial_z A_s \begin{pmatrix} i\beta J_{m+1}(\xi r) \\ \beta J_{m+1}(\xi r) \end{pmatrix} e^{si\beta z} \right. \\
&\quad \left. + si\beta \partial_z B_s \begin{pmatrix} \beta J_{m-1}(\xi r) \\ i\beta J_{m-1}(\xi r) \end{pmatrix} e^{si\beta z} \right\} e^{i(-m\theta - \omega t)}
\end{aligned}$$

From the equation (5.71) we get

$$\begin{aligned} \mathcal{L} \begin{pmatrix} E_r \\ E_\theta \end{pmatrix} &= \frac{1}{2\pi} \sum_s \sum_m \int_{-\infty}^{\infty} d\omega \int_0^{\infty} d\xi \xi \left\{ -\beta^2 A_s \begin{pmatrix} i\beta J_{m+1}(\xi r) \\ \beta J_{m+1}(\xi r) \end{pmatrix} e^{si\beta z} \right. \\ &\quad \left. + -\beta^2 B_s \begin{pmatrix} \beta J_{m-1}(\xi r) \\ i\beta J_{m-1}(\xi r) \end{pmatrix} e^{si\beta z} \right\} e^{i(-m\theta - \omega t)} \end{aligned} \quad (5.73)$$

By inserting this into the equations (5.71) we end up with the two equations

$$\begin{aligned} &\frac{1}{2\pi} \sum_m \int_{-\infty}^{\infty} d\omega \int_0^{\infty} d\xi \xi \left\{ -2\beta \partial_z A_+ \begin{pmatrix} i\beta J_{m+1}(\xi r) \\ \beta J_{m+1}(\xi r) \end{pmatrix} e^{i\beta z} \right. \\ &\quad \left. - 2i\beta \partial_z B_+ \begin{pmatrix} \beta J_{m-1}(\xi r) \\ i\beta J_{m-1}(\xi r) \end{pmatrix} e^{i\beta z} + \partial_z Q J_m(\xi r) \right\} e^{-i(m\theta + \omega t)} = \\ &\frac{1}{2\pi} \sum_m \int_{-\infty}^{\infty} d\omega \int_0^{\infty} d\xi \xi \left\{ M_1 \begin{pmatrix} i\beta J_{m+1}(\xi r) \\ \beta J_{m+1}(\xi r) \end{pmatrix} + M_2 \begin{pmatrix} \beta J_{m-1}(\xi r) \\ i\beta J_{m-1}(\xi r) \end{pmatrix} \right\} e^{-i(m\theta + \omega t)} \end{aligned} \quad (5.74)$$

By comparing both sides we see that the equations can be split into two differential equations for the two amplitudes A_+ and B_+ as

$$2i\beta \partial_z A_+ e^{i\beta z} = M_1 \quad (5.75)$$

$$2i\beta \partial_z B_+ e^{i\beta z} = M_2 \quad (5.76)$$

where the terms M_1 and M_2 can be found in terms of the nonlinearities N_1 and N_2 . By taking the Fourier transform in time and Fourier series in angular direction we get

$$\begin{pmatrix} \widehat{N}_1 \\ \widehat{N}_2 \end{pmatrix} = \int_0^{\infty} d\xi \xi \left\{ M_1 \begin{pmatrix} i\beta J_{m+1}(\xi r) \\ \beta J_{m+1}(\xi r) \end{pmatrix} + M_2 \begin{pmatrix} \beta J_{m-1}(\xi r) \\ i\beta J_{m-1}(\xi r) \end{pmatrix} \right\} \quad (5.77)$$

We can list these in component form

$$\begin{aligned}
i\beta \int_0^{\infty} d\xi \xi M_1 J_{m+1}(\xi r) + \beta \int_0^{\infty} d\xi \xi M_2 J_{m-1}(\xi r) &= \widehat{N}_1 \\
\beta \int_0^{\infty} d\xi \xi M_1 J_{m+1}(\xi r) + i\beta \int_0^{\infty} d\xi \xi M_2 J_{m-1}(\xi r) &= \widehat{N}_1
\end{aligned}$$

Then solving the system with respect to the quantities M_1 and M_2 will give

$$\int_0^{\infty} d\xi \xi M_1 J_{m+1}(\xi r) = \frac{1}{2i\beta} (\widehat{N}_1 + i\widehat{N}_2) \quad (5.78)$$

$$\int_0^{\infty} d\xi \xi M_2 J_{m-1}(\xi r) = \frac{1}{2i\beta} (i\widehat{N}_1 + \widehat{N}_2) \quad (5.79)$$

and by using the inverse Hankel transform we will obtain the quantities M_1 and M_2 as

$$M_1 = \frac{1}{2i\beta} \int_0^{\infty} dr r (\widehat{N}_1 + i\widehat{N}_2) J_{m+1}(\xi r) \quad (5.80)$$

$$M_2 = \frac{1}{2i\beta} \int_0^{\infty} dr r (i\widehat{N}_1 + \widehat{N}_2) J_{m-1}(\xi r) \quad (5.81)$$

If we take the z derivative of the z component in (5.71) we get

$$\begin{aligned}
\partial_z E_z &= \frac{1}{2\pi} \sum_s \sum_m \int_{-\infty}^{\infty} d\omega \int_0^{\infty} d\xi \xi \{ -i\beta \xi A_s J_m(\xi r) e^{si\beta z} \\
&\quad + \beta \xi B_s J_m(\xi r) e^{si\beta z} - s\xi \partial_z A_s J_m(\xi r) e^{si\beta z} - si\xi \partial_z B_s J_m(\xi r) e^{si\beta z} \\
&\quad + \frac{1}{2} \partial_z Q J_m(\xi r) \} e^{-i(m\theta + \omega t)} \quad (5.82)
\end{aligned}$$

From the construction of the modes we have

$$\begin{aligned} \mathcal{R} \begin{pmatrix} E_r \\ E_\theta \end{pmatrix} &= \frac{1}{2\pi} \sum_s \sum_m \int_{-\infty}^{\infty} d\omega \int_0^{\infty} d\xi \xi \{ -i\beta\xi A_s J_m(\xi r) e^{i\beta z} \\ &\quad + \beta\xi B_s J_m(\xi r) e^{i\beta z} \} e^{-i(m\theta + \omega t)} \end{aligned} \quad (5.83)$$

We now insert the z derivative (5.82) and the relation (5.82) into the z component of (5.71), and use the constraint (5.67) to get

$$\begin{aligned} \frac{1}{2\pi} \sum_m \int_{-\infty}^{\infty} d\omega \int_0^{\infty} d\xi \xi \{ -2\xi \partial_z A_+ J_m(\xi r) e^{i\beta z} - 2i\xi \partial_z B_+ J_m(\xi r) e^{i\beta z} \\ + \partial_z Q J_m(\xi r) \} e^{-i(m\theta + \omega t)} &= \frac{1}{2\pi} \sum_m \int_{-\infty}^{\infty} d\omega \int_0^{\infty} d\xi \xi \{ M_3 J_m(\xi r) \} e^{-i(m\theta + \omega t)} \end{aligned} \quad (5.84)$$

We use the Hankel transform and the spectral evolution equations (5.75) and (5.76) to get the equation

$$\partial_z Q = M_3 + \frac{\xi}{i\beta} M_1 + \frac{\xi}{\beta} M_2$$

The spectral evolution equations then sums up to the three equations

$$2i\beta \partial_z A_+ e^{i\beta z} = M_1 \quad (5.85)$$

$$2i\beta \partial_z B_+ e^{i\beta z} = M_2 \quad (5.86)$$

$$\partial_z Q = M_3 + \frac{\xi}{i\beta} M_1 + \frac{\xi}{\beta} M_2 \quad (5.87)$$

where the constraints

$$\partial_z A_+ e^{i\beta z} + \partial_z A_- e^{-i\beta z} = 0$$

$$\partial_z B_+ e^{i\beta z} + \partial_z B_- e^{-i\beta z} = 0$$

holds. The electrical field components expressed through the spectral amplitudes as the expansion are

$$\begin{aligned} \begin{pmatrix} E_r \\ E_\theta \\ E_z \end{pmatrix} (z, r, \theta, t) &= \frac{1}{2\pi} \sum_s \sum_m \int_{-\infty}^{\infty} d\omega \int_0^{\infty} d\xi \xi \{ A_s \begin{pmatrix} i\beta J_{m+1}(\xi r) \\ \beta J_{m+1}(\xi r) \\ -s\xi J_m(\xi r) \end{pmatrix} e^{si\beta z} \\ &+ B_s \begin{pmatrix} \beta J_{m-1}(\xi r) \\ i\beta J_{m-1}(\xi r) \\ -si\xi J_m(\xi r) \end{pmatrix} e^{si\beta z} + \frac{1}{2} Q \begin{pmatrix} 0 \\ 0 \\ J_m(\xi r) \end{pmatrix} \} e^{-im\theta - i\omega t} \quad (5.88) \end{aligned}$$

where we know that this will produce a real electrical field through the relations

$$A_+(\xi, \omega, m) = (-1)^{m+1} i B_-^*(\xi, -\omega, -m) \quad (5.89)$$

$$B_+(\xi, \omega, m) = (-1)^{m-1} i A_-^*(\xi, -\omega, -m) \quad (5.90)$$

$$Q(\xi, -\omega, -m) = (-1)^m Q^*(\xi, \omega, m) \quad (5.91)$$

and the nonlinearity relations are calculated through

$$M_1 = \frac{1}{2i\beta} \int_0^{\infty} dr r (\widehat{N}_1 + i\widehat{N}_2) J_{m+1}(\xi r) \quad (5.92)$$

$$M_2 = \frac{1}{2i\beta} \int_0^{\infty} dr r (i\widehat{N}_1 + \widehat{N}_2) J_{m-1}(\xi r) \quad (5.93)$$

$$M_3 = \int_0^{\infty} dr r \widehat{N}_3 J_m(\xi r) \quad (5.94)$$

where the original nonlinearities are

$$\begin{aligned}
N_1 &= \mu_0 \partial_{tt} P_r^{NL} \\
N_2 &= \mu_0 \partial_{tt} P_\theta^{NL} \\
N_3 &= \frac{(1 + \chi(i\partial_t)^{-1})}{\epsilon_0} \left(\frac{1}{r} \partial_r (r P_r^{NL}) + \frac{1}{r} \partial_\theta P_\theta^{NL} + \partial_z P_z^{NL} \right)
\end{aligned}$$

The spectral equations has to satisfy the constraint (5.38)

$$-\frac{1}{c^2} \partial_{tt} (1 + \chi(i\partial_t)) q + \nabla_\perp^2 q = \mu_0 \partial_{tt} P_z^{NL} \quad (5.95)$$

where

$$q = \frac{1}{2\pi} \sum_m \int_{-\infty}^{\infty} d\omega \int_0^{\infty} d\xi \xi Q J_m(\xi r) e^{-i(m\theta + \omega t)}$$

We got this from the Maxwell equations, without making any assumptions, and this is a true solution to the Maxwell equations. The Q mode is a longitudinal mode, such modes has been mentioned before [19], and is more known in plasma physics than in optics. These modes often require extreme conditions to even start forming, and we will not be close to that domain. In general we set the mode $Q = 0$. For the rest of the equation we are going to do the same as the TE model, and let the left travelling waves be zero in all space and time. Then the simplified system will contain of

$$2i\beta \partial_z A_+ e^{i\beta z} = M_1 \quad (5.96)$$

$$2i\beta \partial_z B_+ e^{i\beta z} = M_2 \quad (5.97)$$

where

$$\begin{aligned}
\begin{pmatrix} E_r \\ E_\theta \\ E_z \end{pmatrix} (z, r, \theta, t) &= \frac{1}{2\pi} \sum_m \int_0^\infty d\omega \int_0^\infty d\xi \xi \left\{ A_+ \begin{pmatrix} i\beta J_{m+1}(\xi r) \\ \beta J_{m+1}(\xi r) \\ -\xi J_m(\xi r) \end{pmatrix} e^{i\beta z} \right. \\
&\quad \left. + B_+ \begin{pmatrix} \beta J_{m-1}(\xi r) \\ i\beta J_{m-1}(\xi r) \\ -i\xi J_m(\xi r) \end{pmatrix} e^{i\beta z} \right\} e^{-im\theta - i\omega t} + (*) \quad (5.98)
\end{aligned}$$

and the collection of nonlinear terms M_1 and M_2 were

$$M_1 = \frac{1}{2i\beta} \int_0^\infty dr r (\widehat{N}_1 + i\widehat{N}_2) J_{m+1}(\xi r) \quad (5.99)$$

$$M_2 = \frac{1}{2i\beta} \int_0^\infty dr r (i\widehat{N}_1 + \widehat{N}_2) J_{m-1}(\xi r) \quad (5.100)$$

$$(5.101)$$

In general it is possible to make a few simplifications to the model. By assuming the wave to be cylindrically symmetric, which is the same as setting $m = 0$, we get

$$\begin{aligned}
\begin{pmatrix} E_r \\ E_\theta \\ E_z \end{pmatrix} (z, r, \theta, t) &= \frac{1}{2\pi} \int_0^\infty d\omega \int_0^\infty d\xi \xi \left\{ A_+ \begin{pmatrix} i\beta J_1(\xi r) \\ \beta J_1(\xi r) \\ -\xi J_0(\xi r) \end{pmatrix} e^{i\beta z} \right. \\
&\quad \left. + B_+ \begin{pmatrix} \beta J_{-1}(\xi r) \\ i\beta J_{-1}(\xi r) \\ -i\xi J_0(\xi r) \end{pmatrix} e^{i\beta z} \right\} e^{-i\omega t} + (*) \quad (5.102)
\end{aligned}$$

To summarize we assumed the fields could be expressed in cylindrical coordinates. This assumption put the constraint on the fields as we can only well represent fields unpopulated at the point $r = 0$.

In a few turns we could reduce the set of equations to three equations determining the evolution of the electrical field components along the propagation direction z . We found a modal expansion for these through the use of Hankel transforms and Fourier series in the spatial dimensions, and a Fourier transform in the temporal dimension.

A complete transformation could be found through considering the transform of A , B and Q alone, while ensuring the electrical field is real. We used this expansion to find evolution equation for the modes, where we again have the nonlinearities expressed as functions of the polarization.

5.2 Rescaling the Vector Model

For the case where we only assume UPPE conditions we are considering the evolution of the positive frequencies of A and B . For the general case of waves traveling to the right and left, including longitudinal waves, we also have to include negative frequencies, and the mode Q .

The respective evolution equation for the three modes present in the model was

$$\begin{aligned} 2i\beta\partial_z A_+ e^{i\beta z} &= M_1 \\ 2i\beta\partial_z B_+ e^{i\beta z} &= M_2 \\ \partial_z Q &= M_3 + \frac{\xi}{i\beta} M_1 + \frac{\xi}{\beta} M_2 \end{aligned} \quad (5.103)$$

where

$$M_1 = \frac{1}{2i\beta} \int_0^\infty dr r (\widehat{N}_1 + i\widehat{N}_2) J_{m+1}(\xi r) \quad (5.104)$$

$$M_2 = \frac{1}{2i\beta} \int_0^\infty dr r (i\widehat{N}_1 + \widehat{N}_2) J_{m-1}(\xi r) \quad (5.105)$$

$$M_3 = \int_0^\infty dr r \widehat{N}_3 J_m(\xi r) \quad (5.106)$$

the nonlinear terms was defined as

$$N_1 = \mu_0 \partial_{tt} P_r^{NL} \quad (5.107)$$

$$N_2 = \mu_0 \partial_{tt} P_\theta^{NL} \quad (5.108)$$

$$N_3 = -\frac{(1+L)^{-1}}{\epsilon_0} \left(\frac{1}{r} \partial_r (r P_r^{NL}) + \frac{1}{r} \partial_\theta P_\theta^{NL} + \partial_z P_z^{NL} \right) \quad (5.109)$$

where the related expansion formula was given as

$$\begin{aligned} \begin{pmatrix} E_r \\ E_\theta \\ E_z \end{pmatrix} (z, r, \theta, t) &= \frac{1}{2\pi} \sum_m \int_{-\infty}^{\infty} d\omega \int_0^{\infty} d\xi \xi \left\{ A_+ \begin{pmatrix} i\beta J_{m+1}(\xi r) \\ \beta J_{m+1}(\xi r) \\ -\xi J_m(\xi r) \end{pmatrix} e^{i\beta z} \right. \\ &- B_+ \begin{pmatrix} i\beta J_{m+1}(\xi r) \\ \beta J_{m+1}(\xi r) \\ -i\xi J_m(\xi r) \end{pmatrix} e^{i\beta z} + \frac{1}{2} Q \begin{pmatrix} 0 \\ 0 \\ J_m(\xi r) \end{pmatrix} \left. \right\} e^{-m\theta - i\omega t} + (*) \end{aligned} \quad (5.110)$$

The model itself was derived from the equations

$$\begin{aligned} \partial_{zz} E_\theta &= \frac{1}{r} \partial_{\theta z} E_z - \partial_r \left(\frac{1}{r} \partial_r (r E_\theta) \right) + \partial_r \left(\frac{1}{r} \partial_\theta E_r \right) \\ &+ \frac{1}{c^2} \partial_{tt} ((1 + \chi(i\partial_t)) E_\theta) + \mu \partial_{tt} P_\theta^{NL} \end{aligned} \quad (5.111)$$

$$\begin{aligned} \partial_{zz} E_r &= \partial_{zr} E_z + \frac{1}{r} \partial_\theta \left(\frac{1}{r} (\partial_r (r E_\theta)) \right) - \frac{1}{r} \partial_\theta \left(\frac{1}{r} \partial_\theta E_r \right) \\ &+ \frac{1}{c^2} \partial_{tt} ((1 + \chi(i\partial_t)) E_r) + \mu_0 \partial_{tt} P_r^{NL} \end{aligned} \quad (5.112)$$

$$\begin{aligned} \partial_z E_z &= -\frac{1}{r} \partial_r (r E_r) - \frac{1}{r} \partial_\theta E_\theta \\ &- (\epsilon_0 (1 + \chi(i\partial_t)))^{-1} \left(\frac{1}{r} \partial_r (r P_r^{NL}) + \frac{1}{r} \partial_\theta P_\theta^{NL} + \partial_z P_z^{NL} \right) \end{aligned} \quad (5.113)$$

The nonlinearities will be assumed still to be some function where their dimension can be expressed as $\epsilon_0 E_0$.

We introduce the same variables with corresponding dimensional constants as

the TE model, by assuming that the electrical field will consist of equal strength in all directions.

$$z = z_0 z', \quad r = r_0 r', \quad t = t_0 t' \quad E_i = E_0 E'_i$$

By inserting this into the equations, and dividing by all unnecessary constants we end up with

$$\begin{aligned} \partial_{z'z'} E'_\theta &= \frac{\alpha}{r'} \partial_{\theta z'} E'_z - \alpha^2 \partial_{r'} \left(\frac{1}{r'} \partial_{r'} (r' E'_\theta) \right) + \alpha^2 \partial_{r'} \left(\frac{1}{r'} \partial_\theta E'_r \right) \\ &+ \partial_{t't'} ((1 + \chi(i\omega_0 \partial_{t'})) E'_\theta) + \partial_{t't'} P_\theta^{NL} \end{aligned} \quad (5.114)$$

$$\begin{aligned} \partial_{z'z'} E'_r &= \alpha \partial_{z'r'} E'_z + \frac{\alpha^2}{r'} \partial_\theta \left(\frac{1}{r'} (\partial_{r'} (r' E'_\theta)) \right) - \frac{\alpha^2}{r'} \partial_\theta \left(\frac{1}{r'} \partial_\theta E'_r \right) \\ &+ \partial_{t't'} ((1 + \chi(i\omega_0 \partial_{t'})) E'_r) + \partial_{t't'} P_r^{NL} \end{aligned} \quad (5.115)$$

$$\begin{aligned} \partial_{z'} E'_z &= - \frac{\alpha}{r'} \partial_{r'} (r' E'_r) - \frac{\alpha}{r'} \partial_\theta E'_\theta \\ &- ((1 + \chi(i\omega_0 \partial_{t'})))^{-1} \left(\frac{\alpha}{r'} \partial_{r'} (r' P_r^{NL}) + \frac{\alpha}{r'} \partial_\theta P_\theta^{NL} + \partial_{z'} P_z^{NL} \right) \end{aligned} \quad (5.116)$$

where we used the relation $z = ct_0$. Again the constant of proportionality is expressed as

$$\alpha = \frac{z_0}{r_0}$$

The equations are now dimensionless, and the coefficients will be determined by the relation of initial propagation of the beam. In the TE model we used the relation $t_0 \omega_0 = 1$, which we will use here too, and also introduce the relation $r_0 \xi_0 = 1$ for the spectral domain produced by the Hankel transform.

Introducing this to the dispersion relation we get

$$\beta' = \frac{1}{z_0} \sqrt{(\omega') n^2(\omega' \omega_0) - \frac{z_0^2}{r_0^2} \xi^2} = \frac{1}{z_0} \sqrt{(\omega') n^2(\omega' \omega_0) - \alpha^2 \xi^2}$$

Observe that the dispersion relation is proportional to the constant α .

Following the same procedure as with the TE model, we analyse the expansion to find the dimensions of the modes in terms of the initial electrical field.

$$E_0 E'_r(z', r', \theta, t') = \frac{A_0}{t_0 z_0 r_0^2} \frac{1}{2\pi} \sum_m \int_{-\infty}^{\infty} d\omega' \int_0^{\infty} d\xi' \xi' \{ A'_+ i\beta' J_{m+1}(\xi' r') e^{i\beta' z'} - B'_+ \beta' J_{m+1}(\xi' r') \} e^{-m\theta - i\omega' t'} + (*)$$

The dimensions here are to be thought of as the relation between the electrical field and the expanded amplitudes

$$E_0 \sim \frac{A_0}{t_0 z_0 r_0^2}$$

For the Q mode we have to consider the last integral

$$E_0 E'_z(z', r', \theta, t') = \frac{1}{2\pi} \sum_m \int_{-\infty}^{\infty} d\omega' \int_0^{\infty} d\xi' \xi' \left\{ -\frac{A_0}{r_0^3 t_0} \xi A'_+ J_m(\xi' r') - \frac{A_0}{r_0^3 t_0} \xi' B'_+ J_m(\xi' r') + \frac{Q_0}{t_0 r_0^2} \frac{1}{2} Q' J_m(\xi' r') \right\} e^{-im\theta - i\omega t'} + (*)$$

Removing excessive terms will lead to

$$E'_z(z', r', \theta, t') = \frac{1}{2\pi} \sum_m \int_{-\infty}^{\infty} d\omega' \int_0^{\infty} d\xi' \xi' \left\{ -\alpha \xi A'_+ J_m(\xi' r') - \alpha \xi' B'_+ J_m(\xi' r') + \frac{Q_0}{t_0 r_0^2 E_0} \frac{1}{2} Q' J_m(\xi' r') \right\} e^{-im\theta - i\omega t'} + (*)$$

With the establishment of the relation between A_0 and E_0 , and the requirement of the transform to be dimensionless, we see that Q_0 has to be of the dimension

$$Q_0 = E_0 r_0^2 t_0$$

For the differential equations of the modes A and B we have the dimensions

$$\frac{A_0}{z_0^2} 2i\beta' \partial_{z'} A'_+ e^{i\beta' z'} = M_0 M'_1 \quad (5.117)$$

and in the right hand side we first consider the terms N_1 and N_2 .

$$N_0 N'_1 = \frac{E_0}{z_0^2} \partial_{t' t'} P_r^{NL'}$$

By inserting these constants in (5.117), together with a t_0 from the time Fourier transform, we get the right hand side to be

$$M_0 M'_1 = \frac{t_0 E_0 r_0^2}{z_0} \frac{1}{2i\beta'} \int_0^\infty dr' r' (\widehat{N}'_1 + i\widehat{N}'_2) J_{m+1}(\xi' r')$$

Now we compare the sides

$$\frac{A_0}{z_0^2} \sim M_0 \sim \frac{t_0 E_0 r_0^2}{z_0} = \frac{A_0}{z_0^2}$$

by the relation from the expansion. We see here that the equations are now dimensionless. In the dimensionless quantities the two differential equations reads

$$\begin{aligned} 2i\beta' \partial_{z'} A'_+ e^{i\beta' z'} &= M'_1 \\ 2i\beta' \partial_{z'} B'_+ e^{i\beta' z'} &= M'_2 \end{aligned}$$

Where the last differential equation involves the Q mode. For M_3 we get

$$M_0 M'_3 = t_0 r_0^2 N_0 \int_0^\infty dr' r' \widehat{N}_3' J_m(\xi' r')$$

where

$$\begin{aligned} N_0 N'_3 &= (1 + \chi(i\partial_{t'})) \left(\frac{E_0}{r' r_0} \partial_{r'} (r' P_r^{NL'}) + \frac{E_0}{r' r_0} \partial_\theta P_\theta^{NL'} + \frac{E_0}{z_0} \partial_{z'} \right) \\ N_0 N'_3 &= \frac{E_0}{z_0} (1 + \chi(i\partial_{t'})) \left(\frac{\alpha}{r'} \partial_{r'} (r' P_r^{NL'}) + \frac{\alpha}{r'} \partial_\theta P_\theta^{NL'} + \partial_{z'} P_z^{NL'} \right) \end{aligned}$$

thus we have

$$M_0 = \frac{t_0 r_0^2 E_0}{z_0}$$

For the differential equation itself we have

$$\begin{aligned} \frac{Q_0}{z_0} \partial_{z'} Q' &= \frac{t_0 r_0^2 E_0}{z_0} M'_3 + \alpha \frac{t_0 E_0 r_0^2}{z_0} \frac{\xi'}{i\beta'} M'_1 + \alpha \frac{t_0 E_0 r_0^2}{z_0} \frac{\xi'}{\beta'} M'_2 \\ \partial_{z'} Q' &= M'_3 + \alpha \frac{\xi'}{i\beta'} M'_1 + \alpha \frac{\xi'}{\beta'} M'_2 \end{aligned}$$

The final rescaled system of equations is thus

$$\begin{aligned} 2i\beta' \partial_{z'} A'_+ e^{i\beta' z'} &= M'_1 \\ 2i\beta' \partial_{z'} B'_+ e^{i\beta' z'} &= M'_2 \\ \partial_{z'} Q' &= M'_3 + \alpha \frac{\xi'}{i\beta'} M'_1 + \alpha \frac{\xi'}{\beta'} M'_2 \end{aligned} \tag{5.118}$$

where the nonlinearities are found as

$$\begin{aligned}
M'_1 &= \frac{1}{2i\beta'} \int_0^\infty dr' r' (\widehat{N}'_1 + i\widehat{N}'_2) J_{m+1}(\xi' r') \\
M'_2 &= \frac{1}{2i\beta'} \int_0^\infty dr' r' (i\widehat{N}'_1 + \widehat{N}'_2) J_{m+1}(\xi' r') \\
M'_3 &= \int_0^\infty dr' r' \widehat{N}'_3 J_m(\xi' r')
\end{aligned} \tag{5.119}$$

where

$$\begin{aligned}
N'_1 &= \partial_{t't'} P_r^{NL'} \\
N'_2 &= \partial_{t't'} P_\theta^{NL'} \\
N'_3 &= (1 + \chi(i\partial_{t'})) \left(\frac{\alpha}{r'} \partial_{r'} (r' P_r^{NL'}) + \frac{\alpha}{r'} \partial_\theta P_\theta^{NL'} + \partial_{z'} P_z^{NL'} \right)
\end{aligned} \tag{5.120}$$

the transformation relevant to our system is

$$\begin{aligned}
\begin{pmatrix} E'_r \\ E'_\theta \\ E'_z \end{pmatrix} (z', r', \theta, t') &= \frac{1}{2\pi} \sum_m \int_{-\infty}^\infty d\omega' \int_0^\infty d\xi' \xi' \{ A'_+ \begin{pmatrix} i\beta' J_{m+1}(\xi' r') \\ \beta J_{m+1}(\xi' r') \\ -\alpha \xi' J_m(\xi' r') \end{pmatrix} e^{i\beta' z'} \\
&- B'_+ \begin{pmatrix} i\beta' J_{m+1}(\xi' r') \\ \beta J_{m+1}(\xi' r') \\ -i\alpha \xi' J_m(\xi' r') \end{pmatrix} e^{i\beta' z'} + \frac{1}{2} Q' \begin{pmatrix} 0 \\ 0 \\ J_m(\xi' r') \end{pmatrix} \} e^{-m\theta - i\omega' t'} + (*)
\end{aligned} \tag{5.121}$$

In this section we introduced new dimensionless variables to the equations. Contrary to the TE model we have left the constant of proportionality between the transverse direction and the longitudinal direction. This constant is typically set by the incident laser beam.

We further investigated all the amplitudes dimensions, and made sure every part of the numerical system is dimensionless. The numerical model is now about solving the set of equations (5.118) where we use (5.119) for the nonlinearities and

(5.120) gives the nonlinearities in terms of polarization.

5.3 Numerical Vectorial

The vectorial model is quite similar to the TE model. Now we have to solve three differential equations at the same time, instead of one. Fortunately many of the methods implemented can be directly transferred to the new model, such as the Fourier transform algorithm and solving a system of differential equations.

We are going to consider the cylindrically symmetric version of equations for the numerical part of the problem. We will do so by the proposed method of setting $m = 0$ throughout the model.

5.3.1 The model

We end up with three evolution equations for the three modes present. These three equations has the right hand side in the same form as the TE model. If the polarization can be expressed as the Kerr effect

$$NL_i(z, r, \theta, t) = (\mathbf{E}(z, r, \theta, t) \cdot \mathbf{E}(z, r, \theta, t))E_i(z, r, \theta, t) \quad (5.122)$$

it will represent a double convolution in the spectral domain for the radial dimension, and the time dimension. The Fourier transform implementation is directly transferable from the TE model. The discretization i needed in order to utilize FFT algorithm is $i = 2^M$ where $M \in \mathbb{N}$. For the radial direction, the discretization j should be large enough for the relevant function $f(r)$, to be well represented.

The Hankel transform implementation for cylindrical coordinates is discussed in Appendix A. This implementation uses a N^2 multiplication and addition algorithm, where the domain 0 to ∞ has to be discretized. Other Hankel transforms uses a $M \log(M)$ multiplication and $M^2 + M \log(M)$ additions algorithms, where they focus on the advantage of FFT to do the Hankel transform. This requires the domain to be from $-\infty$ to ∞ .

$$F_\nu(\xi) = \int_0^\infty d\xi \xi f(r) J_\nu(\xi r) \quad (5.123)$$

The Hankel transform (5.123) requires the sampling of the function $f(r)$ to be sampled with the rate $r_n = j_{n,\nu}R/j_{N,\nu}$ where $j_{n,\nu}$ is the n 'th zero of the Bessel function ν and N is the last zero of the series. R is the maximum value of the domain of interest where $f(r) = 0 \forall r > R$. The nature of the Bessel function zeroes gives a nonuniform sampling close to the origin.

The general full transformation for the electrical field components is

$$\begin{aligned} \begin{pmatrix} E_r \\ E_\theta \\ E_z \end{pmatrix} (z, r, t) &= \frac{1}{2\pi} \int_{-\infty}^{\infty} d\omega \int_0^\infty d\xi \xi \left\{ A_+ \begin{pmatrix} i\beta J_1(\xi r) \\ \beta J_1(\xi r) \\ -\alpha \xi J_0(\xi r) \end{pmatrix} e^{i\beta z} \right. \\ &+ B_+ \begin{pmatrix} -i\beta J_1(\xi r) \\ -\beta J_1(\xi r) \\ -i\alpha \xi J_0(\xi r) \end{pmatrix} e^{i\beta z} + \frac{1}{2} Q \begin{pmatrix} 0 \\ 0 \\ J_0(\xi r) \end{pmatrix} \left. \right\} e^{-i\omega t} + (*) \end{aligned} \quad (5.124)$$

where we observe that the two field components E_r and E_θ is found by the Hankel transform of order $\nu = 1$, while the last components is found by the transform of order $\nu = 0$. Zeroes of the Bessel functions $j_{n,\nu}$ is different for each ν , and the electrical field components will be on different grids compared to each other. This creates a problem when we reconstruct them from the modes.

For electrical field components we cannot express them around $r = 0$, but the nature of the Hankel transforms ensures the modes to be populated around the point $\xi = 0$. The main problem is that $j_{0,0} < j_{0,1}$, which means that in order to reconstruct E_z we have to extrapolate the first point.

Extrapolation is in general a bad thing to do, and to avoid it we tried four different approaches. The first approach was to keep the E_z component on the same grid as E_r and E_θ , and solve

$$\partial_z E_z = -\frac{\alpha}{r} \partial_r (r E_r) - (1 + \chi(i\partial_t))^{-1} \left(\frac{\alpha}{r} \partial_r (r P_r^{NL}) + \partial_z P_z^{NL} \right)$$

directly. For the first term it is possible to use a higher order finite difference method, and such a method was implemented and can be found in Appendix A. The second term requires an iterative method for evaluating $\partial_z E_z$ on the right hand side. Numerically it is a non trivial thing to do, and other methods were pursued.

We instead turn to interpolation methods. The first method to work around the difficulty is to assume cylindrically symmetric components, we can assume that the modes will be symmetric around the point $\xi = 0$, and we can produce the modes A and B at the first point¹ of \mathcal{H}_0 . This method will put serious constraints on the amount of fields we are able to simulate.

Another interpolation method is discussed in [20], and it can be shown [21][22] that any function sampled at the grid $r_{n,\nu}$ can be reconstructed at the arbitrary point r by

$$f(r) = \sum_{n=1}^{\infty} f(r_{n,\nu}) S_k(r)$$

where

$$S_k(r) = \frac{2r_{n,\nu} J_\nu(Tr)}{T(r_{n,\nu}^2 - r^2) J_{\nu+1}(Kr_{n,\nu})}$$

In order for this sum to converge to the point of the original function $f(r)$ the whole domain where $f(r_{n,\nu})$ is defined as to be summed. The method itself proves to be time consuming and infeasible for the amount of iterations we seek to do.

The last method comes from the Hankel transform (5.123) itself. The Bessel functions can in general be written as the sum

¹We will use \mathcal{H}_i as short for the Hankel transform of order $\nu = i$.

$$J_\nu(x) = \left(\frac{x}{2}\right)^\nu \sum_{k=n}^{\infty} \frac{(-1)^k}{\Gamma(k+1)\Gamma(-n+k+1)} \left(\frac{x}{2}\right)^{2k}$$

where it is obvious that $J_\nu(0) = 0 \forall \nu > 1$. Thus we know the value of the Hankel transform itself at the point $\xi = 0$. This is the fastest method found to work around this problem, and was the one ultimately used. To perform the interpolation a cubic spline method was used. Such an implementation can also be found in the Appendix A.

To evolve we modes we have to solve three differential equations

$$\begin{aligned} 2i\beta' \partial_{z'} A'_+ e^{i\beta' z'} &= M'_1 \\ 2i\beta' \partial_{z'} B'_+ e^{i\beta' z'} &= M'_2 \\ \partial_{z'} Q' &= M'_3 + \alpha \frac{\xi'}{i\beta'} M'_1 + \alpha \frac{\xi'}{\beta'} M'_2 \end{aligned} \quad (5.125)$$

Each of these modes consists of $j \times i$ points, and we have to solve equally amount of differential equations. These can be solved simultaneously through the standard ODE solver. For the right hand side we follow the algorithm

1. From the modes A and B we can reconstruct the two field components E_r and E_θ .
2. The last field component is found through interpolating A and B from the grid J_1 to J_0 through the method described, and then do the inverse transform including the mode Q to reconstruct E_z .
3. Do the necessary operations for the polarization expressions M_1 , M_2 and M_3 .
4. Insert the expressions for the right hand side of the evolution equations for E_r and E_θ

5. For the last evolution equation, both M_1 and M_2 has to be interpolated to the grid J_0 before we can insert it into the right hand side of last equation in (5.125).

For the method described it is clear that to reconstruct the electrical field components we have to do i Hankel transforms, and j Fourier transforms for each component. Since these have to be done sequentially we can use parallel programming to speed up the calculation time.

5.3.2 Parallel programming in the model

On the right hand side of the evolution equations we evaluate the nonlinearity in the real domain. The implementation to get from the spectral domain to the real domain involves taking the Fourier transform N times, and Hankel transform M times. These transforms are taken directly on vectors and are thus independent of each other. Such a system is what we call ridiculously parallel.

The implementation was done with a for loop doing each transform sequentially. The easiest way to parallelize such a loop is to use the open multi processing (OpenMP) parallelization. Since no memory is shared between the two different transforms there is no need to put any constraints on the parallelization.

The implementation of OpenMP is easy, and in order to parallelize a loop one simply uses

```
int main(){
    #pragma omp parallel for
    int i;
    for (i = 0; i < N; i++){
        fouriertransform or
        hankeltransform
    };
};
```

and the loop will be distributed amongst the processors available. The package OpenMP is included into the implementation by adding the flag

```
gcc -fopenmp programname.c -o programname
```

to the makefile. This is the parallelization used for both Fourier transform and Hankel transform of the electrical field components and the amplitudes. The same approach can be done for doing the interpolation and the arithmetic operations done on the grid.

5.3.3 Experimental setup

In the experimental case we want to simulate right travelling waves. We know the existence of longitudinal modes requires extreme conditions, we will leave the mode $Q = 0$ for all z . The chosen function

$$f_0(r, t) = e^{-\gamma_1(t-vz)^2 - \gamma_2(r-r_0)^2} \cos(\omega_0 t)$$

will initialize the modes. The model is derived upon cylindrical coordinates, it has the obvious singularity at the point $r = 0$, and the constants for the function f_0 has to be chosen in such a way that the modes will not represent a electrical field populated at the point $r = 0$.

In general one can choose to populate A , B or both A and B initially. For the UPPE conditions we make the same approach as for the TE model, and we pad the negative frequencies of the initial condition with zeroes. Whenever the right hand side is evaluated, we pad the negative frequencies with zeroes. Thus we ensure the produced wave is always travelling to the right.

5.3.4 Verification

As we did with the TE model, we will include left and right travelling waves through both positive and negative frequencies. We will also include the Q mode for longitudinal direction. This will then be a test for the complete system. In order to verify the numerical model we now have to solve three equations simultaneously. The three equations are the origin of the model

$$\begin{aligned}
\partial_{zz}E_\theta &= -\alpha\partial_r\left(\frac{1}{r}\partial_r(rE_\theta)\right) + \partial_{tt}((1 + \chi(i\partial_t))E_\theta) + \partial_{tt}P_\theta^{NL} \\
\partial_{zz}E_r &= \alpha\partial_{zr}E_z + \partial_{tt}((1 + \chi(i\partial_t))E_r) + \partial_{tt}P_r^{NL} \\
\partial_zE_z &= -\frac{\alpha}{r}\partial_r(rE_r) - (1 + \chi(i\partial_t))^{-1}\left(\frac{\alpha}{r}\partial_r(rP_r^{NL}) + \partial_zP_z^{NL}\right)
\end{aligned} \tag{5.126}$$

The polarization in r and θ direction we will assume to be expressed as

$$P_r^{NL} = \rho_r, \quad P_\theta^{NL} = \rho_\theta$$

The longitudinal direction is only included in the evolution of Q mode. This mode for UPPE conditions is always zero, and thus irrelevant. For verifying the equation we have to involve the development of this mode for completeness. What we will do is to avoid the right hand side by assuming we can express the source as

$$-(1 + \chi(i\partial_t))^{-1}\left(\frac{\alpha}{r}\partial_r(rP_r^{NL}) + \partial_zP_z^{NL}\right) = \partial_{tt}\rho_z$$

Inserting the new definitions of the polarizations into the equations (5.126), will give the source terms in analytical expressions through the functions

$$-\partial_{tt}f_i(z, r, t) = E_i(z, r, t)$$

where i denotes a direction in space. The representation ensures the magnetic field to exist. The functions f_i we define as the wavepacket functions

$$f_i(z, r, t) = e^{-(t-zv_i)^2 - (r-r_i)^2} \cos(\omega_i t)$$

where each of the constants are different for each of the components. The system requires five initial conditions, two for the components E_r and E_θ and one for

E_z . From the transformation and the constraint[15] we have the five following equations for the modes A_+ , A_- , B_+ , B_- and Q

$$\begin{aligned} \begin{pmatrix} E_r \\ E_\theta \\ E_z \end{pmatrix} (z, r, t) &= \frac{1}{2\pi} \sum_s \int_{-\infty}^{\infty} d\omega \int_0^{\infty} d\xi \xi \left\{ A_s \begin{pmatrix} i\beta J_1(\xi r) \\ \beta J_1(\xi r) \\ -s\alpha \xi J_0(\xi r) \end{pmatrix} e^{si\beta z} \right. \\ &+ B_s \begin{pmatrix} -i\beta J_1(\xi r) \\ -\beta J_1(\xi r) \\ -si\alpha \xi J_0(\xi r) \end{pmatrix} e^{si\beta z} + \frac{1}{2} Q \begin{pmatrix} 0 \\ 0 \\ J_0(\xi r) \end{pmatrix} \left. \right\} e^{-i\omega' t} \end{aligned} \quad (5.127)$$

and

$$\begin{aligned} \begin{pmatrix} \partial_z E_r \\ \partial_z E_\theta \end{pmatrix} (z, r, t) &= \frac{1}{2\pi} \sum_s \int_{-\infty}^{\infty} d\omega \int_0^{\infty} d\xi \xi \left\{ si\beta A_s \begin{pmatrix} i\beta J_1(\xi r) \\ \beta J_1(\xi r) \end{pmatrix} e^{si\beta z} \right. \\ &+ si\beta B_s \begin{pmatrix} -i\beta J_1(\xi r) \\ -\beta J_1(\xi r) \end{pmatrix} e^{si\beta z} \left. \right\} e^{-i\omega t} + (*) \end{aligned} \quad (5.128)$$

This gives us five equations for five unknowns to solve for the initial condition for each point of the modes. The system was solved by LU factorization, such implementations are standard in any numerical library.

5.4 Numerical Results

As we did with the TE model we will show the experimental results first, then proceed to show the verification of the numerical model.

5.4.1 Experimental results

The chosen material to simulate the wave is air. The nonlinearity is assumed to be of the type Kerr effect. We will assume the same type of intensity for the laser as we had for the TE model. The constant of nonlinearity will thus be

$$\zeta = \eta E_0^2 = 0.00128$$

The refractive index will be the same Sellmeier expansion

$$n(\omega) = 1 + \frac{5.85096 \times 10^{-16}}{1.99884 \times 10^{-11} - \omega^2} + \frac{2.01822 \times 10^{-14}}{8.29399 \times 10^{-10} - \omega^2}$$

For the vectorial model we also have to specify the proportionality constant, and have set this to be $\alpha = 0.001$. The time domain runs from -10 to 10 , discretized in 1024 points. For the radial direction we have chosen the domain from 0 to 10, and discretization of 124 points.

The plots are all at the point $z = 5$. This ensures the wave has gone through enough iterations to move.

The model was initialized with the A mode only. We have chosen the function

$$f(r, t) = e^{-0.5t^2 - (5-r)^2} \cos(10t)$$

to initiate the mode.

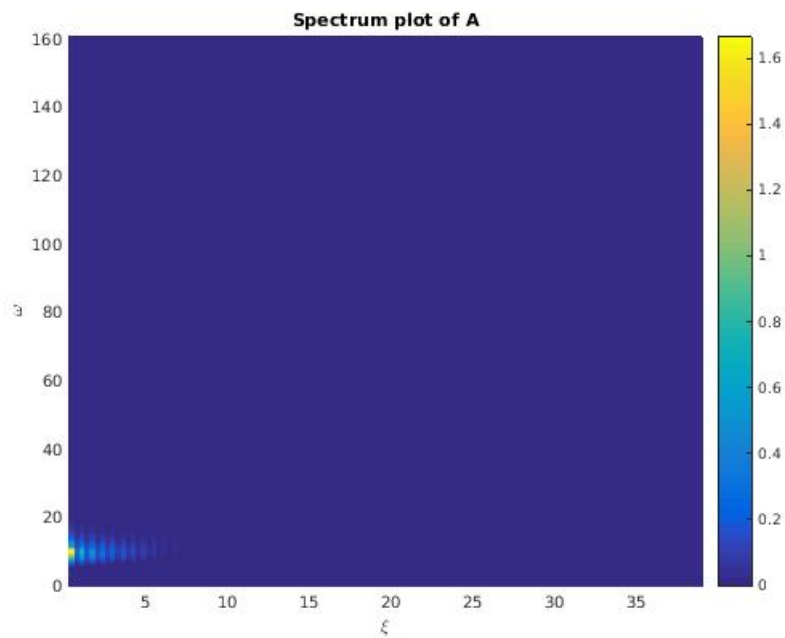


FIGURE 5.1: The figure shows the mode A at the point $z = 5$. The discretization in ξ direction is 125 while discretization in ω is 1025.

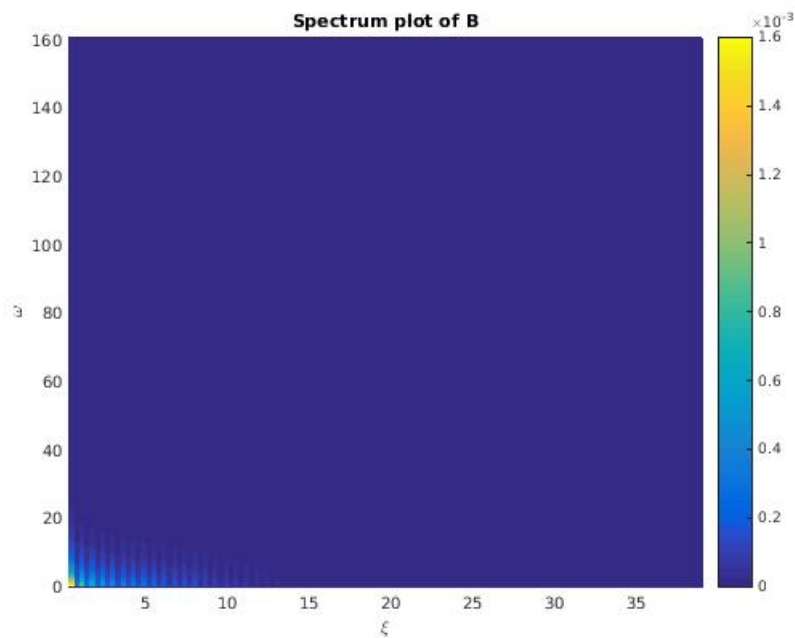


FIGURE 5.2: The figure shows the mode B at the point $z = 5$. The discretization in ξ direction is 125, while discretization in ω is 1025.

The two figures (5.1) and (5.2) show the modes at the point $z = 5$. At start we only initiated the mode A. The mode B will be constructed by the nonlinearity itself. The mode A is in the order $\mathcal{O}(1)$, while the B mode is in order $\mathcal{O}(10^{-3})$.

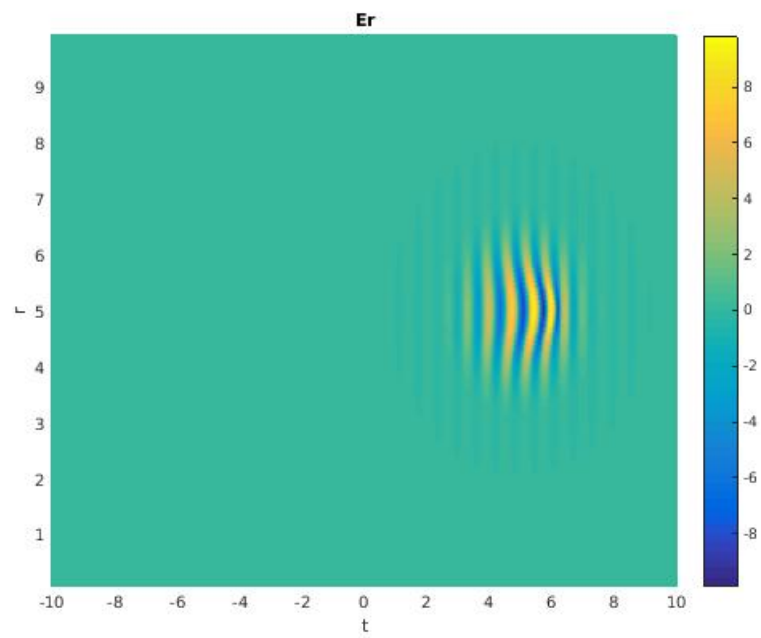


FIGURE 5.3: The figure shows the field component E_r at the point $z = 5$. The discretization in r is 125 points, while discretization in time is 1025.

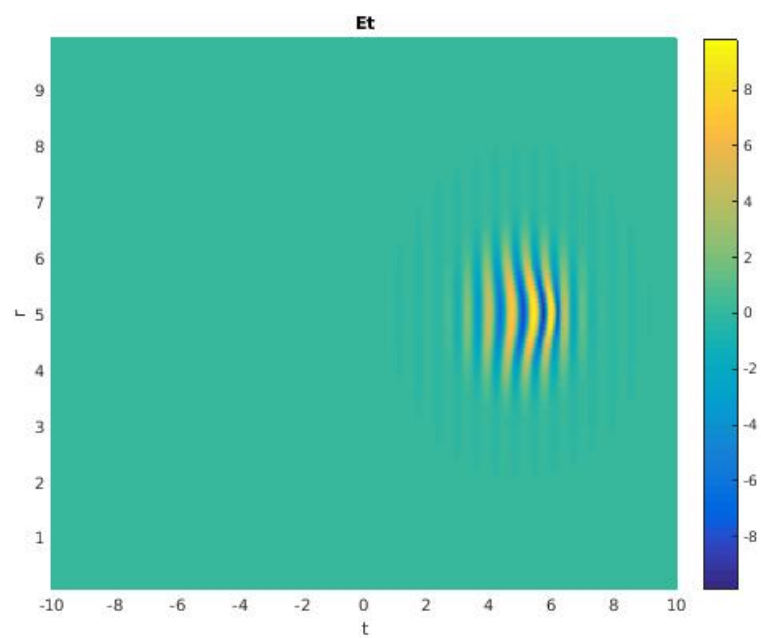


FIGURE 5.4: The figure shows the field component E_θ at the point $z = 5$. The discretization in r is 125 points, while discretization in time is 1025.

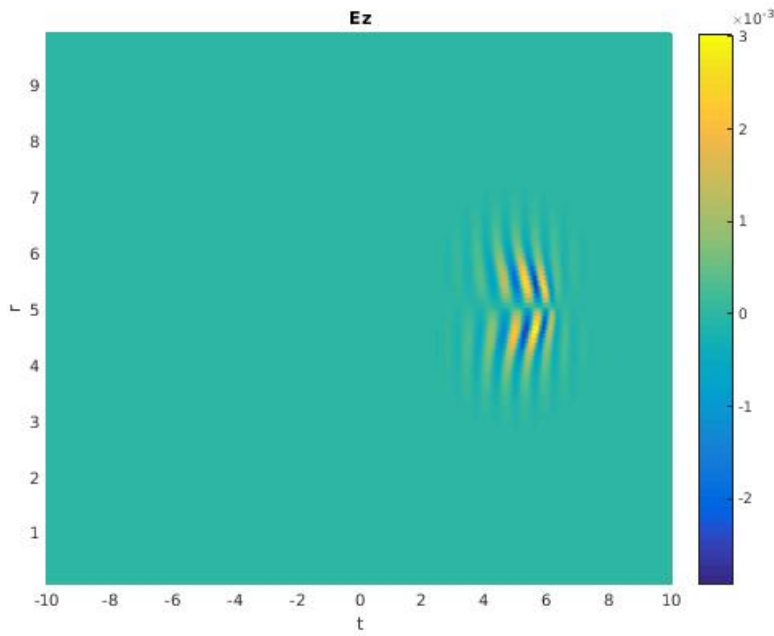


FIGURE 5.5: The figure shows the field component E_z at the point $z = 5$. The discretization in r is 125 points, while discretization in time is 1025.

The figures (5.3), (5.4) and (5.5) show the electrical field components at the point $z = 5$. The first two components E_r and E_θ is in the order of $\mathcal{O}(10)$, while the last one E_z is in the order of $\mathcal{O}(10^{-3})$.

5.4.2 Verification

To verify the model we used the constant refractive index $n(\omega) = 1$. The nonlinearity constant ζ is not included in the evaluation since we assume the polarization to be the source alone. For the proportionality constant the value $\alpha = 0.001$ is chosen. The discretization is again 1025 for time and 125 for radial direction.

The system is tested with the following functions

$$\begin{aligned}
 f_r(r, z, t) &= e^{-(t-0.4z)^2 - (r-4)^2} \cos(9t) \\
 f_\theta(r, z, t) &= e^{-(t-2z)^2 - (r-5)^2} \cos(10t) \\
 f_z(r, z, t) &= e^{-(t-3z)^2 - (r-6)^2} \cos(11t)
 \end{aligned}$$

Thus all the exact waves travels with different speeds and oscillates differently. The chosen representation shows the exact solution against the numerical model in the same plot. The plots are for time represented at the point $r = 4.8$ and $z = 3.0$

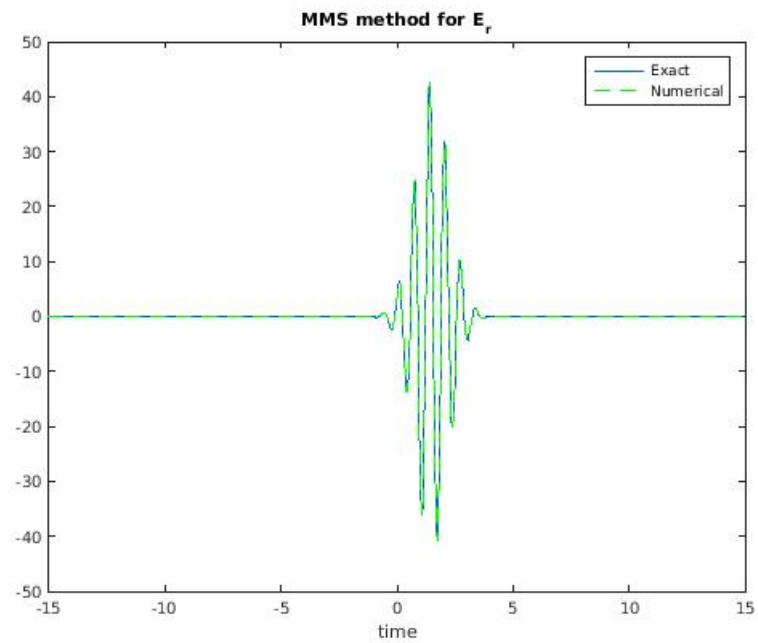


FIGURE 5.6: The figure shows the numerical value of the component E_r plotted against its exact value. The radial point is $r = 4.8$ while the x-axis is time. The y-axis shows the strength of the electrical field along time.

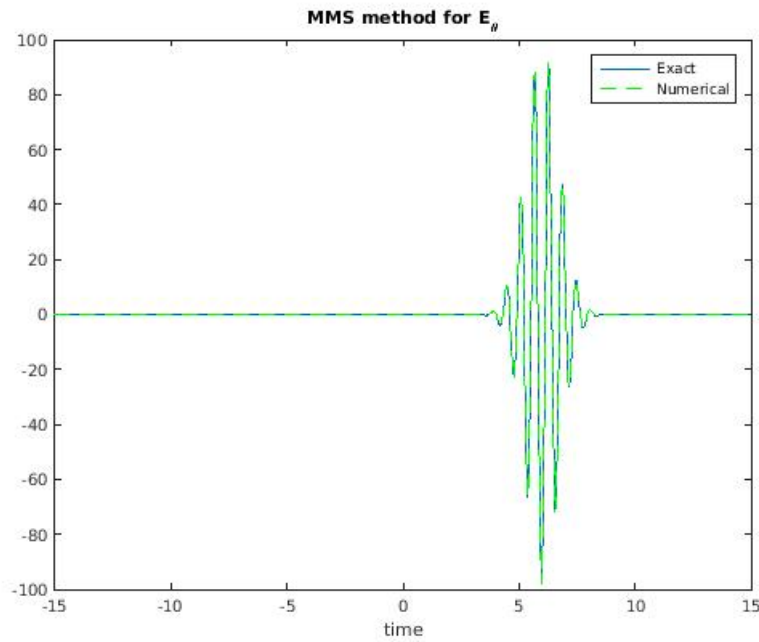


FIGURE 5.7: The figure shows the numerical value of the component E_θ plotted against its exact value. The radial point is $r = 4.8$ while the x-axis is time. The y-axis shows the strength of the electrical field along time.

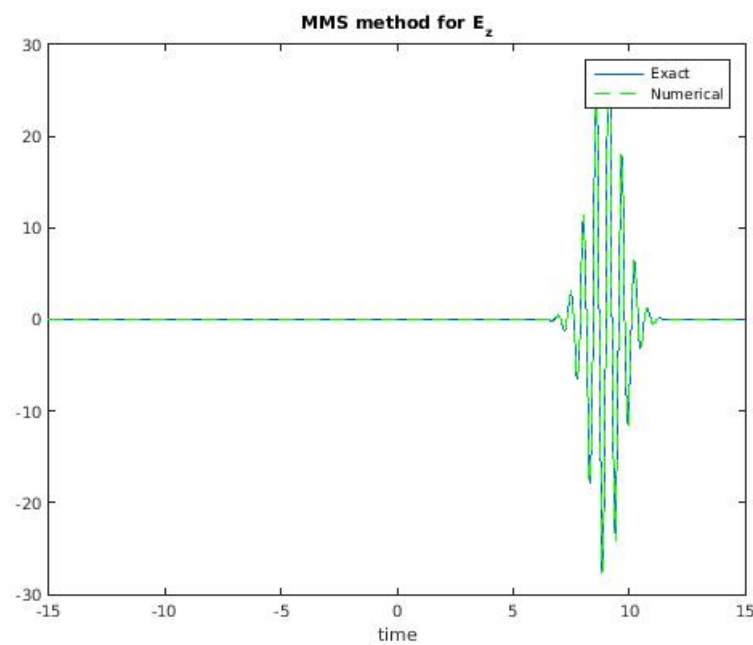


FIGURE 5.8: The figure shows the numerical value of the component E_z plotted against its exact value. The radial point is $r = 4.8$ while the x-axis is time. The y-axis shows the strength of the electrical field along time.

In all the figures (5.6), (5.7) and (5.8) we have perfect overlap between the numerical value and the exact value.

5.5 Discussion

To verify the CV model is more tedious than verifying the TE model. We have to include both the negative frequencies of A and B , and the longitudinal Q mode. Some of the numerical calculation of these modes is not included in the model we seek a solution to, the UPPE conditions. When unnecessary numerical work is done, it should be expected to give more unnecessary numerical error as well.

In the transform implementation both the Hankel transform and Fourier transform are integral approximations. In general we will expect the error estimate from such implementations to be less than $\mathcal{O}(h^2)$. For the Fourier transform this will be true, and for the Hankel transform we have a nonuniform grid close to the origin. We can expect the error close the origin to manifest itself in an unexpected way.

For the cubic spline interpolation we have the error estimation of $\mathcal{O}(h^4)$, which is much stronger than the integral approximations. However, close to the origin we are interpolating on a nonuniform grid, where the steplength can vary in our disfavour dependant on the discretization chosen. The first point is approximated to be zero through the Bessel function. For bad sampling, the first step in ξ direction will be long compared to the rest, and thus create a larger margin for error associated with the interpolation. Thus we can not disregard numerical error from the interpolation close to the origin.

For the last component we propagate the mode Q . The implementation simulates Q on the grid relevant for the Bessel function of order $\nu = 0$, that requires interpolation of both M_1 and M_2 in order to find the right hand side. The amount of interpolation and transforms needed to propagate it is a reason for stronger numerical errors than should be expected for the general UPPE model.

To get a view of how the error is through the verification of the model, we will show plots of the three components at the point $z = 3.0$. These plots will be a mesh of the total error in radial direction and in time.

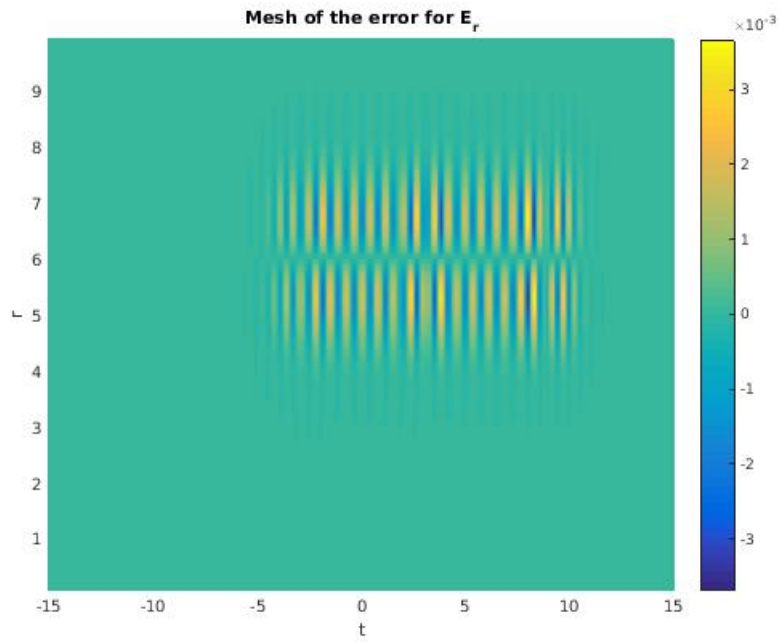


FIGURE 5.9: The mesh of the error of the component E_θ , the x-axis has time, while the y-axis has radial direction.

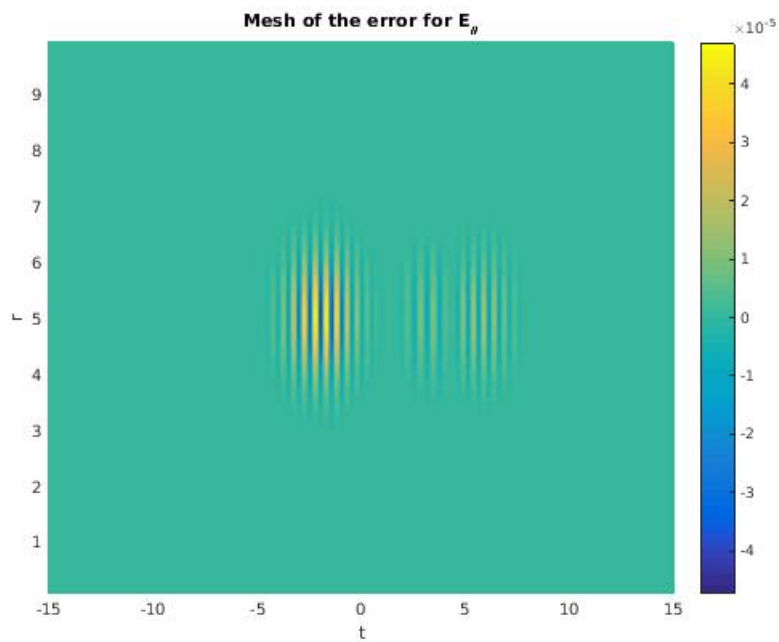


FIGURE 5.10: The mesh of the error of the component E_r , the x-axis has time, while the y-axis has radial direction.

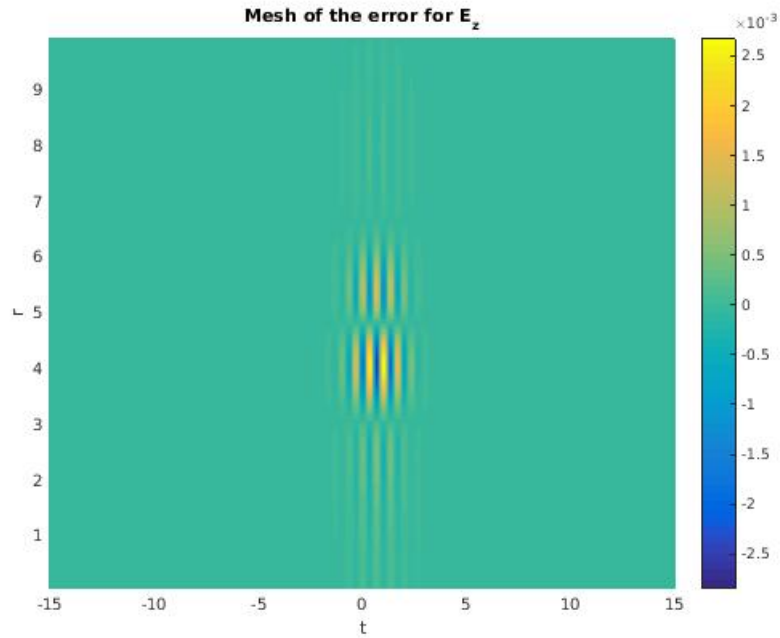


FIGURE 5.11: The mesh of the error of the component E_z , the x-axis has time, while the y-axis has radial direction.

From the figures (5.10), (5.9) and (5.11), we observe that the error is in the region 10^{-5} to 10^{-3} , which was typical for the tests ran with the model. In comparison with the numerical results we had for the verification tests, the peak value was at 10^2 , which in total gives us six digits of significance. The general the error is within a reasonable margin of what we can expect.

In the last figure (5.11) we have an error spreading along the radial axis. The error can be assumed to be an artefact from the zeroth order Hankel transform, which by definition is not zero at the origin, if the function $f(\xi)$ is nonzero. The artefact can be further investigated through the inclusion of the azimuthal direction. The second mode for instance will include Hankel transform of order $\nu = 1$ and $\nu = 2$ to reconstruct the fields. However, for the UPPE conditions we assume the Q mode to be zero, and the longitudinal component E_z is a result of A and B proportional to α . If α is small we would expect E_z to be small or not even exist. The two other components does not posses this radial error, and it can be a property of the Q mode itself. If this is true the error will be close to nonexistent for the UPPE conditions model. In general the errors within the model is within an acceptable amount.

Most of the time spent in the numerical model is in the transform. The most time consuming of them is the Hankel transform, which has a complexity of N^2 multiplications and additions. For our simulations we have chosen a Gaussian in the radial direction. These functions does not need a very fine discretization to be well represented. If the goal is to simulate complex functions in the radial direction the time consumption from the Hankel transform will become even more significant. The time spent can be reduced by the means of inner parallel programming for the Hankel transform.

For the cylindrical case we chose to simulate simple radially directed functions, thus the need for a true fine discretization was not present. For long distance propagation the run time was significant. For time reduction we used the basic for loop parallelization OpenMP. For test runs of the numerical UPPE scheme, which requires a reconstruction of electrical field components and back to spectral domain for the nonlinearities, we experienced a 2.8 times faster run speed. This test was done with only three cores available, and is the total time of the whole implementation. The parallelization can be classified as almost linear, and we can expect it to stay linear for a few more cores before we reach saturation.

Chapter 6

Summary

In this thesis we have successfully implemented a model which predicts the development of the electrical field in cylindrical coordinates under the assumption of UPPE conditions. In order to get to this point we developed a minor model from the TE field, where we first introduced the pseudo spectral method, and the periodic Fourier transform. The CV model included the implementation of the Hankel transform, cubic spline interpolation and LU factorization.

For electrical fields with the shape of cylindrical vector modes a typical plane wave formulation have to include many modes to represent the wave. Our model will highly reduce the amount of modes we have to include in order to produce a proper representation. The advantage of the representation will maintain as long as the propagating wave does not excite too many of the modes. We can conclude that the model is limited, but in some circumstances, potentially a much more effective representation of the electrical field in terms of simulation.

The models were tested with the Method of Manufactured Solutions, and the result was atleast six digits of significance. The verification method assumed the full generalized model, without the assumption of the UPPE conditions. However, all the same numerical implementations are still in use for this model, and the test has verified them as a coherent unit. The verification tests requires us to modify the equations in order to find an exact solution. For a full model it will make sense to simulate real waves, and compare to the experimental results. The experimental results will almost never be the same as a numerical results where

perfect conditions are assumed.

The numerical implementation does only include the cylindrically symmetric case. For our discretization of 1024×125 it requires approximately 2GB memory, where the whole implementation is mode specific. The memory requirement will thus linearly increase with the increase of modes, adding an adequate discretization of the azimuthal direction may require in the region of 200GB of memory. Such a computer was not available at the present time.

6.1 Future work

The future of the model should be to implement the azimuthal direction. The difference between our cylindrically symmetric version and the general version is the inclusion of m . Doing so will be trivial, all we have to do is the exact same thing for each m in the series.

The obvious requirement would be a supercomputer with adequate amount of memory. Throughout our implementation we have introduced a scheme which has a ridiculously parallel right hand side. Adding the azimuthal direction will require the model to do as many transforms as the discretization in the azimuthal direction is. Which in turn will render the implementation even more parallelizable.

In our implementation we used a cubic spline interpolation. The rest of the implementation has a general highest accuracy of $\mathcal{O}(h^2)$, which is the same as the linear interpolation. If the discretization in m is large, the amount of interpolation will also increase linearly. Thus the general speed of the algorithm can be increased if linear interpolation is possible.

Most of the time is spent within the Hankel transform. The form of implementation we have chosen is regarded as a fast algorithm. Other implementations use double FFT algorithms in order to do a Hankel transform. The FFT algorithms uses a uniform grid, thus we can escape the interpolation by such an implementation.

Appendix A

Appendix A

A.1 Fourier Transform

We will now derive the shift and rescaling process needed in order to apply the FFT algorithm to a regular Fourier transform. The procedure is specific for the representation chosen by the library you use. We use the programming language C and the GSL library is relevant for us. The FFT is represented as

$$v_s = \sum_{r=0}^{n-1} u_r e^{-2\pi i \frac{sr}{n}}, \quad u_r = \frac{1}{n} \sum_{s=0}^{n-1} v_s e^{2\pi i \frac{sr}{n}} \quad (\text{A.1})$$

where they denote the first one as the FFT forward, and the second as the FFT backward.

The expansions we have derived in our numerical models are defined as the continuous integrals

$$f(t) = \frac{1}{\sqrt{2\pi}} \int_{-\infty}^{\infty} d\omega F(\omega) e^{-i\omega t}, \quad F(\omega) = \frac{1}{\sqrt{2\pi}} \int_{-\infty}^{\infty} dt f(t) e^{i\omega t} \quad (\text{A.2})$$

The integrals can be approximated by the midpoint rule. We discretize the variables ω and t as

$$a_j = (j - \frac{1}{2})\Delta t, \quad b_l = (l - \frac{1}{2})\Delta\omega, \quad j, l \in \mathbb{Z} \quad (\text{A.3})$$

Between each of these steps we will use the midpoint rule, the mid point of each step will then be

$$t_j = \frac{1}{2}(a_{j+1} + a_j), \quad \omega_l = \frac{1}{2}(b_{l+1} + b_l) \quad (\text{A.4})$$

where we get the step length to be defined as

$$a_{j+1} - a_j = \Delta t, \quad t_j = j\Delta t \quad (\text{A.5})$$

$$b_{l+1} - b_l = \Delta\omega \quad \omega_l = l\Delta\omega \quad (\text{A.6})$$

Applying this to the continuous integrals in (A.2) we get them in the following form

$$f(t) = \frac{1}{\sqrt{2\pi}} \sum_{l=-\infty}^{\infty} \int_{b_l}^{b_{l+1}} d\omega F(\omega) e^{-\omega t} \approx \frac{\Delta\omega}{\sqrt{2\pi}} \sum_{j=-\infty}^{\infty} F(\omega_l) e^{-it\omega_l}$$

$$F(\omega) = \frac{1}{\sqrt{2\pi}} \sum_{j=-\infty}^{\infty} \int_{a_j}^{a_{j+1}} dt f(t) e^{i\omega t} \approx \frac{\Delta t}{\sqrt{2\pi}} \sum_{j=-\infty}^{\infty} f(t_j) e^{i\omega t_j}$$

Now we assume the functions are bounded, such that

$$F_l \equiv F(\omega_l) \approx 0, \quad \text{for } |l| > N$$

$$f_j \equiv f(t_j) \approx 0, \quad \text{for } |j| > N$$

The sums can be truncated at the same N.

$$f(t) \approx \frac{\Delta\omega}{\sqrt{2\pi}} \sum_{j=-N}^N F(\omega_j) e^{-it\omega_j}, \quad F(\omega) \approx \frac{\Delta t}{\sqrt{2\pi}} \sum_{j=-N}^N f(t_j) e^{i\omega t_j}$$

This is true for the general condition of periodic functions. The minimum and maximum period of such functions must be

$$P_{max} = \frac{2\pi}{\Delta\omega}, \quad P_{min} = \frac{2\pi}{\Delta\omega N}$$

In order for the function f to be well represented on the grid of t_j , the period has to at least be of the size $2\delta t$. From this we can deduce the minimum of the frequency domain to be

$$\Delta t = \frac{\pi}{N\Delta\omega} \tag{A.7}$$

This (A.7) will be the relation between the discretization in time domain and spectral domain for the numerical calculations. For periodic functions it is common to associate the last term N with the first term $-N$. This is how periodic functions is formed. The end product of this procedure is the following two identities

$$f_j = \frac{\Delta\omega}{\sqrt{2\pi}} \sum_{l=-N}^{N-1} F_l e^{-i\pi \frac{j l}{N}}, \quad F_l = \frac{\Delta t}{\sqrt{2\pi}} \sum_{j=-N}^{N-1} f_j e^{i\pi \frac{j l}{N}} \tag{A.8}$$

We observe that the last term in the exponent is close to what we have in the FFT algorithms (A.1). The difference is, our representation has a negative in front of the rs sum in the inverse, while the FFT has a positive sign here. What we will do is to associate FFT inverse with our forward, and vice versa.

Now we are going to reformulate the indexing in order to approximate the FFT algorithms (A.1 proposed by the GSL library).

First we have to introduce new indexes in order to rectify the sums. The GSL sum is from 0 to n , so we introduce the new indexes according to

$$\begin{aligned} r &= N + l, & l &= -N, \dots, 0, \dots, N - 1 \\ s &= N + j, & j &= -N, \dots, 0, \dots, N - 1 \end{aligned}$$

This modification gives the new relations

$$f_{s-N} = \frac{\Delta\omega}{\sqrt{2\pi}} \sum_{r=0}^{2N-1} F_{r-N} e^{-i\pi(N-r-s+\frac{rs}{N})}, \quad F_{r-N} = \frac{\Delta t}{\sqrt{2\pi}} \sum_{s=0}^{2N-1} f_{s-N} e^{i\pi(N-r-s+\frac{rs}{N})} \quad (\text{A.9})$$

We have too many terms in our representation to properly associate it with the FFT algorithm. To get rid of some of them we introduce the scaling constants according to

$$F_{r-N} = \beta_r u_r, \quad f_{s-N} = \alpha_s v_s$$

The scaling constants β_r and α_s we represent as

$$\beta_r = b_0 e^{i\pi(N-r)}, \quad \alpha_s = a_0 e^{-i\pi s}$$

Inserting this into the equations (A.9) we get

$$v_s = \frac{\Delta\omega}{\sqrt{2\pi}} \sum_{r=0}^{2N-1} \frac{b_0}{a_0} e^{-i\pi(\frac{rs}{N})}, \quad u_r = \frac{\Delta t}{\sqrt{2\pi}} \sum_{s=0}^{2N-1} \frac{a_0}{b_0} e^{i\pi(\frac{rs}{N})}$$

Now we see that the constants a_0 and b_0 has to satisfy the relations

$$\frac{\Delta\omega b_0}{\sqrt{2\pi}a_0} = 1, \quad \frac{\Delta t a_0}{\sqrt{2\pi}b_0} = \frac{1}{2N}$$

From this we observe that

$$\frac{b_0\Delta\omega}{a_0\sqrt{2\pi}} = 1 \Rightarrow \frac{b_0\Delta\omega\Delta t}{a_0\sqrt{2\pi}\Delta t} \Rightarrow \frac{b_0\sqrt{2\pi}}{a_0\Delta t} = 2N$$

These are the same, thus we only have to impose one of them. We make the choice of the constants as

$$a_0 = \Delta\omega, \quad b_0 = \sqrt{2\pi} \tag{A.10}$$

Inserting this into the transforms and setting $2N = n$ we arrive at the formulas of (A.1).

Thus we have deduced the algorithm in order to make use of the fft scheme to make Fourier transforms. To do a Fourier transform we have to go to the quantity u_r , and for the inverse we have to get the quantity v_s . These are found through

$$v_s = \frac{1}{\Delta\omega} e^{-i\pi s} f_{s-N}, \quad u_r = \frac{1}{\sqrt{2\pi}} e^{-i\pi(N-r)} f_{r-N}, \quad r, s \in 0, \dots, n-1$$

To get the quantities in reverse we have to use

$$F_{r-N} = \sqrt{2\pi} e^{i\pi(N-r)} u_r, \quad f_{s-N} = \Delta\omega e^{i\pi s} v_s, \quad j, l = -N, \dots, N-1$$

We have now derived the relation between the functions we are interested in f and F , and their corresponding vector associated with FFT. In order to do a forward transform we first find v from f , conduct the FFT on v to get u , last we go from u to F .

A.2 Hankel Transform

This section goes through the algorithm for implementing the Hankel transform, the implementation is inspired by [23]. We start by defining the transform in the continuous domain as

$$F_\nu(k) = \int_0^\infty f(r)J_\nu(kr)rdr, \quad \nu \geq -1/2 \quad (\text{A.11})$$

$$f(r) = \int_0^\infty F_\nu(k)J_\nu(kr)kdk, \quad \nu \geq -1/2 \quad (\text{A.12})$$

where the following integral exists and is absolutely convergent.

$$\int_0^\infty dx f(x)x^{1/2}$$

and the function $f(x)$ satisfies the Dirichlet conditions. We will now assume that the function $f(x) = 0$ for all $x \geq R_{max}$. We can then define

$$y = \frac{kR_{max}}{j_N}$$

where j_N us the Nth zeroif $J_\nu(x)$. Through the variable change $r = xR_{max}$ we get the transform on the following form

$$F_\nu\left(\frac{yj_n}{R_{max}}\right) = R_{max}^2 \int_0^1 f(xR_{max})J_\nu(xyj_N)xdx \quad (\text{A.13})$$

$$f(xR_{max}) = \frac{j_N^2}{R_{max}^2} \int_0^\infty F_\nu\left(\frac{yj_n}{R_{max}}\right) J_\nu(xyj_N)ydy \quad (\text{A.14})$$

By expanding this function with Lommel's generalization of Fourier Bessel series, we get

$$f(xR_{max}) = \begin{cases} \sum_{m=1}^{\infty} \frac{2A_m}{J_{\nu+1}(j_m)} J_{\nu}, & 0 \leq x \leq 1, \\ 0, & 1 < x \leq \infty \end{cases} \quad (\text{A.15})$$

where j_m indicates the m th zero of the Bessel function, with the zeroes in ascending order. The coefficients A_m is then found through

$$A_m = \int_0^1 x f(xR_{max}) J_{\nu}(j_m x) dx$$

We can now assume that $A_m = 0$ for all $m \geq N$. This can be done without any loss of generality, since we can choose N and T arbitrarily large anyway. By taking the transform of equation (A.15) we get the result

$$F_{\nu}\left(\frac{j_m}{R_{max}}\right) = R_{max}^2 A_m, \quad \text{when } y = \frac{j_m}{j_N} \quad (\text{A.16})$$

and

$$F_{\nu}\left(\frac{y j_N}{R_{max}}\right) = \sum_{m=1}^{N-1} \frac{2F_{\nu}\left(\frac{j_m}{R_{max}}\right) J_{\nu}(r j_N) j_m}{J_{\nu+1}(j_m)(j_m^2 - y^2 j_N^2)}, \quad 0 \leq y \leq \infty \quad (\text{A.17})$$

When using (A.16) in (A.15) we get

$$f(xR_{max}) = \begin{cases} \sum_{m=1}^{N-1} \frac{2F_{\nu}\left(\frac{j_m}{R_{max}}\right)}{J_{\nu+1}(j_m) R_{max}^2} J_{\nu}(j_m x), & 0 \leq x \leq 1, \\ 0, & 1 < x \leq \infty \end{cases} \quad (\text{A.18})$$

This equation is the relationship between the function $f(xR_{max})$ and the values of its transform for particular values of r . In order to retrieve a similar relationship for the reverse transform we use an identity relationship[23]

$$\frac{4}{J_{\nu+1}(j_m)j_N^2} \sum_{p=1}^{N-1} \frac{J_p(j_m j_p / j_N) J_\nu(j_i j_p / j_N)}{j_{\nu+1}(j_p)} = \delta_{m,i}, \quad m, i < N \quad (\text{A.19})$$

which is the orthogonality relation. If we set $x = j_p / j_N$ and multiply both sides by $J_\nu(j_p j_i / j_n)$ and sum we get

$$F_\nu(j_i / R_{max}) = \frac{1}{R_{max}^2} \sum_{m=1}^{N-1} \frac{2J_\nu(j_p j_i / j_N)}{J_{\nu+1}^2(j_p)} f(j_p R_{max} / j_N) \quad (\text{A.20})$$

From this we can shorten the expression to yield

$$f(i) = \frac{1}{R_{max}^2} \sum_{m=1}^{N-1} Y_\nu(m, i) F_\nu(m), \quad F_\nu(m) = \frac{R_{max}^2}{j_N^2} \sum_{m=1}^{N-1} Y_\nu(m, i) f(i) \quad (\text{A.21})$$

where

$$F_\nu(m) = F_\nu(j_m / R_{max}), \quad f(i) = f(j_i R_{max} / j_N), \quad Y_\nu(i, m) = 2J_\nu(j_i j_m / j_N) / J_{\nu+1}^2(j_m) \quad (\text{A.22})$$

These are the algorithms we need in order to do a Hankel transform. The scaling constants needed in order to do a forward transform is $\frac{1}{R_{max}^2}$ while a inverse is $\frac{R_{max}^2}{j_N^2}$. These transforms are actually the same transform, thus we only need one of them in order to do both. the difference between them is the coefficient.

Example A.1. *1 We are going to start with the function*

$$f(x) = \begin{cases} 1, & x < a \\ 0, & x > a \end{cases} \quad (\text{A.23})$$

Which has the analytic Hankel transform of

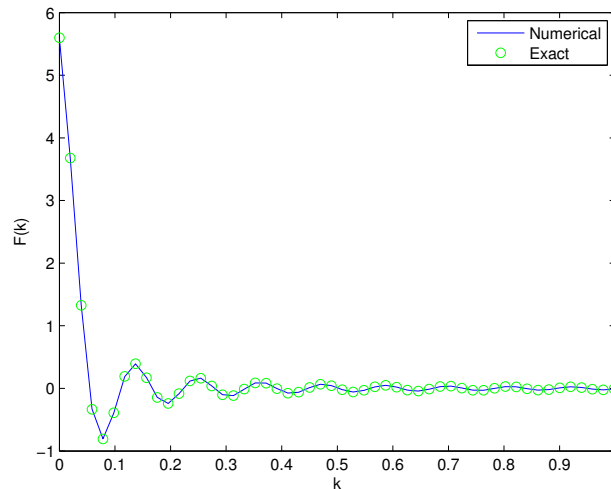


FIGURE A.1: Figure shows the numerical Hankel transform of the heaviside function, with a step at $a = 3.5$ plotted against the exact one. The discretization in this picture is $R_{max} = 10$ and divided into $N = 512$. Thus giving 52 points within the picture. We have chosen to zoom in on the left most part of the graph, as it is here the interesting parts of the function are. We can see that they overlap perfectly.

$$F(r) = aJ_0(ar)/r \quad (\text{A.24})$$

In this experiment we chose to use $a = 3.5$ and set the maximum of x to be $R_{max} = 10$. Thus we are ensured that the function is zero at that point. We cut the interval short to further enhance the picture closer to zero where the most of the fluctuations are.

123

Example A.2. *2 The next example we are going to do is the Gaussian. Since most of our calculations evolves around Gaussian functions it is instructive to further validate the method in this retrospect.*

$$f(x) = e^{-\frac{1}{2}a^2x^2} \quad (\text{A.25})$$

which has the analytical Hankel transform of

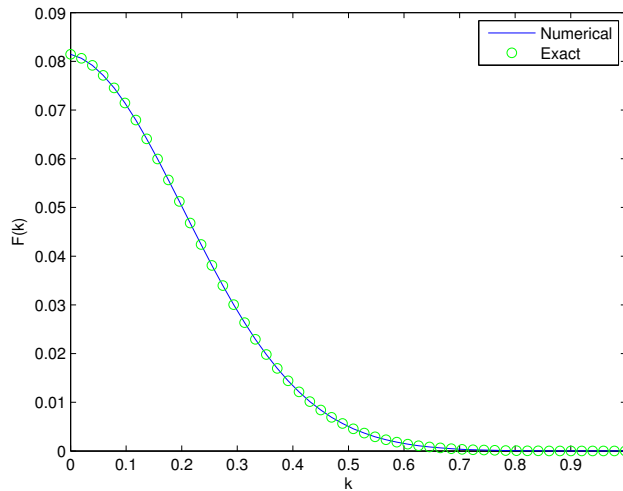


FIGURE A.2: Figure shows the numerical Hankel transform of a Gaussian function, plotted against the exact one. The discretization in this picture is $R_{max} = 10$ and divided into $N = 512$. Thus giving 52 points within the picture. We have chosen to zoom in on the left most part of the graph, as it is here the interesting parts of the function are. We can see that they overlap perfectly.

$$F(r) = \frac{1}{a^2} e^{-\frac{r^2}{2a^2}} \quad (\text{A.26})$$

In order to ensure enough decay of the function, we have chosen $a = 1$ and $R_{max} = 10$ in this picture.

A.3 Interpolation

Interpolation is a method used to evaluate a function of discrete points at points not present in the grid. Assume the grid is given by integer values $f(1)$, $f(2)$ etc. If the function itself needs to be evaluated at the point $f(1.5)$ an interpolation scheme is needed.

The three main interpolation schemes is the linear, quadratic and the cubic spline. For the linear interpolation we have

$$y(x) = y_a + (y_b - y_a) \frac{x - x_a}{x_b - x_a} \quad (\text{A.27})$$

where (x_a, y_a) and (x_b, y_b) is the function y at the point x known from a discrete perspective. A straight line will be drawn between these, and $y(x)$ can be found on the line between these points. The drawback with this type of interpolation is accuracy in functions with a big derivative.

For the quadratic, or polynomial interpolation it is assumed

$$p(x) = a_n x^n + a_{n-1} x^{n-1} + a_{n-2} x^{n-2} + \dots + a_2 x^2 + a_1 x + a_0 \quad (\text{A.28})$$

If p interpolate the data points we have

$$p(x_i) = y_i, \quad \forall i \in \{0, 1, \dots, n\} \quad (\text{A.29})$$

This gives the system

$$\begin{pmatrix} x_0^n & x_0^{n-1} & x_0^{n-2} & \dots & x_0 & 1 \\ x_1^n & x_1^{n-1} & x_1^{n-2} & \dots & x_1 & 1 \\ \vdots & \vdots & \vdots & & \vdots & \vdots \\ x_n^n & x_n^{n-1} & x_n^{n-2} & \dots & x_n & 1 \end{pmatrix} \begin{pmatrix} a_n \\ a_{n-1} \\ \vdots \\ a_0 \end{pmatrix} = \begin{pmatrix} y_0 \\ y_1 \\ \vdots \\ y_n \end{pmatrix} \quad (\text{A.30})$$

In order to interpolate, we have to solve this system, then insert the given a_n into equation (A.28) and the function can be found at any x . However, solving a system such as (A.30) includes solving a Vandermonde system, the condition number of such systems may be large, and thus render the interpolation highly inaccurate. This phenomena is called Runge's phenomena.

The last of the three is the cubic spline interpolation. It assumes the function split into n pieces such that

$$S_i(x) = a_i(x - x_i)^3 + b_i(x - x_i)^2 + c_i(x - x_i) + d_i, \quad \text{for } x \in \{x_i, x_{i+1}\} \quad (\text{A.31})$$

There are $4n$ parameters, $2n$ of them can be found by the endpoints of the interval

$$S_i(x_i) = y_i, \quad S_i(x_{i+1}) = y_{i+1} \quad (\text{A.32})$$

By forcing smooth and continuous function in both the derivative and double derivative we have

$$S'_{i-1}(x_i) = S'_i(x_i), \quad S''_{i-1}(x_i) = S''_i(x_i) \quad (\text{A.33})$$

This can be applied for $i \in \{1, \dots, n-1\}$. Thus we get $2(n-1)$ constraints. The last two constraints can be chosen, three popular choices is the natural

$$S''_0(x_0) = 0, \quad S''_{n-1}(x_n) = 0 \quad (\text{A.34})$$

clamped

$$S'_0(x_0) = f'(x_0), \quad S'_{n-1}(x_n) = f'(x_n) \quad (\text{A.35})$$

or periodic boundaries. We then define the following

$$h_i = x_{i+1} - x_i \quad (\text{A.36})$$

$$b_i = \frac{y_{i+1} - y_i}{h_i} \quad (\text{A.37})$$

$$v_i = 2(h_{i-1} + h_i) \quad (\text{A.38})$$

$$u_i = 6(b_i - b_{i-1}) \quad (\text{A.39})$$

$$z_0 = z_n = 0 \quad (\text{A.40})$$

where $z_i = S''(x_i)$ for $i = 0, \dots, n$. This will reduce to the following tridiagonal system

$$\begin{pmatrix} v_1 & h_1 & & & & & \\ h_1 & v_2 & h_3 & & & & \\ & h_2 & v_3 & h_3 & & & \\ & & \ddots & \ddots & \ddots & & \\ & & & \ddots & \ddots & h_{n-2} & \\ & & & & h_{n-2} & v_{n-1} & \end{pmatrix} \begin{pmatrix} z_1 \\ z_2 \\ z_3 \\ \vdots \\ z_{n-2} \\ z_{n-1} \end{pmatrix} = \begin{pmatrix} u_1 \\ u_2 \\ u_3 \\ \vdots \\ u_{n-2} \\ u_{n-1} \end{pmatrix} \quad (\text{A.41})$$

where

$$\begin{aligned} a_i &= \frac{z_{i+1}}{6h_i} \\ b_i &= \frac{z_i}{6h_i} \\ c_i &= \frac{y_{i+1}}{h_i} - \frac{z_{i+1}h_i}{6} \\ d_i &= \frac{y_i}{h_i} - \frac{h_i z_i}{6} \end{aligned}$$

Which goes back into (A.31) and forms the interpolating function.

Example A.3. *Example* The test of the numerical scheme is done using a Gaussian function of the type

$$f(x) = e^{-x^2}$$

The grid is chosen from -10 to 10 with nonuniform discretization. A numerical solution is thus found through the cubic spline interpolation

In the first figure (A.3) we see the numerical solution calculated with the cubic spline method against the exact solution. Both these functions are here evaluated on the same nonuniform grid.

The last figure (A.4) shows the relative error between the exact solution and the numerical solution. The magnitude of the error is in the order of 10^{-3} .

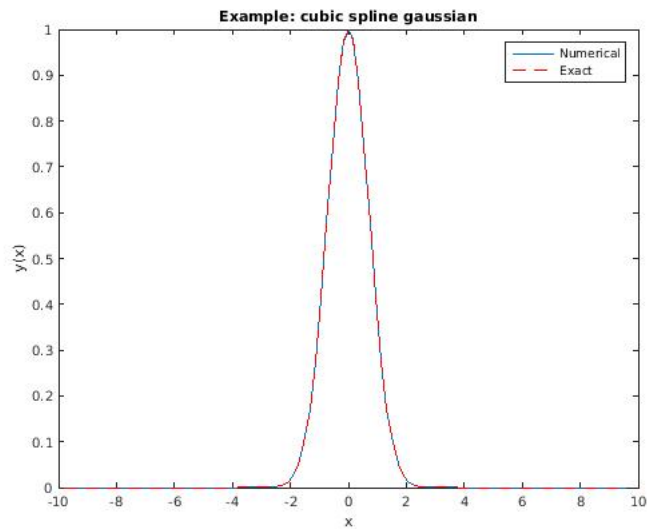


FIGURE A.3: The exact solution and numerical interpolated solution plotted against each other on a nonuniform grid.

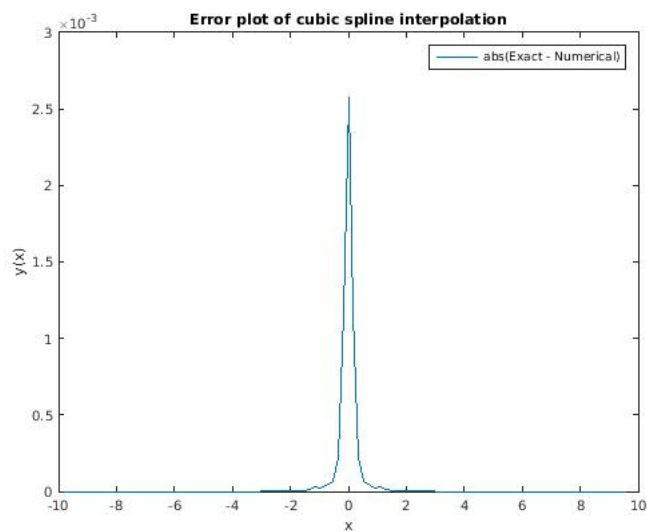


FIGURE A.4: The relative error of the numerical solution against the exact solution.

A.4 The First Order Finite Difference Method

When we do calculations we always want the highest order of accuracy we can get. The usual first order difference methods are the forward-, backward- and center difference methods.

$$f'(x) = \frac{f(x + dx) - f(x)}{dx} \quad (\text{A.42})$$

$$f'(x) = \frac{f(x) - f(x - dx)}{dx} \quad (\text{A.43})$$

$$f'(x) = \frac{f(x + dx) - f(x - dx)}{2dx} \quad (\text{A.44})$$

They all come from the same type of Taylor expansion, where we expand the function $f(x)$ around the point x we want to find the derivative of. For the forward method we have

$$f(x) = f(x_0) + \frac{d}{dx}f(x_0)(x - x_0) + \frac{d^2}{dx^2}f(x_0)\frac{(x - x_0)^2}{2!} + \dots$$

To find the forward method we isolate the first derivative by truncating higher terms

$$\frac{d}{dx}f(x_0) = \frac{f(x) - f(x_0)}{(x - x_0)}$$

The error we get from this can be calculated as

$$\frac{d}{dx}f(x_0) - \frac{f(x) - f(x_0)}{(x - x_0)} = \frac{d^2}{dx^2}f(x_0)\frac{(x - x_0)}{2!} \dots$$

This error is atleast of magnitude $(x - x_0)$. That is first order. The same can be applied for the backward difference, and the result will be the same. In order to get the central difference we need the Taylor expansion of the backward as well, it is

$$f(x) = -f(x_0) + \frac{d}{dx}f(x_0)(x - x_0) + \frac{d^2}{dx^2}f(x_0)\frac{(x - x_0)^2}{2!} - \dots$$

if we adding the forward from the backward we get

$$f(x_0 + h) + f(x_0 - h) = \frac{d}{dx}f(x_0)(h) + \frac{d}{dx}f(x_0)(h) + O(h^3)$$

What we observe from this is that the accuracy is higher, it is actually double the accuracy of the two former methods. Inspired by this we will adopt a notation for calculating the derivative of a known vector as a second order Taylor expansion. If we assume we have a vector $f_1, \dots, f_i, \dots, f_N$ of values evaluated on a grid $x_1, \dots, x_i, \dots, x_N$. Then the derivative can be approximated to the second order by the three point list

1. For the first element we have a special case, we cannot solve as central difference, since f_0 does not exist. What we do is to solve the following system of equations

$$\begin{aligned} f_1 &= a \\ f_2 &= a + b(x_1 - x_2) + c(x_1 - x_2)^2 \\ f_3 &= a + b(x_1 - x_3) + c(x_1 - x_3)^2 \end{aligned}$$

2. The middle elements are clear, we will adopt something similar to the central difference scheme in order to achieve double accuracy magnitude

$$\begin{aligned} f_{i-1} &= a + b(x_i - x_{i-1}) + c(x_i - x_{i-1})^2 \\ f_i &= a \\ f_{i+1} &= a + b(x_i - x_{i+1}) + c(x_i - x_{i+1})^2 \end{aligned}$$

3. At the end we will have the same problem as the beginning, thus we will use a reverse scheme of what we used at the beginning

$$f_{N-2} = a + b(x_N - x_{N-2}) + c(x_N - x_{N-2})^2$$

$$f_{N-1} = a + b(x_N - x_{N-1}) + c(x_N - x_{N-1})^2$$

$$f_N = a$$

This results in a system of equations to be solved for the particular derivatives of the function which takes the form

$$\mathbf{A}x = \mathbf{b}$$

Solving this system will also give the derivatives at a higher order at the endpoints than the forward and backward differences can give.

Appendix B

Appendix B

B.1 The Sellmeier formula

For most cases it is rather difficult to find a mathematical exact formula for the refractive index. Since the rise of the laser itself, studies has been done and it is actually possible to measure the refractive index. This graph can then be approximated analytically by a method of curve fitting.

The Sellmeier formula is an empirical relationship between the refractive index and the wavelength. It was first discovered in 1871 by Wilhelm Sellmeier (ref). The most common form of the equation for glasses is

$$n^2(\lambda) \approx 1 + \frac{B_1\lambda^2}{\lambda^2 - C_1} + \frac{B_2\lambda^2}{\lambda^2 - C_2} + \frac{B_3\lambda^2}{\lambda^2 - C_3} \quad (\text{B.1})$$

where n is the refractive index, λ is the wavelength, and the constants $B_1, B_2, B_3, C_1, C_2, C_3$ can be found experimentally and are called the Sellmeier coefficients. For some cases where the refractive index is close to 1 it is possible to use a simplified version of the formula.

$$n(\lambda) - 1 \approx \frac{B_1\lambda^2}{\lambda^2 - C_1} + \frac{B_2\lambda^2}{\lambda^2 - C_2} + \frac{B_3\lambda^2}{\lambda^2 - C_3} \quad (\text{B.2})$$

where some but always all of the constants are needed in order to approximate

the refractive index of the medium. This case is more often discussed in the case of rare gases.

These formulas follows the universal notation of λ as the wavelength. The wavelength in the Sellmeier formulas are typically given in terms of micrometers. In order for us to do numerics on these formulas we have to first relate these towards the typical wavelengths, and scale them to appropriate factors for our system. We will use the linear formula between the wavelength and the frequency as

$$\lambda \times 10^6 = \frac{2\pi c}{\omega} \quad (\text{B.3})$$

We can insert these into the equation in order to get the refractive index on the form of frequency instead of the wavelength, doing so for the typical glass equation we get

$$n^2(\omega) \approx 1 + \frac{B_1 \left(\frac{2\pi c \times 10^{-6}}{\omega}\right)^2}{\left(\frac{2\pi c \times 10^{-6}}{\omega}\right)^2 - C_1} + \frac{B_2 \left(\frac{2\pi c \times 10^{-6}}{\omega}\right)^2}{\left(\frac{2\pi c \times 10^{-6}}{\omega}\right)^2 - C_2} + \frac{B_3 \left(\frac{2\pi c \times 10^{-6}}{\omega}\right)^2}{\left(\frac{2\pi c \times 10^{-6}}{\omega}\right)^2 - C_3} \quad (\text{B.4})$$

which through a few manipulations can be rewritten in the more convenient way as

$$n^2(\omega) \approx 1 + \frac{\beta_1}{\alpha_1 - \omega^2} + \frac{\beta_2}{\alpha_2 - \omega^2} + \frac{\beta_3}{\alpha_3 - \omega^2} \quad (\text{B.5})$$

where all we have done is to redefine the constants in such a way that everything is included in them. The last part of this is off course the scaling matter. We will need this in a scaled form, as such we will set $\omega = \omega' \omega_0$

$$n^2(\omega' \omega_0) \approx 1 + \frac{\beta_1}{\alpha_1 - (\omega' \omega_0)^2} + \frac{\beta_2}{\alpha_2 - (\omega' \omega_0)^2} + \frac{\beta_3}{\alpha_3 - (\omega' \omega_0)^2} \quad (\text{B.6})$$

This is the function that will be used throughout the numerical calculations.

B.2 The Cylindrical Derivative Operators

Within this thesis the cylindrical vector operators such as curl and divergence are used. These will be listed here for convenience of the reader.

The unit vectors in cylindrical vector space is

$$\hat{\mathbf{x}} = \cos(\phi)\hat{\rho} - \sin(\phi)\hat{\phi}$$

$$\hat{\mathbf{y}} = \sin(\phi)\hat{\rho} + \cos(\phi)\hat{\phi}$$

$$\hat{\mathbf{z}} = \hat{\mathbf{z}}$$

A vector field is defined as

$$\mathbf{A} = A_\rho\hat{\rho} + A_\phi\hat{\phi} + A_z\hat{\mathbf{z}}$$

The gradient of the scalar field f is then

$$\nabla f = \partial_\rho f \hat{\rho} + \frac{1}{\rho} \partial_\phi f \hat{\phi} + \partial_z f \hat{\mathbf{z}}$$

The divergence of the field \mathbf{A} is

$$\nabla \cdot \mathbf{A} = \frac{1}{\rho} \partial_\rho (\rho A_\rho) + \frac{1}{\rho} \partial_\phi A_\phi + \partial_z A_z$$

And finally the curl of the field \mathbf{A} is

$$\nabla \times \mathbf{A} = \left(\frac{1}{\rho} \partial_\phi A_z - \partial_z A_\phi \right) \hat{\rho} + (\partial_z A_\rho - \partial_\rho A_z) \hat{\phi} + \frac{1}{\rho} (\partial_\rho (\rho A_\phi) - \partial_\phi A_\rho) \hat{\mathbf{z}}$$

Appendix C

Appendix C

This appendix is dedicated to inform the people interested in more specific details of the implementation. In the following is dedicated to how we chose to set up the program for the vectorial model in order to best keep track of all its components.

Main.c The main function we decide the size of the domain, its discretization and runs all initialization functions. Solving the ODE is also implemented in this part, together with the right hand side.

Initialization.c This is where we define the structures to store all domain vectors. We also find the initial value of the electrical field and modes in a separate function implemented here, for verification we also include the LU factorization in this section.

FFT.c Both inverse and forward fourier transform implementation.

Hankel.c Both inverse and forward hankel transform implementation.

Interpolation.c Interpolation schemes both in the spectral and real domain.

Functions.c To save space and keep the other implementations clean we have all the analytic functions needed in this segment.

Source.c All the needed analytical functions for the source test is included in this file.

Throughout the implementation we have chosen not to store the matrices and the auxiliary vectors needed throughout the functions. The reason to do so is the shared memory complexity when using parallel programming.

When utilizing multi core programming it is most powerful when none of the processes has to wait for another one to finish. However, this requires us to allocate and deallocate memory to avoid leaks along the way. In general optimization can be done on this aspect, as some of the matrices may be better left at static presence.

Throughout the implementation there is several step which one might check in order to verify if the implementation is correct. When the modes are found for the first time, these can be checked against the reality conditions of the field. Over the whole frequency domain these shall be satisfied. The next step is to check whether the reconstruction works by verifying the electrical field with its initial condition. When first propagating the model through the verification method it is easiest done by assuming the longitudinal component is zero $E_z = 0$ for all time and space. Doing so will make interpolation unnecessary. In the last segment it is to include the longitudinal component, where we will have to include both the interpolation and the Q mode. The process described is the one we followed when implementing the algorithm, and gives a natural progression of the numerical scheme, where every part can be truly verified.

Bibliography

- [1] Per Jakobsen. A uppe propagation scheme for cylindrical vector modes. 2012.
- [2] Qiwen Zhan. Adv. opt. *Photon*, 2009.
- [3] Hongcheng Want and Weilong She. Nonparaxial optical kerr vortex soliton with radial polarization. *Optical Express*, 2006.
- [4] Zasim Mzumder Joseph W. Haus and Qiwen Zhan. Azimuthal modulation instability for a cylindrically polarized wave in a nonlinear kerr medium. *Optical Express*, 2005.
- [5] P. Di. Porto A Ciattoni, B. Crosignani and A. Yariv. Rev, lett. *Phys.*, 2005.
- [6] J. Durnin. Exact solutions for nondiffracting beams i. the scalar theory. *J. Opt. Am. A*, 1987.
- [7] Micheal Zamboni-Rached Hugo E. Hernansez-Figueroa and Erasmo Recami. Localized waves. *Series in microwave and optical engineering*, Wiley, 2008.
- [8] V. Nilsen. A unidirectional pulse propagation model for extreme nonlinear optics: Derivation and implementation, Desember 2014.
- [9] James Neill Brittingham. Focused wave modes in homogenous maxwell's equations: Transverse electric mode. *J. Appl. Phys*, 1983.
- [10] J.V. Moloney M. Kolesik and M. Mlejnek. Unidirectional optical pulse propagation equation. *Phys. Rev. Lett.*, 2002.
- [11] P. Jakobsen M. Kolesik and J.V. Moloney. Quantifying the limits of unidirectional ultrashort optical pulse propagation. *Physical Review A*, 2012.

-
- [12] G. Russakoff. A derivation of the macroscopic maxwell equations. *American Journal of Physics*, 1970.
- [13] M. Kolesik. Computational methods for nonlinear pde's in ultrashort pulse propagation, 2011.
- [14] R.W. Boyd. Nonlinear optics, 3rd edition, 2008.
- [15] P. Weinberger. John kerr and his effects found in 1877 and 1878. *Philosophical Magazine Letters* 88, 2008.
- [16] P.J. Roache. Cide verification by the method of manufactured solutions. *Trans, ASME, J. Fluids Engineering*, 2002.
- [17] P. Knupp K. Salari. Code verification by the method of manufactured solutions. *Sandia Report, Sandia National Laboratories*, 2000.
- [18] J.V. Moloney-A.C. Newell K. Glasner, M. Kolesik. Canonical and singular propagation of ultrashort pulses in a nonlinear medium. *International Journal of Optics*, 2011.
- [19] Per Jakobsen and J.V. Moloney. The effect of longitudinal electric field components on the propagation of intense ultrashort optical pulses. *Physica*, 2012.
- [20] Andrew W. Norfolk and Edward J. Grace. Reconstruction of optical fields with the quasi-discrete hankel transform. *Optics Express*, 2010.
- [21] A. J. Jerri and D. W. Kreisler. Sampling expansion with derivatives for finite hankel and other transforms. *SIAM J. Math*, 1975.
- [22] L.L. Campbell. A comparison of the sampling theorems of kramer and whitaker. *J. Soc. Indust. Appl. Math*, 1964.
- [23] H. FISK JOHNSON. An improved method for computing a discrete hankel transform. *Elsevier Science Publishers B.V.*, 1986.

